

Distribution Agreement

In presenting this thesis or dissertation as a partial fulfillment of the requirements for an advanced degree from Emory University, I hereby grant to Emory University and its agents the non-exclusive license to archive, make accessible, and display my thesis or dissertation in whole or in part in all forms of media, now or hereafter known, including display on the world wide web. I understand that I may select some access restrictions as part of the online submission of this thesis or dissertation. I retain all ownership rights to the copyright of the thesis or dissertation. I also retain the right to use in future works (such as articles or books) all or part of this thesis or dissertation.

Signature:

Anna Rose Blood

Date

Dearomative Photocatalytic Hydroalkylation and Lipophilic Prodrugs

By
Anna Rose Blood
Master of Science

Chemistry

Dennis Liotta, Ph.D.
Advisor

Simon Blakey, Ph.D.
Committee Member

Bill Wuest, Ph.D.
Committee Member

Accepted:

Kimberly Jacob Arriola, Ph.D, MPH
Dean of the James T. Laney School of Graduate Studies

Date

Dearomative Photocatalytic Hydroalkylation and Lipophilic Prodrugs

By

Anna Rose Blood

B.A., New College of Florida, 2019

Advisor: Dennis Liotta, Ph.D.

An abstract of

A thesis submitted to the faculty of the

James T. Laney School of Graduate Studies of Emory University

in partial fulfillment of the requirements for the degree of

Masters of Science

in Chemistry

2021

Abstract

Dearomative Photocatalytic Hydroalkylation and Lipophilic Prodrugs

By Anna Rose Blood

Dearomatization has become a powerful technique to create dimensional complexity from inexpensive, abundant aromatic precursors. Here, we employed intramolecular cyclization of alkyl radicals for dearomatization of benzylacetamides to form spirocyclic lactams. A strongly reducing organic photocatalyst with a stoichiometric amine reductant was used to afford the 1,4-cyclohexadiene moieties by a reductive radical polar crossover mechanism. The reaction was optimized to favor the dearomatized product over hydrodehalogenation and dimer byproducts. The regioselective method proceeds efficiently on a range of substituted benzylacetamides. Additionally, the dearomatized products can be functionalized to afford a variety of scaffolds, including the commonly prescribed anticonvulsant drug, Gabapentin.

Nucleoside analogues have emerged as effective therapeutics by interfering with endogenous nucleosides to prevent viral replication and tumor proliferation. Here we develop nucleoside prodrug analogues to increase selectivity, and decrease degradation and toxicity. A Tenofovir prodrug was developed with a glycerol backbone with oxygen linkers connecting TFV to inhibit reverse transcriptase, a lipophilic chain to improve cell permeability, and varying lipophilic groups to increase lipoprotein association and direct transport to systemic circulation. The 5-fluorouracil prodrug analogue incorporates the active metabolite FdUMP prevent 5-FU degradation, steric bulk to limit kinase activity, and a metabolically stable chain to decrease premature drug release.

Dearomative Photocatalytic Hydroalkylation and Lipophilic Prodrugs

By

Anna Rose Blood

B.A., New College of Florida, 2019

Advisor: Dennis Liotta, Ph.D.

A thesis submitted to the faculty of the
James T. Laney School of Graduate Studies of Emory University
in partial fulfillment of the requirements for the degree of
Masters of Science
in Chemistry
2021

Dedicated to David Bruch:

a chem fueled maniac, a brilliant scientist, an amazing person, and a great friend,

who went out doing what he loved.

Acknowledgements

First, I would like to thank my advisor, Dr. Liotta, for all the kindness and grace he has shown me since I joined his lab. It was truly wonderful to work for such a thoughtful mentor. He brought me into his lab when I was in a difficult situation, and provided me with comfort and resources to rebuild my passion for science after a particularly difficult year.

Additionally, I'd like to thank my committee, Dr. Blakey and Dr. Wuest, and my previous advisor, Dr. Jui. They have been so helpful throughout my time in the program assisting me to continuously improve as a scientist.

I'd like to give a special thanks to my mentors, Dr. Kelly McDaniel and Dr. Nicole Pribut. They taught me everything I know about research and lab work. I would not be the scientist I am today had I not had the pleasure of learning from them.

Finally, I would like to thank all of my lab mates. I am especially thankful for the members of the Jui lab close-out group including Dr. Cameron Pratt, Dr. Kelly McDaniel, Dr. Henry Zecca, Cecelia Hendy, Racheal Spurlin, Gavin Smith, Mark Maust, and Brock Keen. Their endless support in both science and day-to-day life is the only thing that got me this far. I'd also like to thank the Liotta lab 5th floor crew for helping me over the past few months.

Table of Contents

Dearomatization of Unactivated Arenes via Photocatalytic Hydroalkylation.....	1
Introduction.....	1
Results and Discussion.....	7
Conclusion and Future Work.....	16
Lipophilic Tenofovir Prodrugs.....	18
Introduction.....	18
Results and Discussion.....	26
Conclusion and Future Work.....	31
Fluorodeoxyuridine Monophosphate Prodrugs.....	32
Introduction.....	32
Results and Discussion.....	39
Conclusion and Future Work.....	41
References.....	42
Experimental	48

List of Figures:

Figure 1. Reactivity and reaction scheme.

Figure 2. Selected spiro lactam target compounds.

Figure 3. Photocatalytic oxidative and reductive quenching cycle.

Figure 4. Organic donor acceptor photoredox catalysts.

Figure 5. Dearomative hydroarylation by ipso-radical cyclization and RRPCO.

Figure 6. Photocatalytic reductive dehalogenation.

Figure 7. Dearomatization by ipso-radical spirocyclization for gamma-lactams.

Figure 8. Radical precursors and radical-radical coupling for dimer formation.

Figure 9. Amide substituent effect on cyclization.

Figure 10. Proposed hydroalkylation mechanism, undesired HDH pathways, and effect of water on HDH formation.

Figure 11. Lactam derivatization.

Figure 12. Proposed catalytic cycle.

Figure 13. Cyclic voltammetry experiments.

Figure 14. Electronic effects.

Figure 15. Steric effects.

Figure 16. Future work.

Figure 17. A. Steps of viral replication. B. Phosphodiester bond formation with endogenous nucleotides. C. Prevention of bond formation with reverse transcriptase inhibitors. D. Reverse transcriptase inhibition.

Figure 18. Structures of TFV and its lipophilic prodrugs TAF, TDF, and TXL.

Figure 19. TXL analogues with stable terminal motifs.

Figure 20. Structure of cidofovir prodrugs.

Figure 21. Structure of TXL preliminary analogues and target analogues.

Figure 22. Example of a hybrid TFV prodrug that contains both increased lipophilicity and metabolically stable terminal motifs.

Figure 23. Structures of representative nucleosides, mono- and triphosphates.

Figure 24. dUMP and FdUMP complexation with TS and MeTHF

Figure 25. 5-FU degradation to DHFU by DPD.

Figure 26. Representative 5-FU prodrugs Tegafur, UFT, and S-1.

Figure 27. Prodrugs affecting phosphorylation and metabolic stability.

Figure 28. Target 5-FU prodrug.

List of Schemes:

Scheme 1. Synthesis of 2-benzyloxy glycerol TFV prodrugs.

Scheme 2. Initial synthetic route to 3-benzyloxy glycerol TFV prodrugs.

Scheme 3. Synthesis of 3-benzyloxy glycerol TFV prodrugs.

Scheme 4. Synthesis of prodrugs with alternate protecting groups.

Scheme 5. Synthesis of acetonide protected 5'-C-methyl-5-fluorouridine nucleosides.

Scheme 6. Synthesis of metabolically optimized lipophilic chain.

Scheme 7. Synthesis of metabolically stable lipophilic chain equipped with phosphate group.

List of Tables:

Table 1. Reaction condition optimization for dearomatized spirocyclic lactam.

Table 2. Scope of spirocyclic lactam products.

Table 3. Representative examples of lipophilic analogues to be coupled to TFV.

List of Abbreviations:

AIDS: Acquired immunodeficiency syndrome

CDV: Cidofovir

CAN: Cerium ammonium nitrate

CV: Cyclic voltammetry

CYP: Cytochrome P450

DBU: 1,8-Diazabicyclo[5.4.0]undec-7-ene

DHFU: 5,6-Dihydro-5-fluorouracil

DIPEA: Diisopropylethylamine

DNA: Deoxyribonucleic acid

DPD: Dihydropyrimidine dehydrogenase

dUMP: Deoxyuridine monophosphate

EtOAc: Ethyl acetate

Et₂O: Diethyl ether

FDA: Food and drug administration

FdUMP: Fluorodeoxyuridine monophosphate

FdUTP: Fluorodeoxyuridine triphosphate

FUTP: Fluorouridine triphosphate

GCMS: Gas chromatography mass spectrometry

HAT: Hydrogen atom transfer

HDH: Hydrodehalogenation

HDP-CDV: Hexadecyloxypropyl-cidofovir

HIV: Human immunodeficiency virus

HLM: Human liver microsome

HOMO: Highest occupied molecular orbital

HPLC: High performance liquid chromatography

HSA: Human serum albumin

IBX: 2-iodobenzoic acid

LCMS: Liquid chromatography mass spectrometry

LiAlH₄: Lithium aluminum hydride

LUMO: Lowest unoccupied molecular orbital

mCPBA: *meta*-Chloroperoxybenzoic acid

MeCN: Acetonitrile

MeOH: Methanol

MeTHF: 5,10-Methylene tetrahydrofolate

mRNA: messenger RNA

NADPH: Nicotinamide adenine dinucleotide phosphate

NRTIs: Nucleoside reverse transcriptase inhibitors

NtRTIs: Nucleotide reverse transcriptase inhibitors

ODBG-CDV: 1-*O*-octadecyl-2-*O*-benzyl-*sn*-glycero-cidofovir

PC: Photocatalyst

PC*: Photocatalyst excited state

PLC: Phospholipase C

PMB: *para*-Methoxy benzyl

RNA: Ribonucleic acid

rRNA: Ribosomal ribonucleic acid

RRPCO: Reductive radical polar crossover

SCE: Saturated calomel electrode

TAF: Tenofovir alafenamide

TBAF: *tetra-N*-Butylammonium fluoride

TBS: *tert*-Butyl dimethyl silyl

TDF: Tenofovir disoproxil fumarate

TFA: Trifluoroacetic acid

TFV: Tenofovir

THF: Tetrahydrofuran

THP: Tetrahydropyran

TIPS: triisopropyl silane

TLC: Thin layer chromatography

TMP: Thymidine monophosphate

tRNA: transfer ribonucleic acid

TS: Thymidylate synthase

TTP: Thymidine triphosphate

TXL: Tenofovir Exalidex 4CzIPN: 1,2,3,5-tetrakis(carbazol-9-yl)-4,6-dicyanobenzene

UTP: Uridine triphosphate

5-FU: 5-Fluorouracil

Dearomatization of Unactivated Arenes via Photocatalytic Hydroalkylation

Introduction

Biological targets, such as proteins and enzymes, have intricate three-dimensional structures, creating a demand for therapeutics with complex spatial orientations.¹ On the other hand, aromatic compounds are cheap, abundant, and easy to functionalize, making them ideal precursors for drug

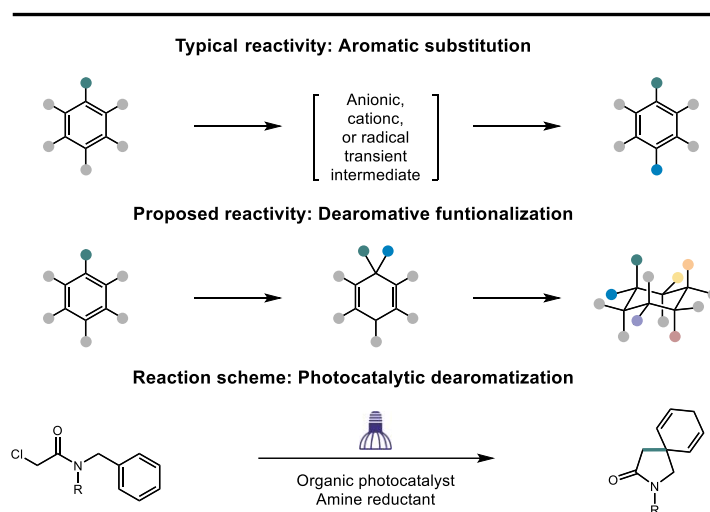


Figure 1. Reactivity and reaction scheme.

synthesis. Consequently, the conversion of simple arenes to complex ring systems is a valuable transformation.² This is made possible by recent advances in dearomatization,³ along with seminal dearomative techniques including the Birch reduction,⁴ enzymatic oxidation,⁵ and high-pressure hydrogenation.⁶ The resulting saturation and sp^3 character leads to an increase in the potential spatial orientations of a compound without a significant increase in the molecular weight, providing more possibilities for the compound to interact with complex biological targets without decreasing its drug-like properties. However, dearomatization presents unique challenges due to the difficulty in overcoming the high thermodynamic aromatic stabilization energy, such as that of benzene (36 kcal/mol).⁷

While aromaticity is temporarily broken to form anionic and cationic intermediates in aromatic substitution reactions, the thermodynamically stable aromatic systems are quickly restored.^{8,9} Transient radical intermediates also typically restore aromaticity by oxidation and deprotonation, such as in Minisci-type reactions.¹⁰ In contrast, reduction of these transient radical

intermediates via reductive radical-polar crossover (RRPCO) followed by protonation would allow for trapping of the dearomatized structures. Applying this process to benzylacetamides would

give rise to spirocyclic lactams, a scaffold found in target compounds such as those shown in Figure 2.^{11,12,13}

While the reaction scheme requires a high-energy reduction, photoredox catalysis offers a simple and mild strategy to undergo high energy electron transfers for otherwise difficult bond formations.¹⁴ As shown in Figure 3, a photocatalyst (PC) absorbs visible light, which raises a single electron from the highest occupied molecular orbital (HOMO) to the lowest unoccupied molecular orbital (LUMO). The electron then changes spin multiplicity from the singlet state to the triplet state by inter-system crossing. This results in a long-lived excited state (PC*), which is both more oxidizing, and more reducing than the analogous ground state photocatalyst. The catalyst can undergo a reductive quenching cycle by reduction from an electron donor, resulting in a strong reductant. Alternatively, it can undergo an oxidative quenching cycle by oxidation from an electron acceptor, resulting in a strong oxidant.¹⁴

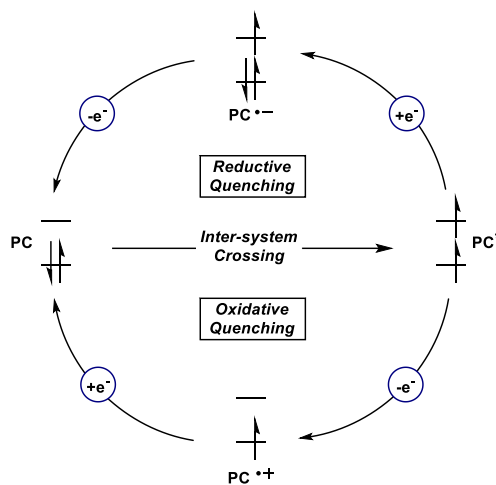
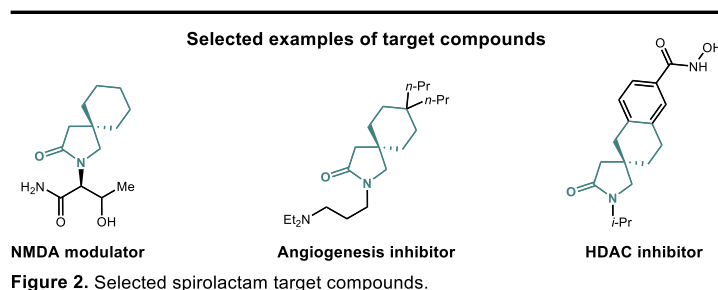


Figure 3. Photocatalytic oxidative and reductive quenching cycle.

Ruthenium and iridium based photocatalysts have been extensively researched, and are commonly employed due to their favorable

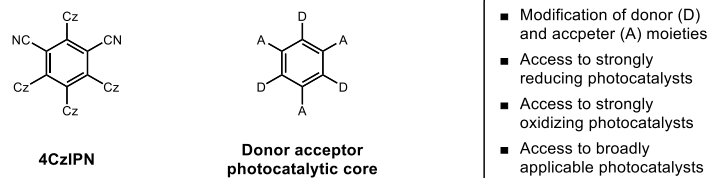


Figure 4. Organic donor acceptor photoredox catalysts.

photophysical properties.¹⁵ However, these are precious metal-based catalysts, making them expensive and unsustainable.¹⁶ First-row transition metal complexes have been developed as more sustainable alternatives,¹⁷ and there has been growing interest in organic photocatalysts.¹⁸ The Zeitler lab recently developed a library of donor-acceptor cyanoarene photocatalysts based off of the previously developed organic photocatalyst, 1,2,3,5-tetrakis(carbazol-9-yl)-4,6-dicyanobenzene (4CzIPN), as shown in Figure 4. The electron donor substituents and the electron acceptor molecular core were adjusted in order to tune the photophysical properties.¹⁹ Modification of these moieties gave rise to purely organic photocatalysts with strong redox potentials.

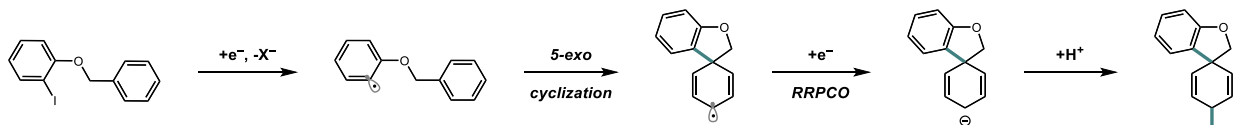


Figure 5. Dearomative hydroarylation by ipso-radical cyclization and RRPCO.

Our group (Jui lab) previously developed a photocatalytic method with an organic photocatalyst for intramolecular arene hydroarylation to form spirocyclic products by dearomatization, shown in Figure 5.²⁰ This method operated through photoexcitation of a donor-acceptor cyanoarene catalyst, 3DPAFIPN, followed by reductive quenching with Hünig's base. Single-electron transfer from the resulting ground state reductant 3DPAFIPN⁻ ($E_{1/2}^{\circ} = -1.59$ V vs SCE) to the aryl halide followed by mesolytic cleavage resulted in regioselective aryl radical formation. Dearomatization of the pendant arene by intramolecular cyclization gave rise to a dienyl radical. A second reduction by RRPCO resulted in anion formation, followed by protonation to afford the desired dearomatized product.

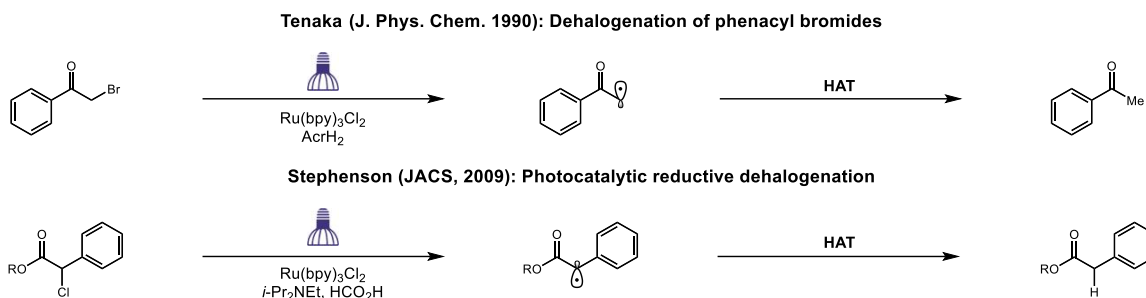


Figure 6. Photocatalytic reductive dehalogenation.

We sought to determine whether this catalytic dearomative RRPCO sequence could be applied to hydroalkylation to form spiro lactams. In order for the alpha-halogenated N-benzylacetamides to undergo a radical cyclization, the alpha-acyl radical must first be generated by reductive dehalogenation. Early work from the Tanaka group (Figure 6, top) demonstrated photocatalytic reductive dehalogenation of phenacyl bromides using a ruthenium photocatalyst and methylacridine as a stoichiometric reductant.²¹ The phenacyl bromide underwent mesolysis upon reduction to form an alpha-acyl radical and a bromide anion. The resulting radical then abstracted a proton from the oxidized methylacridine to form acetophenone. Stephenson later developed a general method for photocatalytic reductive dehalogenation (Figure 6, bottom) using a ruthenium photocatalyst, amine reductant, and a hydrogen atom source that is able to reduce alpha-acyl halides.²² While both of these photocatalytic reactions demonstrate effective reductive dehalogenations of activated halides, formation of these radical intermediates is followed by hydrogen atom transfer. In our system, we sought to achieve functionalization of alpha-acyl radical intermediates via dearomative cyclization followed by reductive radical polar crossover (RRPCO) utilizing a highly reducing organic photocatalyst, avoiding the need for metals.

Dearomative spirocyclization of alpha-acyl radicals to form gamma-lactam scaffolds has been previously reported as shown in Figure 7.^{23,24,25} Seminal work reported by the Zard lab used nickel as an electron transfer reagent for reduction of trichloroacetamides, which was followed by

radical cyclization resulting in dearomatization. The dearomatized radical intermediate then underwent oxidation and chloride addition to afford the spiro lactam products. However, this reaction required stoichiometric nickel and resulted in low regioselectivity. The Miranda group later reported spirocyclic gamma-lactams by dearomative cyclization into para-methoxy substituted benzyloxy. Refluxing peroxide with a xanthate functionalized benzylacetamide resulted in an alpha-acyl radical, which similarly cyclized into the benzene substituent, dearomatizing the arene. This was followed by oxidation and demethylation, resulting in the desired product. In addition to employing rather harsh reaction conditions, this method was limited to cyclohexadienone derivatives. Finally, the Bonjoch group used a copper catalyst to achieve radical generation and dearomative cyclization, followed by a C-Cl bond formation by atom transfer. The allylic chlorine is then hydrolyzed, generating the corresponding alcohol. While this method is highly regioselective, it is limited by use of a copper catalyst and formation of cyclohexadienols.

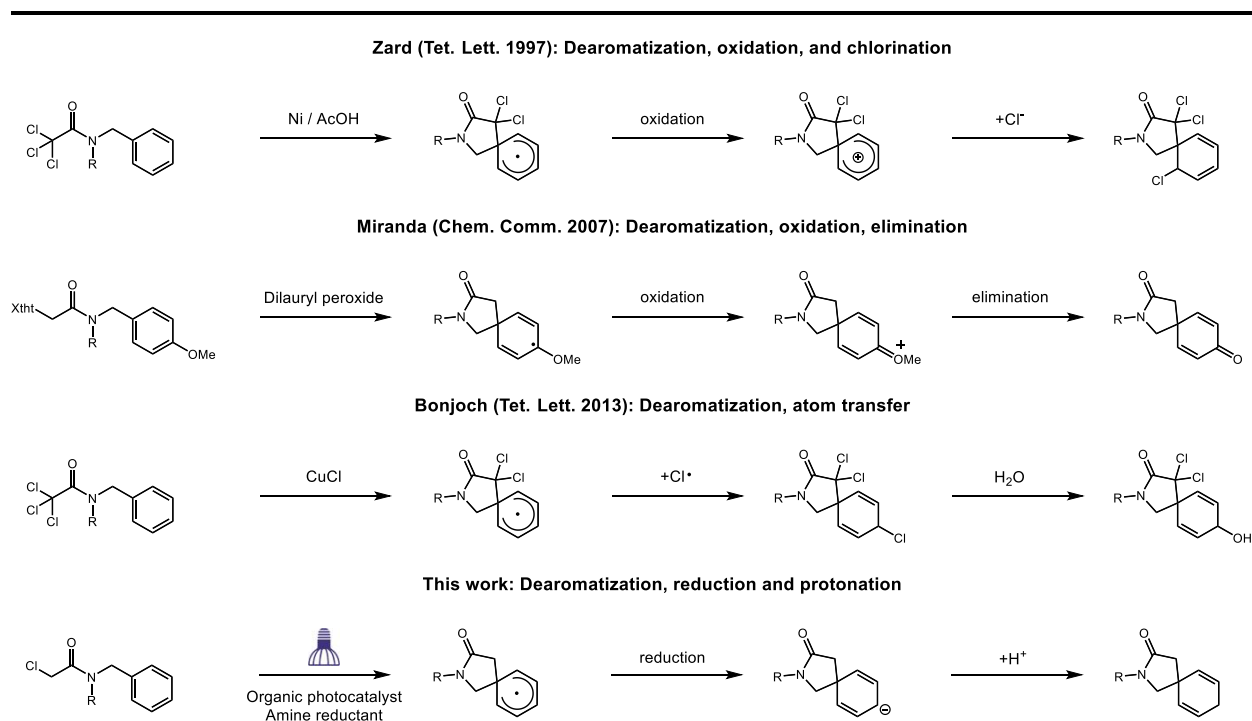


Figure 7. Dearomatization by ipso-radical spirocyclization for gamma-lactams.

In contrast, in our system, we employ a highly reducing organic photocatalyst so the cyclohexadienyl radical intermediate can undergo a second reduction, trapping the dearomatized intermediate and increasing selectivity for the 1,4-cyclohexadiene, while removing the necessity for metal catalysts or harsh reaction conditions. To evaluate the feasibility of the reaction, we employed a highly reducing catalytic system which utilizes photoredox generated alpha-acyl radicals to intramolecularly dearomatize N-benzylacetamides, followed by second reduction and protonation to afford spiro lactam products.

Results and Discussion

Initial efforts focusing on radical cyclization of benzylacetamide substrates utilized the previously developed hydroarylation conditions. Under these conditions, reductive dehalogenation and radical cyclization of a bromodifluoroacetamide gave intermediate **3** (Figure 8). From this intermediate, the desired pathway is radical polar crossover and protonation to furnish dearomatized product **5**. Unfortunately, we found the catalytic reductant competitively reduced the substrate rather than the dienyl radical intermediate leading to dienyl radical buildup and radical-radical coupling to form dimer **7** in 80% yield. Similar results were shown from a trichloroacetamide substrate, which also outcompeted the cyclohexadienyl radical for reduction. In order to prevent dimer formation, the rate of the dienyl radical reduction must be greater than the rate of the dehalogenation reduction. We hypothesized that switching to a substrate with a higher reduction potential such as a chloroacetamide, would increase the rate of the second reduction relative to that of the first, preventing dimerization. Initial cyclization attempts with the chloroacetamide led to product **5** in a 22% yield. However, the less electrophilic CH₂ radical also had a decreased rate of cyclization, resulting in a hydrodehalogenation (HDH) byproduct **6** in 66% yield.

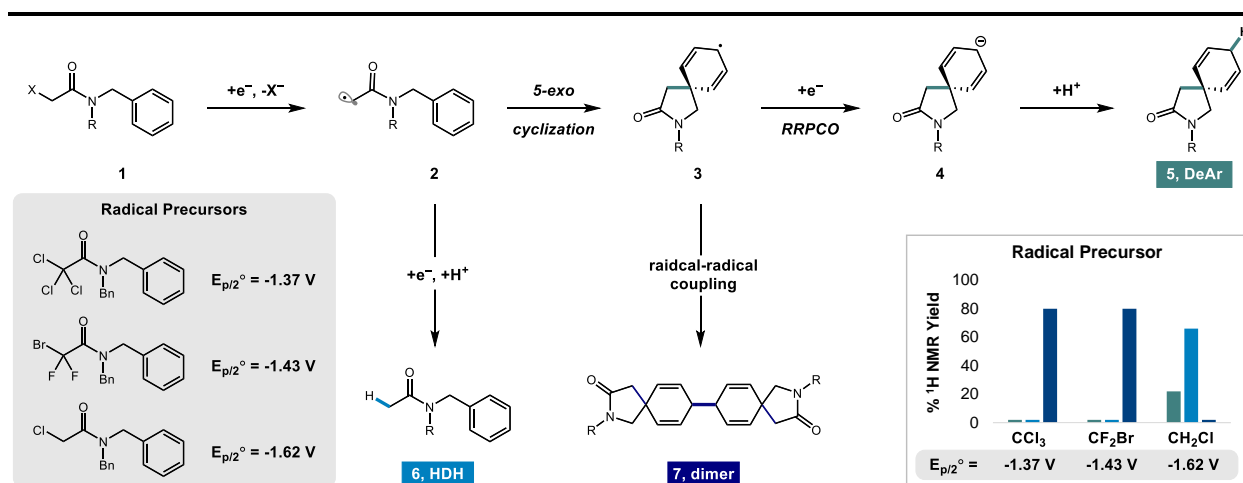


Figure 8. Radical precursors and radical-radical coupling for dimer formation.

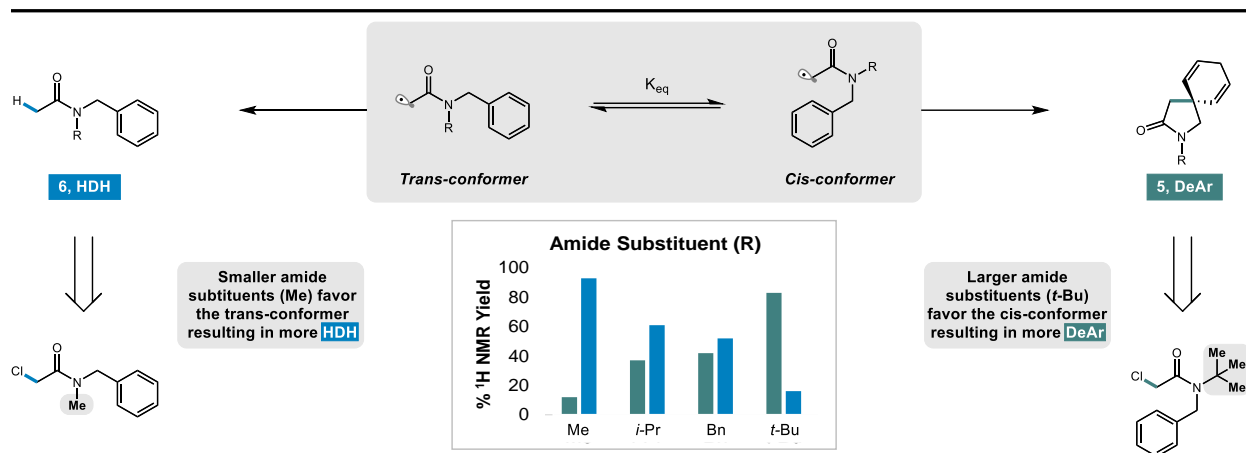


Figure 9. Amide substituent effect on cyclization.

Consistent with dearomative cyclization of benzylacetamides from the Zard lab,¹⁷ the steric properties of the amide substituent affected the efficiency of cyclization relative to HDH production. The amide substituent effects on cyclization were observed by making a range of substrates with varying substituent sizes including methyl, isopropyl, benzyl, and tert-butyl. The results are shown in Figure 9. The highest product yields were obtained from substrates with bulkier amide substituents. As the size of the amide substituent increases, the rotamer equilibrium shifts from favoring the benzyl group in the *trans* position to the *cis* position. In the *cis* conformation, the alpha-acyl radical is located closer to the arene, increasing cyclization relative to HDH. Optimization was carried forward using the tert-butyl substrate, which gave 62% product formation and 34% HDH.

After determining the optimal radical precursor and amide substituent, reaction conditions were optimized. Employing different photocatalysts with varying ground state reduction potentials showed that 3DPAFIPN (3DPAFIPN^{•-}, $E_{1/2}^{\circ} = -1.59$ V vs SCE) was the best catalyst for the reduction. The more strongly reducing photocatalyst 3DPA2FBN (3DPA2FBN^{•-}, $E_{1/2}^{\circ} = -1.92$ V vs SCE) had a high enough reduction potential to increase the rate of substrate reduction relative to that of the dienyl radical intermediate, resulting in 44% dimer formation, while 4CzIPN (4CzIPN^{•-}, $E_{1/2}^{\circ} = -1.24$ V vs SCE) had too low of a reduction potential, resulting in 78% returned

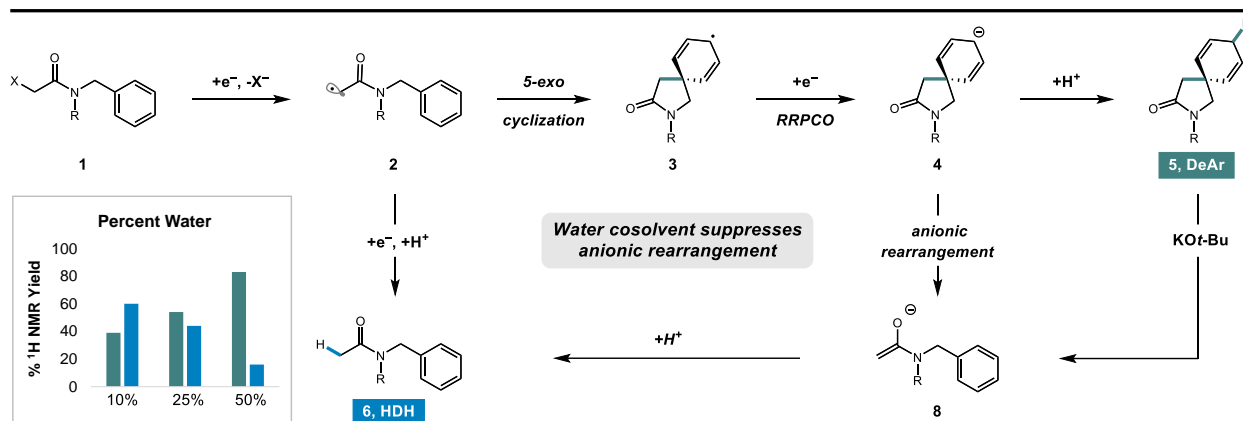


Figure 10. Proposed hydroalkylation mechanism, undesired HDH pathways, and effect of water on HDH formation.

starting material. The effects of the reaction concentration were then considered. The results showed that increasing the concentration decreased the ratio of product to HDH. This is consistent with lower reaction concentrations typically favoring intramolecular reactivity, such as cyclization. As the concentration was increased above 0.05 M, more HDH byproduct was formed.

We found that adding base to the cyclized product resulted in deprotonation of the diallylic proton and anionic rearrangement, resulting in HDH formation, as shown in Figure 10. Therefore, it is expected that the same anionic rearrangement can occur from the intermediate anion **4** during product formation, especially since the reaction takes place in a basic environment due to the amine reductant. To suppress this undesired reaction pathway, the concentration of water was adjusted. Increasing the water concentration to 50% $H_2O/MeCN$ increased the rate of protonation and suppressed anionic rearrangement, resulting in 74% product formation. Finally, increasing the temperature to $50^\circ C$ resulted in 82% product yield with HDH as the only byproduct. Control reactions were carried out to show that the photocatalyst, amine reductant, and blue light were all required for the reaction to take place.

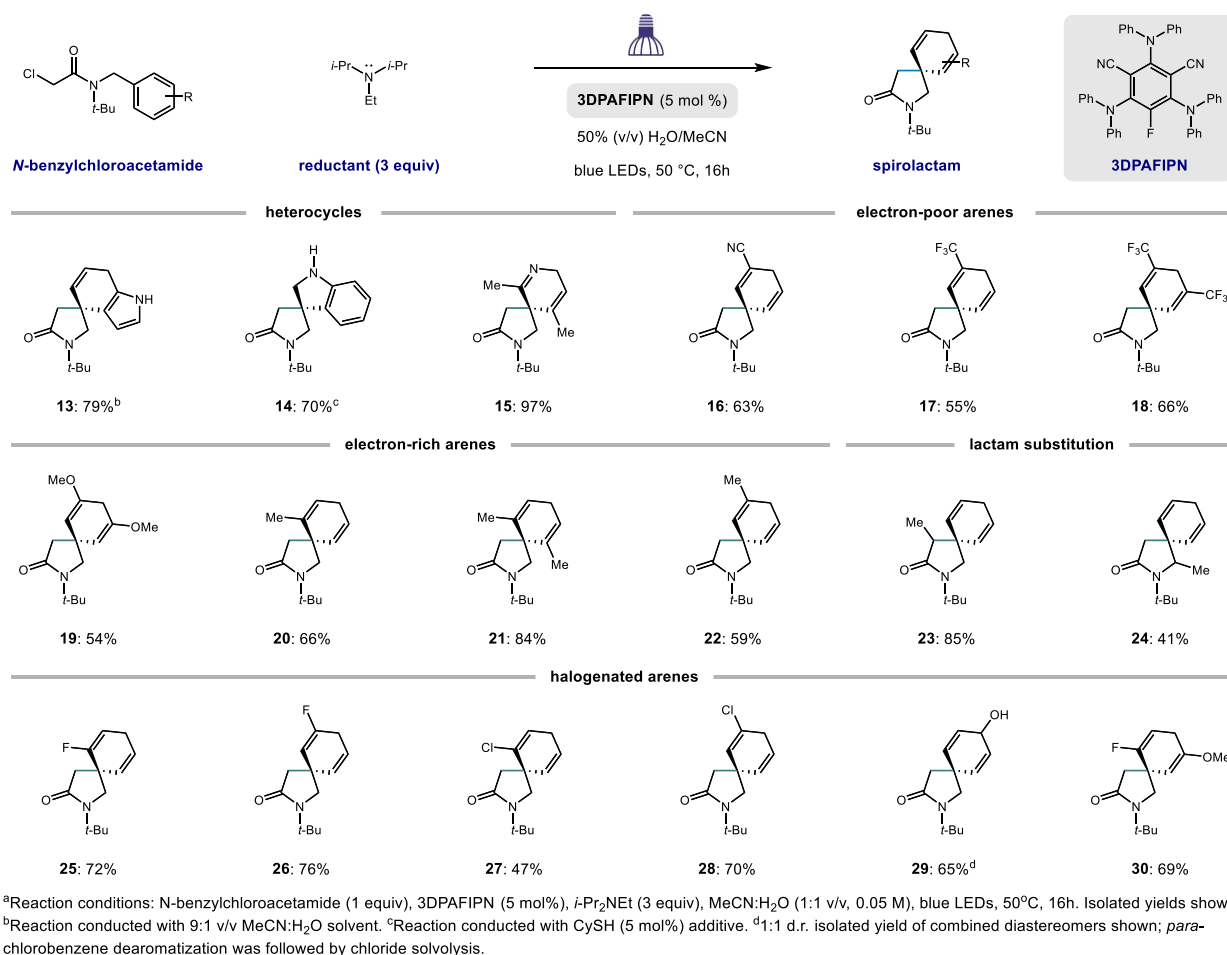
Table 1. Reaction Condition Optimization for Dearomatized Spirocyclic Lactam

Entry	PC	Concentration	Temperature	% water	9	10	11, HDH	12, Dimer	
1	3DPAFIPN	0.05 M	23 °C	50%	-	74	25	-	
2	3DPA2FBN	0.05 M	23 °C	50%	-	29	14	44	
3	4CzIPN	0.05 M	23 °C	50%	78	16	7	-	
4	3DPAFIPN	0.1 M	23 °C	50%	-	67	31	-	
5	3DPAFIPN	0.05 M	50 °C	50%	-	83	18	-	optimized conditions
6	3DPAFIPN	0.05 M	50 °C	0%	-	42	57	-	
7	3DPAFIPN	0.05 M	50 °C	10%	-	39	60	-	
8	3DPAFIPN	0.05 M	50 °C	25%	-	54	44	-	
controls									
9	-	0.05 M	23 °C	25%	100	-	-	-	no PC
9	3DPAFIPN	0.05 M	23 °C	25%	97	-	-	-	no reductant
10	3DPAFIPN	0.05 M	23 °C	25%	99	-	-	-	no light

With optimized conditions in hand (Table 1), the scope of the reaction was evaluated (Table 2). The reaction was highly regioselective, as demonstrated by indole substrates, which undergo selective dearomatization at the benzene or pyrrole, resulting in products **13** (79% yield) and **14** (70% yield), respectively. Pyridine dearomatization also occurred with high efficiency, resulting in **15** (97% yield). However, the scope of pyridines was limited by the substrate synthesis due to polymerization at the acyl chloride with unhindered pyridines. Electron-poor arenes and electron rich arenes gave rise to products **16-22** in good yields (54-85% yield). Products with lactam substitution were achieved by alpha- and gamma-acyl substitution on the starting material, resulting in products **23** (85% yield) and **24** (41% yield), respectively. Ortho- and meta- halogenated substrates reacted to give the corresponding halogenated products **25-28**

and **30** (47-72% yield), while a para-chlorinated substrate reacted to give the alcohol product **29** (65% yield), likely due to hydrolysis of the diallylic chloride.

Table 2. Scope of Spirocyclic Lactam Products.



The utility of the method has been demonstrated by derivatization of the standard dearomatized product **10**, as well as derivatization of other products from the scope (Figure 11). Reacting the standard dearomatized lactam with *m*CPBA results in epoxidation of the alkenes in a diastereomeric mixture (**31**, 82% yield, 6:5:1 dr). Highly efficient conversion to a pyrrolidine was achieved by carbonyl reduction with LiAlH₄ (**32**, quant). Removal of the tert-butyl group in TFA to furnish the deprotected lactam **33** proceeds in quantitative yields. While this transformation

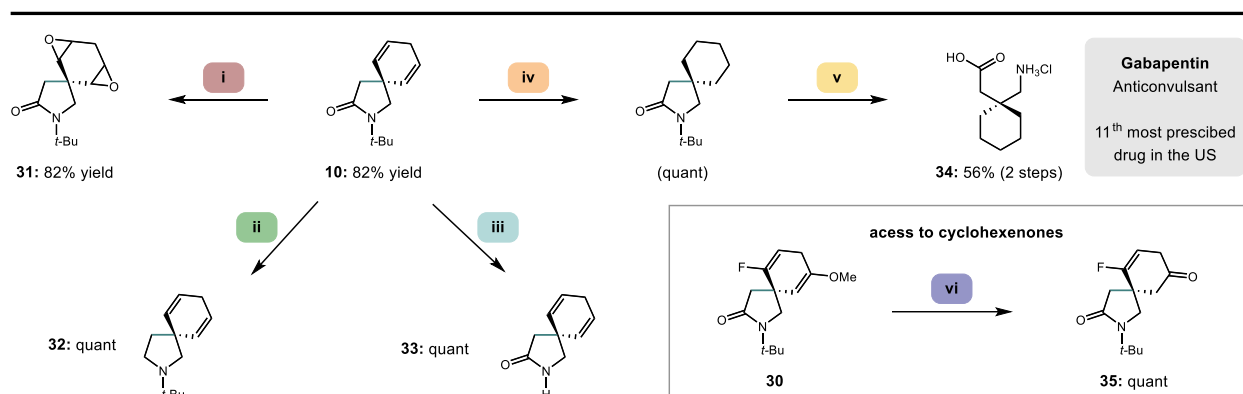


Figure 11. Lactam derivatization. Conditions: (i) *m*CPBA, CH₂Cl₂, 16h; (ii) LiAlH₄ (2 equiv), THF, 16h; (iii) TFA, 150°C, 16h; (iv) H₂, Pd/C, MeOH; (v) HCl (aq), 160°C, 16h; (vi) TFA, CH₂Cl₂, 16h.

requires high temperatures (150°C, 16 h), it is the only known example of successfully removing the tert-butyl from this scaffold while avoiding saponification of the lactam. We optimized this deprotection by first finding the strongest acid that did not result in undesired side reactions, then pushing the reaction forward with heat. Alternatively, using a cumyl protecting group in place of the tert-butyl allows for more mild deprotection conditions (TFA, 50°C). The dearomatized product was also transformed into Gabapentin, which is the most commonly prescribed anticonvulsant,²⁶ and the 11th most prescribed drug in the US.²⁷ This transformation proceeds by hydrogenation of the alkenes using catalytic Pd/C, followed by concurrent lactam deprotection and saponification in a microwave reactor (16 h, 160°C) to furnish the Gabapentin HCl salt (**34**, 56% yield). Additionally, hydrolysis of enol ethers formed from dearomatization of methoxybenzenes gave rise to cyclohexenones with excellent efficiency (**35**, quant).

The proposed catalytic cycle is shown in Figure 12. Photoexcited 3DPAFIPN is reductively quenched by Hünig's base to give 3DPAFIPN^{•-} ($E_{1/2}^{\circ} = -1.59$ V vs. SCE). This high energy ground state reductant is employed in the reductive dehalogenation of chloroacetamide, resulting in mesolytic cleavage to furnish a chloride anion and an alpha-acyl radical. This radical undergoes radical cyclization into the benzyl substituent, dearomatizing the arene and resulting in the cyclohexadienyl radical. The photoexcited catalyst is reductively quenched with another

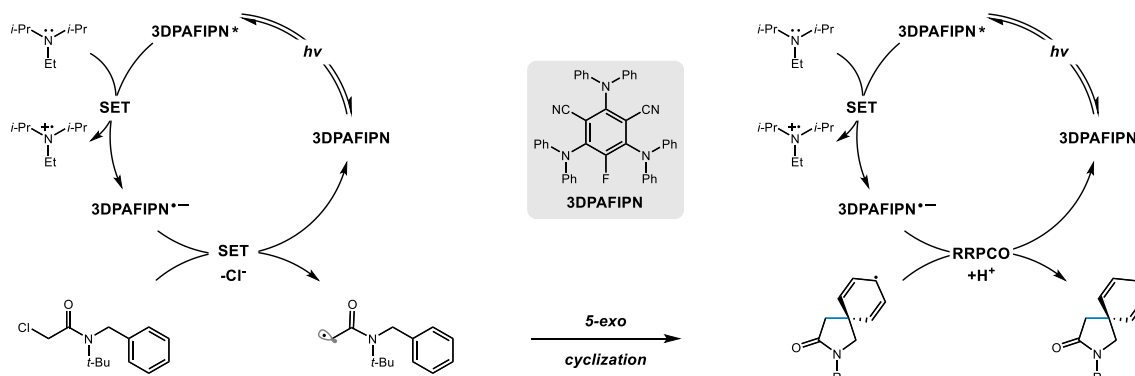


Figure 12. Proposed catalytic cycle.

equivalent of Hünig's base and is used for the second reduction of the cyclohexadienyl radical ($E_{1/2}^{\circ} = -1.40$ V vs. SCE). The resulting anion is then protonated by the aqueous solvent to furnish the dearomatized product. Replacing the water cosolvent with deuterium oxide resulted in >95% deuterium incorporation at the diallylic position, supporting the proposed reductive radical polar crossover mechanism, rather than HAT. Similarly, HDH formation showed 88% deuterium incorporation, supporting a reduction/protonation pathway.

Cyclic voltammetry (CV) experiments were conducted by Kelly McDaniel to support the proposed mechanism and are shown in Figure 13. The voltammogram of the dibenzylacetamide substrate **36** showed an irreversible reduction at $E_{p/2} = -2.12$ V vs SCE. This reduction potential was significantly greater than the expected threshold of the catalyst. However, a

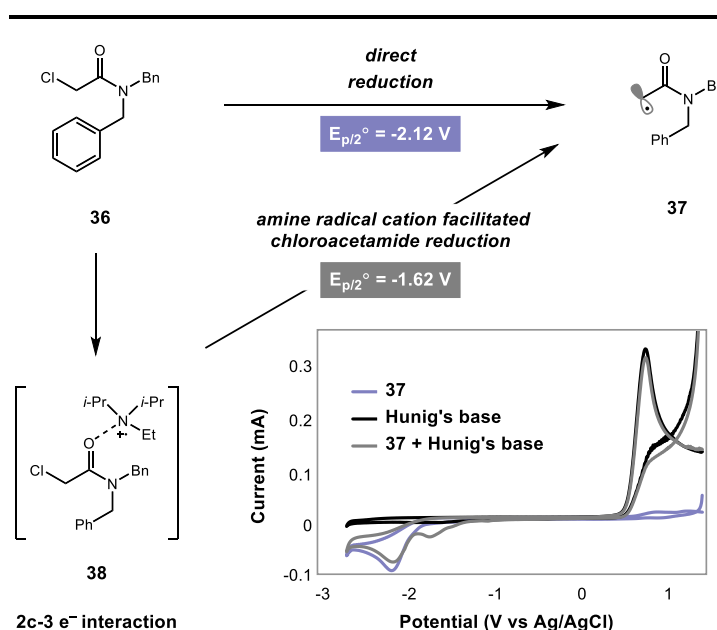


Figure 13. Cyclic voltammetry experiments.

voltammogram more representative of the reaction conditions, which included **36** in addition to **3**

equivalents of Hünig's base, showed an additional reduction at $E_{p/2} = -1.62$ V vs SCE. This reduction potential is more closely aligned to that of $3\text{DPAFIPN}^{\bullet-}$ and is a result of the amine radical cation interacting with the lone pair of the carbonyl. This interaction results in a 2-center-3-electron interaction, shown by intermediate **38**, and decreases the LUMO energy, which has been previously reported in the literature.^{28,29,30}

To gain insight into the electronic effects on the mechanism, a dibenzylchloroacetamide was made with an electron withdrawing substituent on one arene and an electron

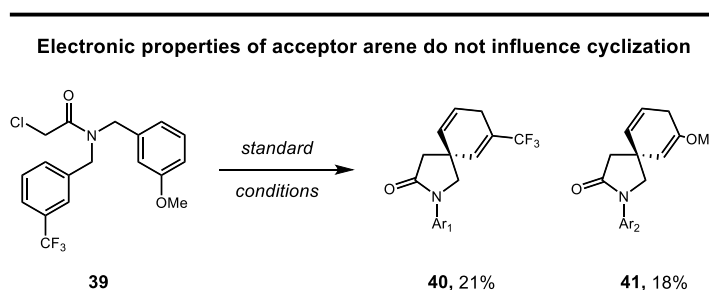


Figure 14. Electronic effects.

donating substituent on the other. Subjecting this substrate to the standard reaction conditions revealed no electronic preference for dearomatization of either ring. As shown in Figure 14, the results gave 21% dearomatization of the electron deficient ring and 18% dearomatization of the electron rich ring, with HDH byproduct accounting for the remaining mass. For this reason, it was expected that the highly efficient pyridine dearomatization (**15**, 97% yield) was attributed to the additional steric influence of the two methyl groups ortho to the position of the cyclization. Computational data was used to further investigate these steric properties.

The computational work was done by Gavin Smith using GaussView, which was used to calculate the minimized geometries of compounds and observe the steric effects of the benzyl substituents. Interatomic

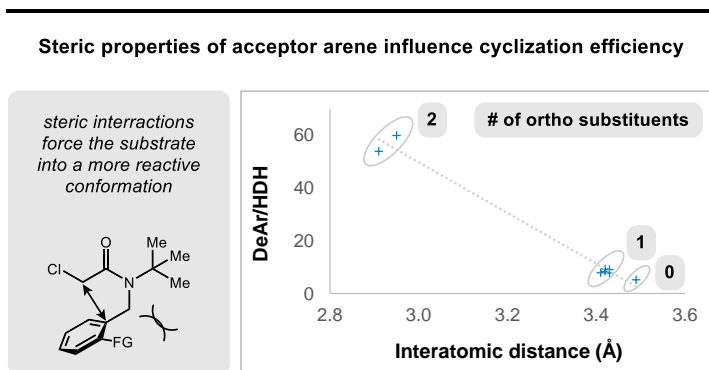


Figure 15. Steric effects.

distances between the two carbons participating in the spirocyclic bond formation were measured. The results shown in Figure 15 indicate that the ratio of dearomatized product to HDH byproduct increased as the interatomic distance between the two carbons decreased due to steric influence. The greatest product yields were seen when two ortho substituents were present, followed by one ortho substituent, and finally no ortho substituents.

Conclusion and Future Work

A simple and efficient method for intramolecular dearomatization by alkyl radical cyclization has been developed. A strong organic photocatalyst/stoichiometric amine reductant system is employed for the net reductive process. The mechanistic studies shown here indicate that the generated amine radical cation interacts with the carbonyl to promote the reductive dehalogenation. Additionally, the results support a reductive radical polar crossover mechanism by means of reduction and protonation to afford a 1,4-cyclohexadiene. Based on experimental results and computational data, the cyclization depends less on the electronic properties of the arene and more on steric influence of the amide or arene substituents.

While the reaction is tolerant of a range of functional groups, we are interested in evaluating extended aromatic systems such as naphthalene to determine if these groups would result in 2-hydronaphthalene systems from reduction of the linked arene, while maintaining aromaticity in the fused ring, or 6-hydronaphthalene systems from propagated dearomatization of both rings, as shown in Figure 16.

Additional future work is based on nitrogen- and oxygen-centered radicals, which are great candidates for dearomative cyclization based on their highly electrophilic character, providing them with the potential for cyclization to form [6.5.0] and [6.6.0] spirocyclic scaffolds. The Knowles lab has previously published a method for 5-

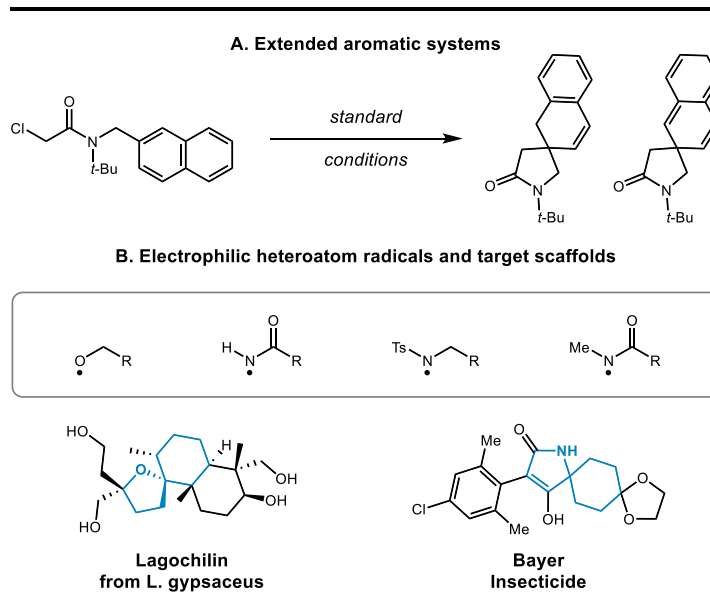


Figure 16. Future work.

exo-cyclization of oxygen centered radicals onto alkenes,³¹ providing promising preliminary data for heteroatom-based radical cyclization onto arenes. Methods for direct homolytic photoactivation of amides, amines, and alcohols to their corresponding heteroatom-based radicals have been reported,^{22,32} so the focus will be activating these radicals for dearomative cyclization onto arenes and heteroarenes.

Lipophilic Tenofovir Prodrugs

Introduction

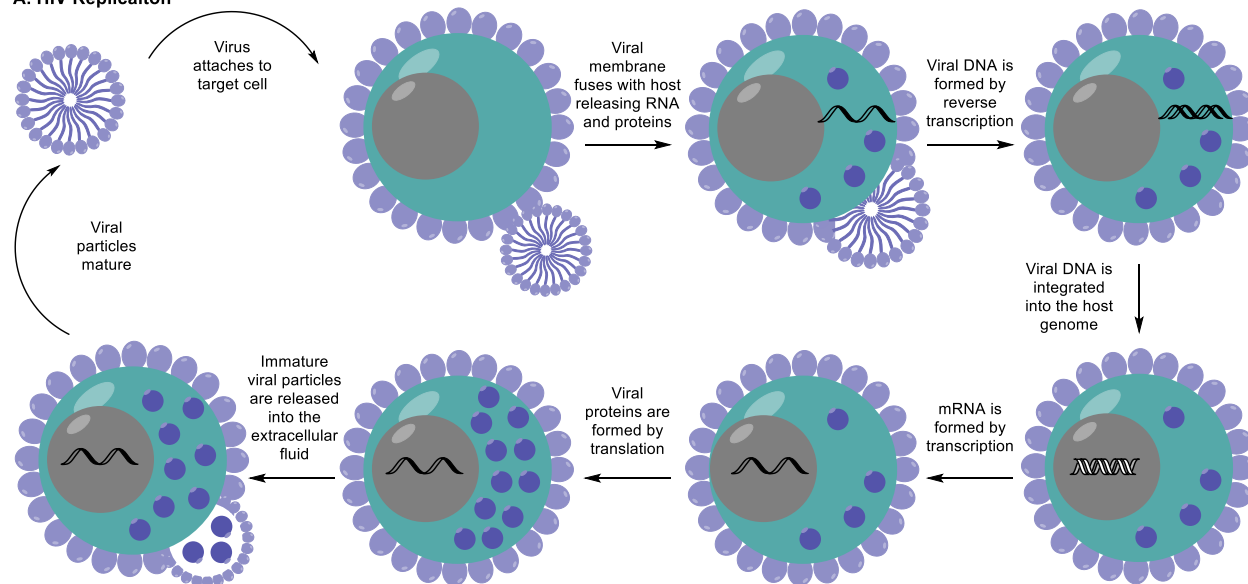
Human immunodeficiency virus (HIV), which can progress to acquired immunodeficiency syndrome (AIDS), weakens the immune system and makes people more susceptible to infection. Last year, an estimated 680 thousand people died from HIV and 1.5 million people acquired it.³³ HIV is a major public health issue, and currently has no cure. While medications have been developed to prevent and treat HIV, further research is necessary to provide safe, reliable, and effective treatment.

The process of HIV replication is illustrated in Figure 17A. When viruses, such as HIV, infect a cell, the viral membrane fuses with the host membrane and releases viral RNA and proteins into the cell. The viral RNA is then converted into viral DNA by reverse transcription, facilitated by the viral enzyme reverse transcriptase.³⁴ The newly formed viral DNA is then integrated into the host genome by another viral enzyme, integrase. HIV and other viruses then use the infected host cells to replicate. They do this by taking advantage of the host cells natural biological mechanisms, transcription and translation. The DNA in the genome of a cell's nucleus undergoes transcription to form messenger RNA (mRNA), which is transported from the nucleus to the cytoplasm, and translated to form proteins. These viral proteins then associate with the host membrane, along with newly transcribed RNA, to form immature viral particles. After leaving the host cell, the new viral particles can infect other cells.³⁵

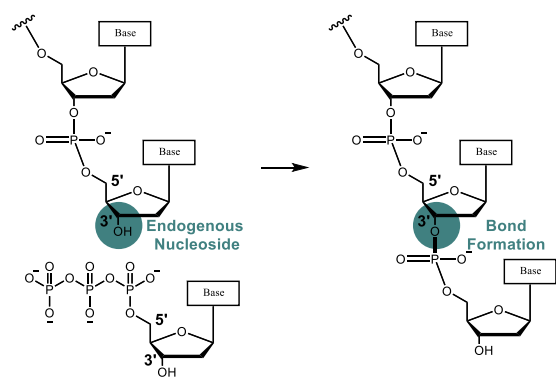
The basic components of the DNA and RNA required for elongation are nucleosides, which are typically comprised of a purine or pyrimidine base, connected to a ribose or deoxyribose sugar. The nucleosides undergo phosphorylation on the 5' alcohol of the sugar to form nucleotides

(nucleoside monophosphates), which undergo two additional phosphorylation events to form nucleoside triphosphates. Nucleoside triphosphates are incorporated into the growing DNA and RNA strands during reverse transcription, and transcription, respectively. The incoming

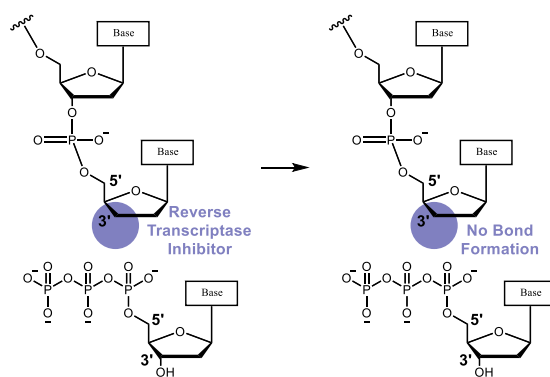
A. HIV Replication



B. Phosphodiester Bond Formation with Endogenous Nucleotides



C. Prevention of Bond Formation with Reverse Transcriptase Inhibitors



D. Reverse Transcriptase Inhibition

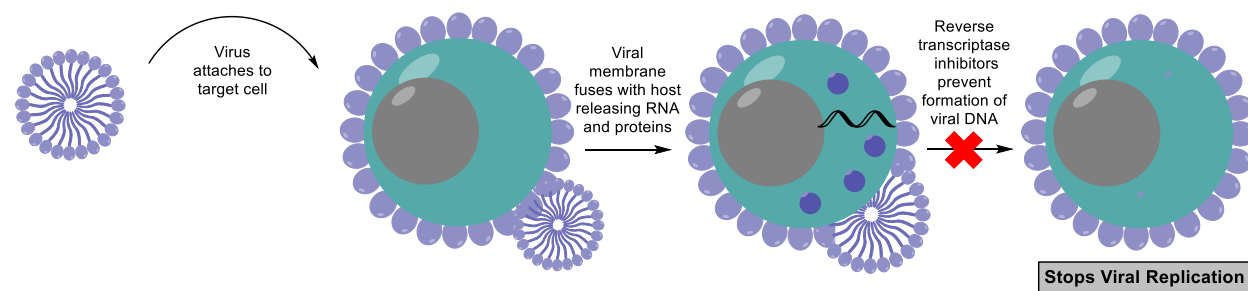


Figure 17. A. Steps of viral replication. B. Phosphodiester Bond Formation with Endogenous Nucleotides. C. Prevention of bond formation with reverse transcriptase inhibitors. D. Prevention of viral replication by use of reverse transcriptase inhibitors.

nucleoside triphosphates form phosphodiester bonds between the 3' alcohol of the sugar on the growing DNA and RNA chains and the 5' phosphate of the incoming nucleoside triphosphate (Figure 17B).

Nucleoside reverse transcriptase inhibitors (NRTIs) and nucleotide reverse transcriptase inhibitors (NtRTIs) have been developed to terminate chain elongation due to lack of a 3' hydroxyl group (Figure 17C).³⁶ When these inhibitor analogues add into the chain in place of endogenous nucleotides, the next incoming nucleoside triphosphate cannot form the phosphodiester bond required for chain elongation. This interferes with reverse transcription of viral RNA to viral DNA, consequently preventing transcription and ultimately translation, inhibiting formation of viral proteins and viral replication, as shown in Figure 17D.^{37,38}

Similar to endogenous nucleosides, NRTIs and NtRTIs undergo three or two intracellular phosphorylation events, respectively to form the active triphosphates,³⁹ which can then be incorporated into the growing viral DNA strand by reverse transcriptase. A major advantage of NtRTIs compared to NRTIs is the phosphonate linkage. The permanently affixed phosphonate permits bypassing the initial phosphorylation step, which is the rate-limiting step for most NRTIs.⁴⁰ This allows the NtRTI analogues to outcompete endogenous nucleotides to form the corresponding active triphosphates and add into the elongating DNA strand.⁴¹ Additionally, the use of a phosphonate linkage in place of an endogenous phosphate linkage (phosphorous-carbon bond rather than a phosphorous-oxygen bond) prevents esterase hydrolysis to the nucleoside.⁴²

Although these inhibitors terminate chain elongation and prevent viral replication, they have limitations. They require daily administration, which is impractical in areas that don't have easy access to health care. Additionally, they lead to drug resistance and toxicity,^{43,44,45} which is amplified with chronic use.³⁶ In addition, the persistent phosphonate on NtRTIs results in dianionic

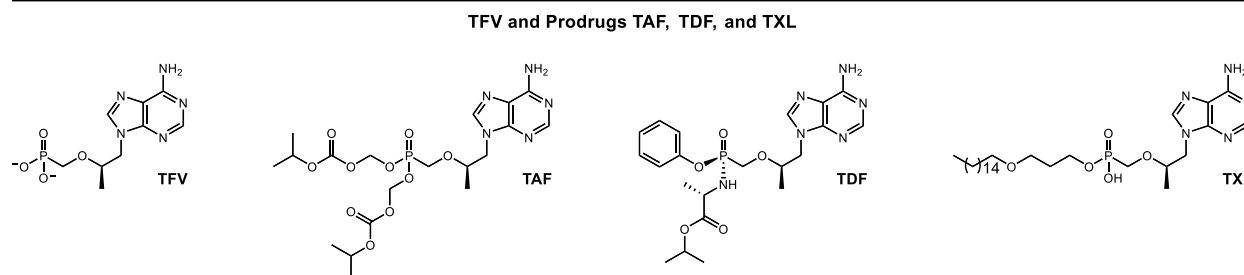


Figure 18. Structures of TFV and its lipophilic prodrugs TAF, TDF, and TXL.

character at physiological pH, causing low oral bioavailability, poor cell permeability, and increased nephrotoxicity due to restricted diffusion across the plasma membrane and accumulation in the kidneys.⁴⁶ In order to improve upon these drawbacks Tenofvir (TFV), which is a common NtRTI used in HIV treatment, is administered in the form of prodrugs.

TFV prodrugs have been developed in order to improve bioavailability, cell permeability, and safety.⁴⁷ This is accomplished by masking the dianionic phosphonate to form a neutral compound. Two FDA-approved TFV prodrugs used in most HIV treatments include Tenofvir Disoproxil Fumarate (TDF),⁴⁸ and Tenofvir Alafenamide (TAF).⁴⁹ A third TFV prodrug is Tenofvir Exalidex (TXL),⁵⁰ however, this one has not yet been approved by the FDA. The structure of TFV and these three common prodrugs are shown in Figure 18.

TDF uses two isopropylloxymethyl carbonates to esterify the phosphonate and mask the dianionic character and is prepared as the fumarate salt. Once TDF enters the target tissues, esterases cleave the carbonates to release TFV,⁵¹ which can then be converted to its active triphosphate form. Compared to TFV, TDF has shown improved cell permeability and anti-HIV activity *in vitro*.⁵² However, the high presence of esterases in other organs and tissue, such as the liver and the plasma, cause the phosphodiester to break down extracellularly and release TFV prematurely.⁴⁸ With chronic treatment, hepatic cleavage can damage the liver,⁴³ and cleavage in plasma can cause toxicity in the bones and kidneys.^{44,53}

TAF is an isopropylalaninyl phenyl ester prodrug of TFV. This structural difference removes the phosphoesters and eliminates the hydrolysis by esterases. Instead, TAF is cleaved to TFV by cathepsin A, which is a protease localized in lysosomes.⁵⁴ While TAF does result in improved safety due to its increased stability in the plasma, most of it is cleaved by carboxylesterase 1⁵⁵ and extracted by the liver.⁵⁶ It has been demonstrated in dogs that only 18% of the drug is available to access HIV infected target cells after undesired metabolism.⁵⁷

TXL is a lipid prodrug of TFV that is cleaved intracellularly by phospholipase C (PLC),⁵⁸ however, it is also largely extracted by the liver. Distinct from the hepatic cleavage of TDF and TAF, TXL undergoes ω -oxidation in the liver by cytochrome P450 (CYP) at the

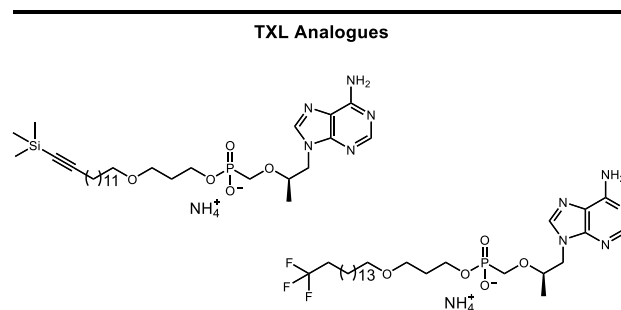
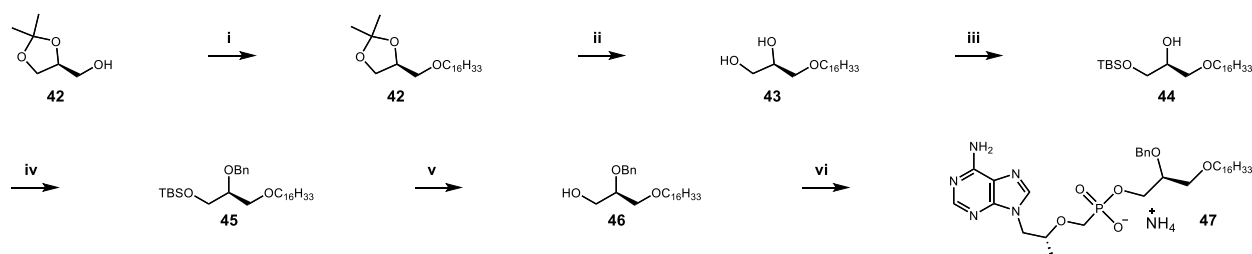


Figure 19. TXL analogues with stable terminal motifs.

terminal methyl group of the lipid which is then broken down by β -oxidase to ultimately release TFV.⁵⁹ In order to bypass this CYP mediated oxidation and cleavage, TXL analogues (Figure 19) were developed by replacing the terminal methyl group with stable motifs.⁶⁰ This decreased hepatic metabolism, which thereby creates potential for increased drug availability to reach infected cells.

While these TXL analogues decreased hepatic metabolism of TFV prodrugs, undesired metabolism could be further decreased by entering lipoproteins and being shuttled directly into systemic circulation through the lymphatic system, bypassing the liver.⁶¹ When a drug is administered orally, it goes through the small intestine and then enters either the portal vein, or the lymphatic system depending on the size and solubility of the drug.^{62,63} Small, soluble drugs enter the portal vein and are transported to the liver, where they can be metabolized by enzymes. After

Synthesis of 2-Benzyloxy Glycerol TFV Prodrugs



Scheme 1. Conditions: i) alkyl bromide (3 equiv), TBAB (0.1 equiv), THF:50% NaOH (1:1), reflux. ii) AcOH:H₂O, rt. iii) TBSCl (1.4 equiv), TEA (1.4 equiv), DMAP (0.05 equiv), DCM, rt. iv) NaH (1.25 equiv), benzyl bromide (1.25 equiv), THF, 0°C to rt. v) HF-pyridine (6 equiv), THF:pyridine, rt. vi) TFV, DCC (1.6 equiv), DMAP (0.1 equiv), NMP, 100°C

dioxolane methanol (**42**). The primary alcohol was alkylated with the 16-atom carbon chain, which is implemented to increase cell permeability. The dioxolane component was then deprotected to open up into a glycerol backbone. The newly formed primary alcohol was protected with a *tert*-butyl dimethyl silyl (TBS) group and the secondary alcohol was equipped with the benzyl group. The TBS group was then deprotected and the resulting primary alcohol was coupled with TFV to form the TXL analogue with the benzyl group on carbon-2 of the glycerol backbone (**47**).

Additionally, our group recently developed a TXL prodrug analogue with an oxyethyl linker (Figure 21, middle), rather than an oxypropyl linker. The oxyethyl linked compound (IC₅₀ value of 3 nM), was shown to be more active than the oxypropyl linked compound, TXL (IC₅₀ value of 18 nM), with a 6-fold difference in potency. Since the glycerol analogue with the benzyloxy group on carbon-2 resembles the oxypropyl linker with a benzyloxy substituent, we propose that forming a hybrid compound with the benzyloxy group on carbon-3 will further increase activity by incorporating

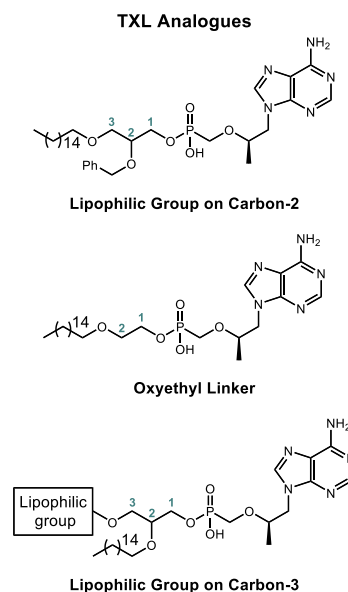


Figure 21. Structure of TXL preliminary analogues and target analogues.

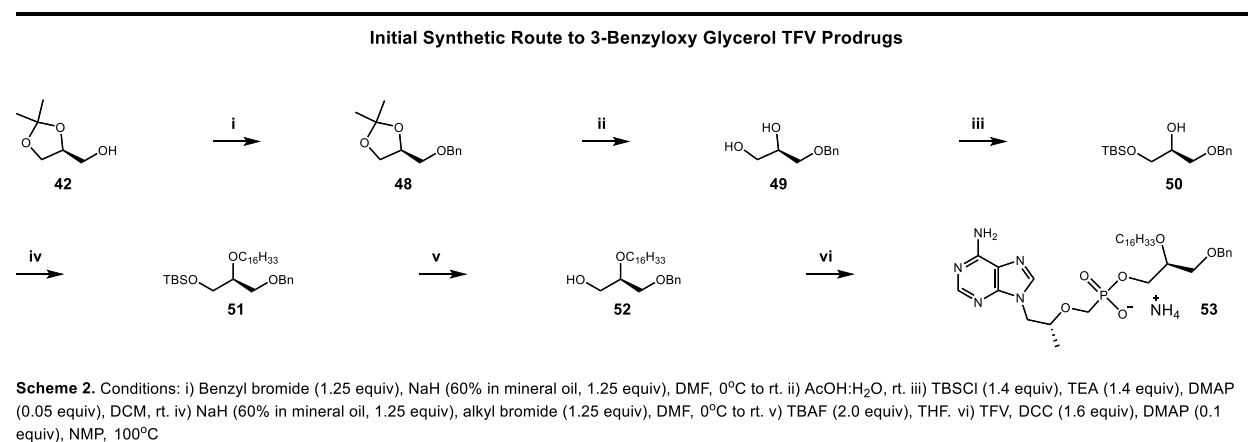
properties of the oxyethyl linked analogue. Switching the carbon chain to the carbon-2 position of glycerol and switching the benzyloxy group to the carbon-3 position of glycerol will achieve this structural design (Figure 21, bottom).

Our goal is to develop TXL analogues with increased lipophilicity to encourage association with chylomicrons, in addition to the lipophilic carbon chain to increase cell permeability. The chylomicron association will allow the prodrug to bypass first-pass metabolism by increased transport into systemic circulation through the lymphatic system. Here, we develop a TXL prodrug analogue with a glycerol backbone that incorporates the carbon chain on carbon-2 of glycerol to take advantage of the potent activity observed with the oxyethyl linker analogue with an IC_{50} value of 3 nm, and additional lipophilic groups such as the benzyloxy on carbon-3 of the glycerol to take advantage of the distribution profile observed with the benzyloxy analogues of CDV, with increased transport to the lungs and decreased transport to the liver.

Results and Discussion

The benzyloxy substituted TXL analogue was selected to be our initial target analogue based off the previous work of Hostetler et. al., which showed that increased lipophilicity due to the presence of the benzyloxy motif had a significant effect on the distribution of the drug. In the absence of this benzyloxy motif, the drug was primarily delivered to the liver. In contrast, by addition of the benzyloxy group, transport to the liver was decreased and rather had increased transport to the lungs. Additionally, based on the previous data gathered on the oxyethyl linked prodrug analogue, which demonstrated significantly increased potency compared to the standard TXL analogue that contains an oxypropyl linker, the glycerol component was designed to be equipped with the carbon chain on carbon-2 and the added lipophilic group on carbon-3 (Figure 21, bottom).

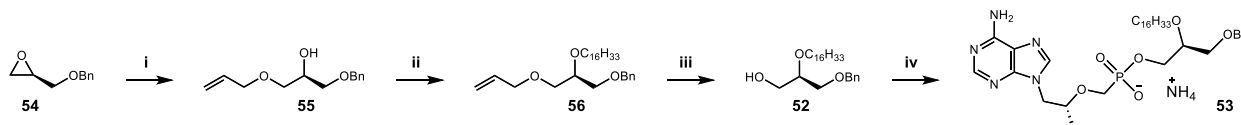
Initially, the synthetic route for the 3-benzyloxy glycerol TFV prodrugs was designed to correspond to the synthetic route for the 2-benzyloxy glycerol TFV prodrugs, as illustrated in Scheme 2. However, several complications arose, which led to the design of a novel synthetic route. The initial strategy started with the dimethyl dioxolane methanol (**42**), similar to the preceding synthesis, and equipped the free primary alcohol with a benzyl group, followed by dioxolane deprotection to open to a benzyl substituted glycerol backbone. We then attempted to



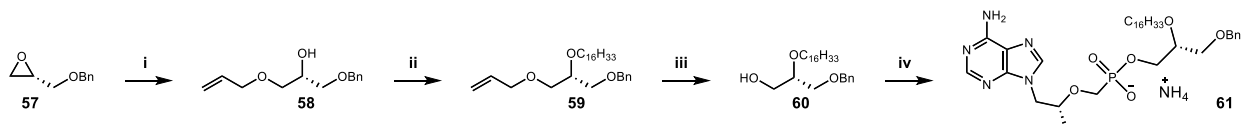
protect the newly formed primary alcohol with a TBS group followed by alkylation of the free secondary alcohol with alkyl bromide, and TBS deprotection with *tetra-N*-butylammonium fluoride (TBAF) to form the desired coupling agent (**52**) to be coupled with TFV. However, this resulted in partial silane rearrangement at steps iii and iv, resulting in both the desired intermediates, in addition to side products with the TBS group on carbon-2 of the glycerol backbone, which significantly decreased the yields at both steps.

The novel synthetic route shown in Scheme 3 bypasses these undesired side reactions by making use of an epoxide starting material and etherification to produce the desired glycerol backbone. The synthesis begins with a chiral glycidyl benzyl ether (**54**, **57**). The epoxide is opened with an allyl alcohol by an SN2 mechanism at the more substituted position to form a chiral secondary alcohol (**55**, **58**). This forms the benzyl substituted triglyceride backbone with an allyl protecting group on the primary alcohol. The secondary alcohol is then alkylated with a primary alkylbromide to form the lipid chain. The allyl group is then deprotected through a palladium pi allyl complex to form the primary alcohol (**52**, **60**), which is coupled to tenofovir to form the target prodrug. Both the R and the S isomers of the standard analogue were formed with this synthesis (**53**, **61**).

A. Synthesis of ammonium (S)-3-(benzyloxy)-2-(hexadecyloxy)propyl (((R)-1-(6-amino-9H-purin-9-yl)propan-2-yl)oxy)methyl)phosphonate



B. Synthesis of ammonium (R)-3-(benzyloxy)-2-(hexadecyloxy)propyl (((R)-1-(6-amino-9H-purin-9-yl)propan-2-yl)oxy)methyl)phosphonate



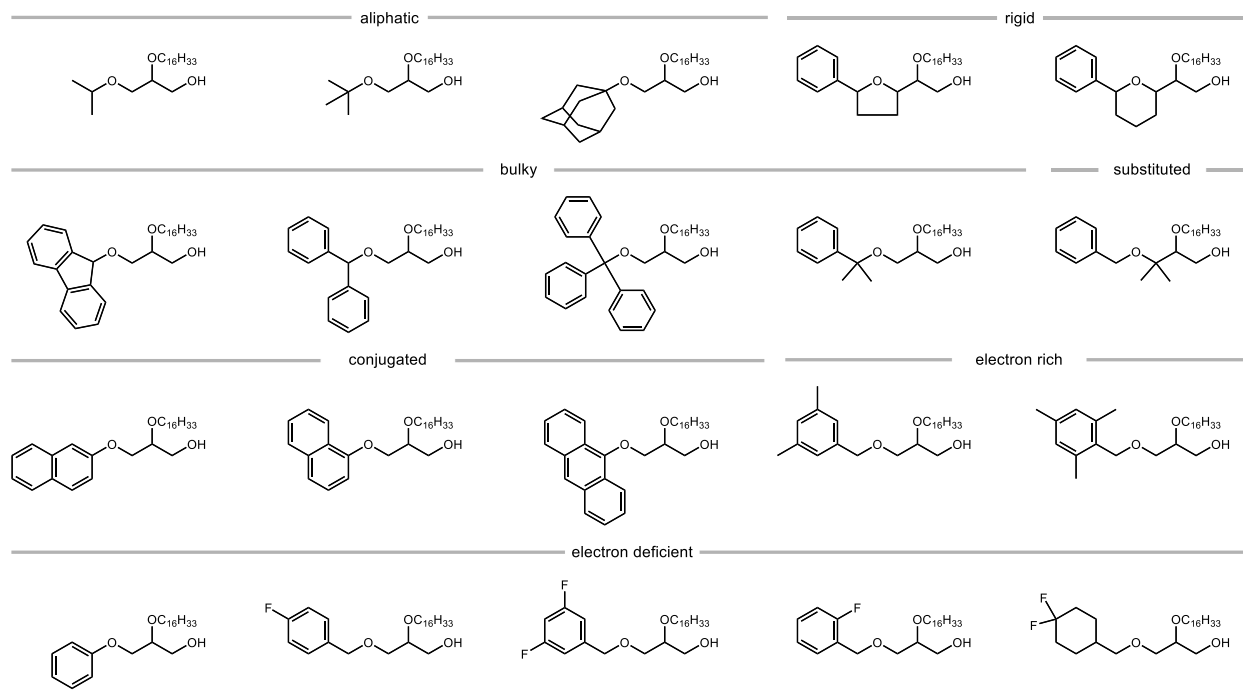
Scheme 3. A. Conditions: i) BF_3OEt_2 (0.25 equiv), allyl alcohol (10.0 equiv), DCM, rt (76%). ii) $\text{C}_{16}\text{H}_{33}\text{Br}$ (2 equiv), NaH (60% in mineral oil, 3.5 equiv), DMF, rt (79%). iii) $\text{Pd}(\text{PPh}_3)_4$ (0.10 equiv), K_2CO_3 (6 equiv), MeOH, 75°C (74%). iv) TFV (1.2 equiv), DCC (1.6 equiv), DMAP (0.1 equiv), NMP, 100°C (17%). B. Conditions: i) BF_3OEt_2 (0.25 equiv), allyl alcohol (10.0 equiv), DCM, rt (99%). ii) $\text{C}_{16}\text{H}_{33}\text{Br}$ (2 equiv), NaH (60% in mineral oil, 3.5 equiv), DMF, rt (55%). iii) $\text{Pd}(\text{PPh}_3)_4$ (0.10 equiv), K_2CO_3 (6 equiv), MeOH, 75°C (52%). iv) TFV (1.2 equiv), DCC (1.6 equiv), DMAP (0.1 equiv), NMP, 100°C (13%).

The analogues were then evaluated *in vitro* using a whole cell HIV assay to measure cellular toxicity and anti-HIV activity. The assay uses a mixture of the drug with human serum albumin (HSA), which is the plasma protein that is most abundant in human blood. This mimics the prodrug bound to HSA in systemic circulation. The drug must then dissociate from HSA, cross the plasma membrane of an HIV-infected cell, and generate TFV by PLC cleavage. The results show that the S isomer has an average CC₅₀ value of 134.8 μM and an average IC₅₀ value of 73 nM, whereas the R isomer has an average CC₅₀ value of 239.8 μM and an average IC₅₀ value of 297 nM. These results illustrate a preference for the S isomer since it is significantly more potent than the R isomer, whereas no significant isomeric preference was observed for the original compounds.

Switching the benzyl group with other lipophilic motifs can affect the rate and efficiency of transport through the chylomicrons, so additional motifs with varying size and lipophilicity will be synthesized and tested. Representative examples of other lipophilic analogues to be coupled to TFV are shown in Table 3. These analogues all have a primary alcohol to be coupled to TFV. Additionally, they have a 16-atom carbon chain on carbon-2 of the glycerol backbone to emulate the efficient oxyethyl linked analogue, as shown in figure 16. Finally, they have varying lipophilic groups on carbon-3 of the glycerol backbone to affect the rate and efficiency of association and transport by chylomicrons. The lipophilic components were selected with varying steric and electronic properties. Aliphatic substituents of various sizes were selected, in addition to aromatic substituents. Some analogues were designed to be rigid, while others are more flexible, and some are symmetric, while others are asymmetric. Additionally, the representative scope includes primary, secondary, and tertiary alcohols, as well as conjugated and unconjugated substituents.

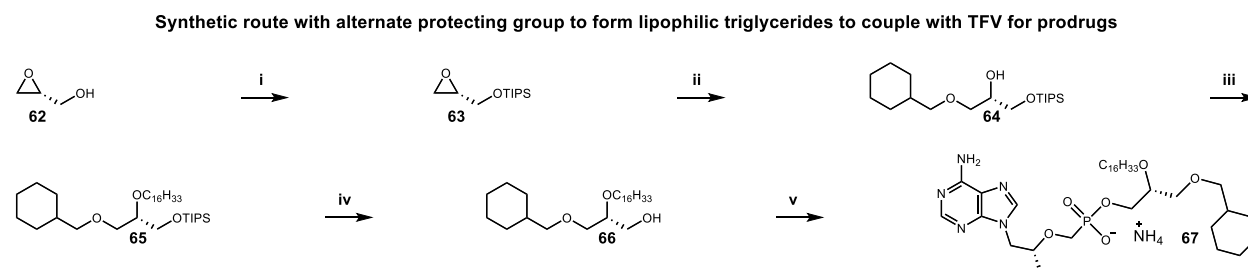
Finally, ortho- meta- and para- substituted analogues were selected with both electron rich and electron deficient rings.

Table 3. Representative examples of lipophilic analogues to be coupled to TFV.



The next target compound selected was the analogue with a cyclohexyl group in place of the benzyl group. Compared to the benzyl group, the cyclohexyl group has different steric and electronic properties because it is larger, more flexible, and saturated. However, it is still a symmetrical primary alcohol, and does not include any electron-rich or deficient substituents, such as halogens. While the standard compound has the benzyl group incorporated in the starting material, the benzyl group would not be an ideal protecting group for other derivatives because deprotection of the benzyl group would likely interfere with some of the desired functional groups. For alternate substituents, a TIPS group was used as the protecting group, which has more steric bulk than the TBS group, resulting in less silyl migration byproduct. The S isomer of the analogues were selected for preparation, in accordance with the preliminary IC₅₀ data.

These alternate analogues follow a similar synthesis to the standard benzyloxy analogues, demonstrated in Scheme 4 with a cyclohexyl substituent. Starting with a chiral glycidol (**62**), the primary alcohol is protected with a triisopropyl silane (TIPS) group. The epoxide is then opened using the desired lipophilic alcohol. This forms the TIPS protected triglyceride backbone with an ether linked lipophilic group and a free secondary alcohol, which is alkylated with a primary alkyl



Scheme 4. Conditions: i) DMAP (0.05 equiv), Imidazole (1.4 equiv), TIPSCl (1.4 equiv), DCM, 0oC - rt (42%), ii) BF₃OEt₂ (0.25 equiv), cyclohexylmethanol (10 equiv), DCM, rt (53%), iii) C₁₆H₃₃Br (2 equiv), NaH (60% in mineral oil, 3.5 equiv), DMF, rt (83%), iv) TBAF (1 M in THF, 4 equiv), THF, rt (65%), v) TFV(1.2 equiv), DCC(1.6 equiv), DMAP (0.1 equiv), NMP, 100°C.

bromide. The compound then undergoes a deprotection to remove the TIPS group, followed by coupling with TFV to form the prodrug analogue, in this case, the cyclohexyl analogue (**67**).

Conclusion and Future Work

Three TXL analogues of TFV prodrugs and the synthetic routes for derivatives have been developed. These analogues consist of a glycerol backbone with the oxygen linkers connecting TFV on carbon-1, a 16-carbon chain on carbon-2, and varying lipophilic groups on carbon-3. These analogues were designed to encourage association with chylomicrons in order to travel through lymphatic vessels and enter systemic circulation, bypassing first-pass metabolism.

After more analogues are synthesized and tested, hybrid structures will be formed by combining the properties of the compounds that have lipophilic groups with the properties of the compounds that contain metabolically stable motifs on the carbon chain, as shown in

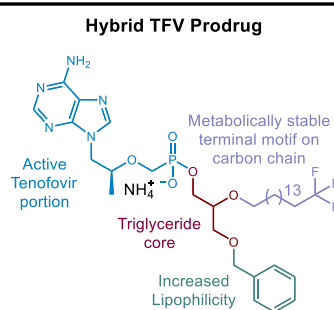


Figure 22. Example of a hybrid TFV prodrug that contains both increased lipophilicity and metabolically stable terminal motifs.

Figure 22. This is expected to cause association with chylomicrons, while decreasing degradation of the drug that is still exposed to first-pass metabolism.

Fluorodeoxyuridine Monophosphate Prodrugs

Introduction

Cancer continues to be one of the leading causes of death globally, despite constant research and improvements in cancer therapy. One large area of cancer treatment research that has been shown to be effective and commonly used in chemotherapy is the development of nucleoside analogues, similar to those used for HIV treatment, described in the previous section. These nucleoside analogues compete with endogenous nucleosides, resulting in cytotoxicity.⁶⁷ 5-Fluorouracil (5-FU) is a common chemotherapeutic nucleoside analogue used to treat a variety of cancers including liver, breast, lung, pancreatic, and most commonly, colorectal cancers.^{68,69,70,71,72}

5-FU is structurally very similar to uracil, differing only by a fluorine atom on carbon-5 of 5-FU in place of the usual hydrogen atom on carbon-5 of uracil (Figure 23). The 5-FU nucleoside can be converted in vivo to any of three active metabolites: fluorouridine triphosphate (FUTP); fluorodeoxyuridine triphosphate (FdUTP); and fluorodeoxyuridine monophosphate (FdUMP). FUTP adds into RNA, FdUTP adds into DNA, and FdUMP can undergo

Structures of Representative Nucleosides, Mono- and Triphosphates

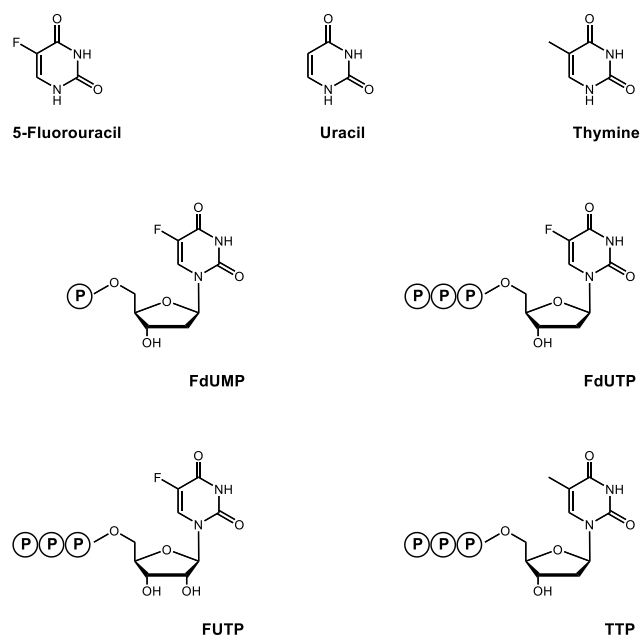


Figure 23. Structure of representative uracil, thymine, and 5-fluorouracil nucleosides, monophosphates, and triphosphates.

phosphorylation events to form FdUTP and add into DNA, or act as a thymidylate synthase (TS) inhibitor in its monophosphate form, all of which interfere with cell replication.

The accumulation of multiple misincorporations of the FUTP and FdUTP metabolites into RNA and DNA can cause destabilization, resulting in cell death. The FUTP metabolite adds into RNA in place of uridine triphosphate (UTP). Misincorporation can interfere with ribosomal RNA (rRNA) synthesis as well as post-transcriptional modification of transfer RNAs (tRNAs).^{73,74,75,76} The FdUTP metabolite adds into DNA in place of thymidine triphosphate (TTP) by acting as a competitive nucleotide substrate for DNA polymerase.⁷⁷ While these misincorporations can have positive effects of destabilization and cell death for cancerous target cells, the metabolites can also misincorporate into healthy cells, causing toxicity.

FdUMP can undergo multiple phosphorylation events to form FdUTP and be incorporated into DNA causing cell death, as described above. However, if it does not undergo the subsequent phosphorylation events, FdUMP can act as a competitive inhibitor for thymidylate synthase (TS). TS is an enzyme that catalyzes the methylation of deoxyuridine monophosphate (dUMP) to

form thymidine monophosphate (TMP) (Figure 24, top). This occurs by formation of a ternary complex of TS, dUMP, and the cofactor 5,10-methylene tetrahydrofolate (MeTHF). After complex formation, the MeTHF cofactor methylates the bound dUMP to form TMP. This reductive methylation of dUMP to TMP catalyzed by TS is the only de novo source of thymidine.⁷⁸ Additionally, TMP is required for DNA replication since thymidine is a DNA specific nucleotide precursor. This makes TS an excellent target for inhibition to cause cytotoxicity.

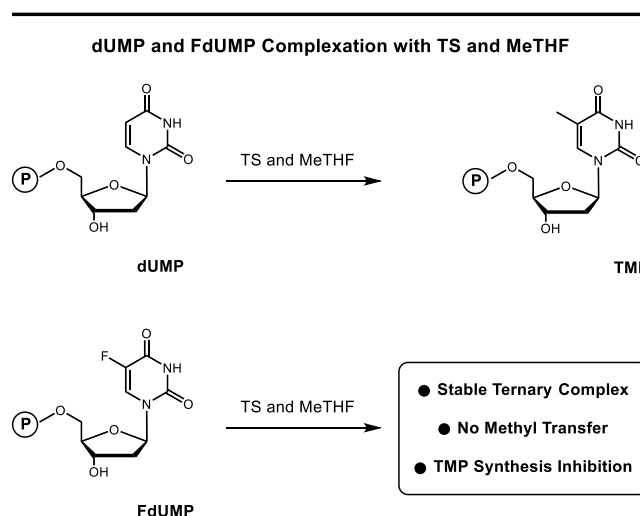
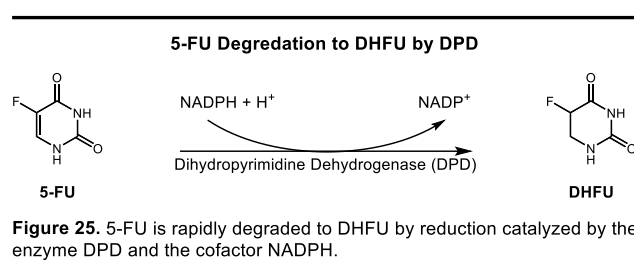


Figure 24. dUMP is converted to TMP by a methyl transfer from MeTHF cofactor, catalyzed by TS. FdUMP inhibits TMP synthesis by forming a stable ternary complex with TS and MeTHF and preventing the methyl transfer.

When FdUMP binds to TS in place of dUMP, a stable complex is formed between the enzyme, the nucleotide analogue, and the MeTHF cofactor. However, the methylation does not occur due to the tightly bound fluorine atom on carbon-5 of FdUMP. The fluorine is bound more tightly than the hydrogen on carbon-5 of dUMP due to the increased bond strength of a carbon-fluorine bond compared to a carbon-hydrogen bond, so no reaction occurs (Figure 24, bottom). However, the FdUMP binds tightly, blocking future binding of dUMP. This inhibits TMP synthesis, preventing DNA replication, and inhibiting the proliferation of tumors.⁷⁹

While 5-FU is one of the most highly prescribed chemotherapy agents, further advancements are necessary in order to improve the drug due to its current limitations.



More than 85% of 5-FU is rapidly reduced to the inactive metabolite 5,6-dihydro-5-fluorouracil (DHFU) by the enzyme dihydropyrimidine dehydrogenase (DPD) and a nicotinamide adenine dinucleotide phosphate (NADPH) cofactor (Figure 25).⁸⁰ Variable levels of DPD activity result in low and unpredictable levels of active metabolite formation,^{81,82,83} and 5-FU has a very short half-life of 10-20 minutes due to the rapid degradation.^{84,85} Additionally, variable expression of TS in tumors results in unpredictable drug response and resistance.⁸⁶

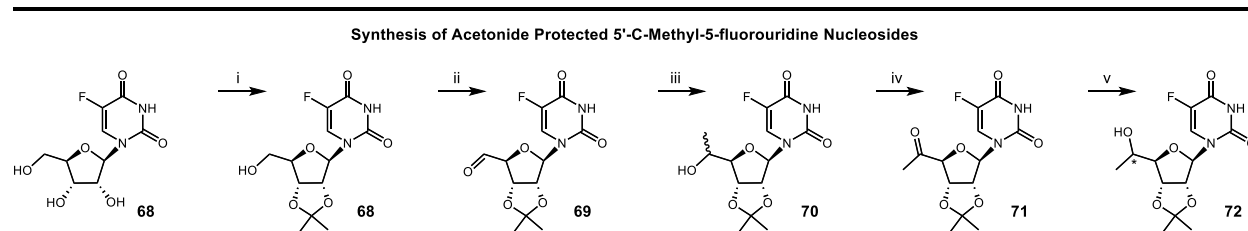
Activity of 5-FU can be improved by use of prodrugs (representative examples shown in Figure 26).⁸⁷ The 5-FU prodrug Tegafur was designed to gradually release 5-FU by cytochrome P450 metabolism.⁸⁸ While Tegafur increased the concentration and time duration of 5-FU present in the blood and tissues, it is still degraded by DPD in large amounts. UFT was then

5-FU is already in its FdUMP form. The increased concentration of FdUMP in the cells could increase TS inhibition, making the drug more active.

Since FdUMP acts as a TS inhibitor while the nucleoside triphosphates misincorporate into RNA and DNA, TS inhibition could also be increased by inhibiting subsequent phosphorylation events that convert FdUMP to nucleoside triphosphate

metabolites. In a recent study, novel nucleosides with 5'-C-methyl substitutions were synthesized (Figure 27, left) in an attempt to reduce nucleotidase activity and increase intracellular concentrations of nucleoside triphosphates.⁸⁹ However, it was found that steric bulk on the 5'-carbon of phosphoester prodrugs interfere with kinases that catalyze di- and triphosphorylation events. Therefore this 5'-C-methyl steric bulk can be used in FdUMP prodrugs to decrease di- and triphosphorylations and target TS inhibition with the FdUMP metabolite.

The synthesis of 5'-C-methyl-5-fluorouridine nucleosides are illustrated in Scheme 5. The synthesis begins with commercially available 5-fluorouridine (**68**), which is first protected to its acetone. The free 5' primary alcohol is then oxidized to an aldehyde with 2-iodobenzoic acid (IBX). The aldehyde undergoes methylation by a Grignard reaction to form a diastereomeric mixture of the secondary alcohol (**70**). IBX oxidation is then used to form the methyl ketone,



Scheme 5. Synthesis of 5'-methyl-5-fluorouridine derivatives. Conditions: (i) Acetone, cat. H_2SO_4 , reflux; (ii) IBX, CH_3CN , 85°C; (iii) CH_3MgBr (3 M in Et_2O), -78°C; (iv) IBX, CH_3CN , 80°C; (v) $\text{RuCl}(\text{p-cymene})[(\text{R},\text{R})\text{-TsDPEN}]$, HCO_2Na , H_2O , EtOAc , rt.

Prodrugs Affecting Phosphorylation and Metabolic Stability

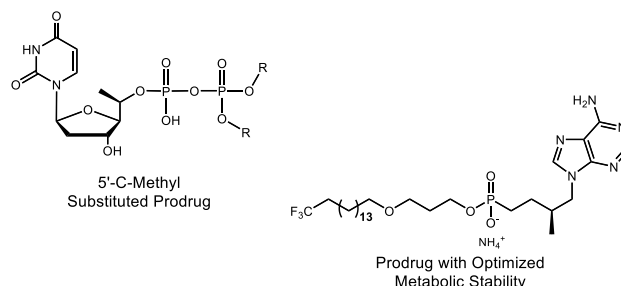
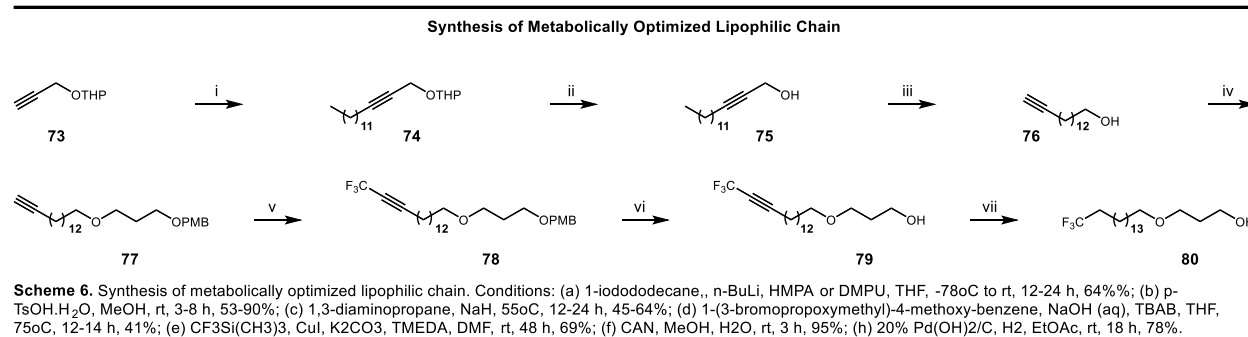


Figure 27. Prodrug with 5'-C-methyl substituent to increase steric bulk and interfere with phosphorylations and prodrug with optimized metabolic stability.

followed by stereoselective reduction with Noyori's asymmetric transfer hydrogenation using a ruthenium catalyst and chiral ligands. This effectively produces the stereospecific secondary alcohol as two separate diastereomers (**72**) in their acetonide protected nucleoside forms. This can be followed by phosphate coupling with a stable phosphate-bound prodrug, and acetonide deprotection for formation of FdUMP prodrugs.

Finally, selectivity and toxicity can be improved by limiting metabolic degradation of the prodrug. This can be achieved with stable terminal groups on the FdUMP prodrugs. Lipophilic carbon chains can be broken down in the liver by ω -oxidation and chain shortening with CYP and β -oxidases, as described for TFV analogues in the previous section.⁵⁹ However, as mentioned following the initial description of the lipophilic carbon chain degradation, TXL analogues of TFV prodrugs were recently designed in order to optimize metabolic stability.⁶⁰ While TXL has a 20-atom chain length with an ether linker and terminal methyl group on the lipophilic carbon chain, the analogues were designed with varying chain lengths, linkers, and ω -terminal groups. They were then evaluated to determine the optimal design for human liver microsome (HLM) stability and reduced ω -oxidase degradation. It was determined that a 20-atom chain with an ether linker and a trifluoromethyl terminal group (Figure 27, right) demonstrated the best *in vivo* profile and provided optimal metabolic stability against hepatic degradation and ω -oxidases.

Applying this metabolically optimized lipophilic chain to other compounds has the potential to limit degradation of other prodrugs besides TXL analogues. Formation of FdUMP prodrugs could limit degradation by DPD, while addition of the metabolically optimized lipophilic chain could limit degradation of the prodrug and premature release of FdUMP. The published synthesis of the optimized chain is illustrated in Scheme 6. The synthesis began with a tetrahydropyran (THP) protected propynol (**73**), which was alkylated by iodododecane to afford



the internal alkyne (**74**). The THP protecting group was then removed, followed by alkyne isomerization by a zipper reaction to form the terminal alkyne (**76**). The intermediate was then used for etherification of 1-(3-bromopropoxymethyl)-4-methoxy-benzene under phase transfer conditions to yield a *para*-methoxy benzyl (PMB) protected ether linked lipophilic chain with a terminal alkyne (**77**). Copper-mediated oxidative trifluoromethylation of the alkyne added the metabolically stable motif. The PMB group was then removed by cerium ammonium nitrate (CAN), followed by hydrogenation in the presence of Pearlman's catalyst to form the saturated lipophilic ether linked chain with a trifluoromethyl group on one end for metabolic stability, and a primary alcohol on the other (**80**) to couple to prodrugs.

Our goal is to create a FdUMP prodrug that improves target selectivity and decreases toxicity. Here, we develop a FdUMP prodrug, shown in Figure 28, that incorporates the FdUMP metabolite to bypass 5-FU degradation, a 5'-C-methyl substituent to limit di- and triphosphorylations, and a 20-atom lipophilic chain with an ether linker, and a metabolically stable trifluoromethyl group on the terminal carbon to decrease metabolic degradation.

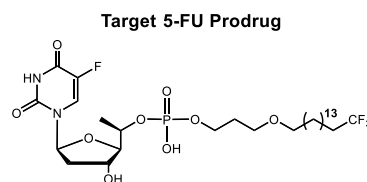


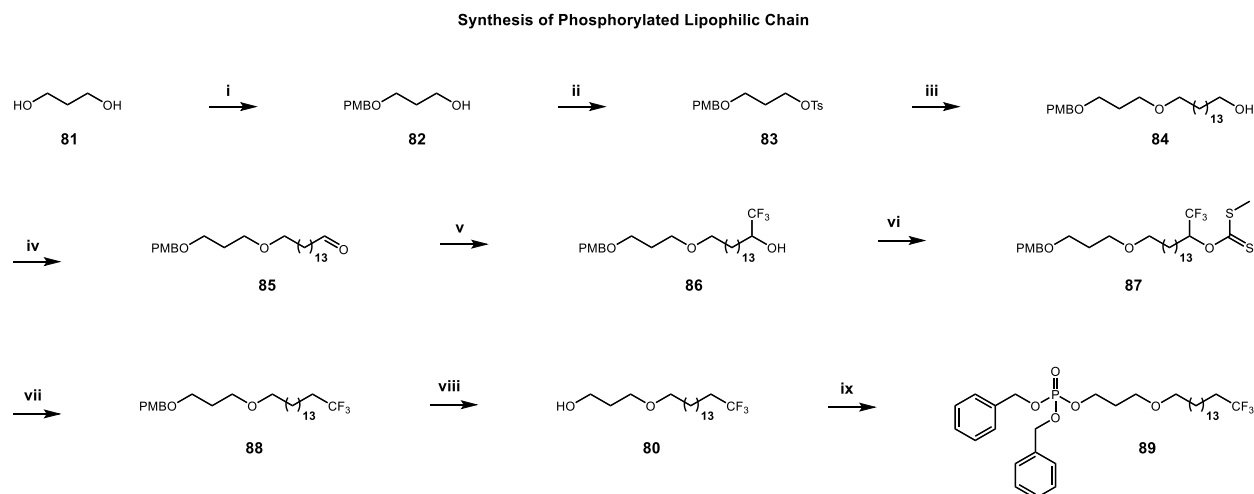
Figure 28. Target compounds of 5-FU prodrugs with active FdUMP metabolite, oxypropyl linker, lipophilic carbon chain, and metabolically stable terminal motifs.

Results and Discussion

The prodrug described here was designed to increase selectivity and decrease toxicity by improving stability in the liver and plasma and increasing concentration of the FdUMP metabolite for TS inhibition. Incorporation of the FdUMP metabolite into the prodrug results in release of FdUMP rather than 5-FU, preventing 5-FU degradation by DPD. The added steric bulk from the 5'-C-methyl-substituent has been shown to limit di- and triphosphorylations, which limits toxic misincorporation of nucleoside triphosphates. Attachment of a 20-atom chain with an ether linker and trifluoromethyl terminal group based off a previous TFV prodrug optimizes metabolic stability. Combining these features should allow increased intracellular release of the active FdUMP metabolite to target cells, increasing selectivity and limiting toxicity effects observed with alternative 5-FU prodrugs.

The lipophilic chain was formed by an alternative method than the published route previously described. In their optimization, Pribut et. al. formed multiple lipophilic chains with the common terminal alkylene intermediate shown in Scheme 6. Since this terminal alkylene handle was not required as an intermediate for our purposes, an alternate synthetic route was used. The novel synthesis of the lipophilic chain is illustrated in Scheme 7. The propane-1,3-diol starting material (**81**) was asymmetrically mono-protected with a PMB group. The remaining alcohol was then equipped with a tosyl group to act as a strong leaving group. The tosyl group was displaced with an etherification by pentadecane-1,15-diol. (The diol was prepared separately by lithium aluminum hydride reduction of pentadecandioic acid.) The primary alcohol was then oxidized to an aldehyde by a Swern oxidation, followed by a reductive trifluoromethylation to attach the metabolically stable terminal group and form a secondary alcohol (**86**). The alcohol was then removed by the 2-step Barton McCombie radical deoxygenation reaction to form the PMB

protected, ether-linked lipophilic chain (**88**). The alcohol was deprotected by a palladium catalyzed hydrogenation, and phosphorylated, forming the metabolically stable lipophilic coupling unit (**89**). The lipophilic unit was then delivered to M. Dasari, and coupled to the 5'-C-methyl-5-fluoronucleoside (**72**), which she formed by her synthetic route, previously described in Scheme 5.



Scheme 7. Synthesis of metabolically stable lipophilic chain equipped with phosphate group. i) PMBCl, NaH (60% in mineral oil, 4 equiv), THF, 70°C (92%). ii) TsCl (1.4 equiv), TEA (1.4 equiv), DMAP (0.05 equiv), DCM, rt (78%). iii) Pentadecane-1,15-diol (3 equiv), TBAB (0.5 equiv), 1:1 50% NaOH/THF, 75°C (47%). iv) Oxalyl chloride (2 equiv), DMSO (5 equiv), TEA (7 equiv), DCM, -78°C - rt (76%). v) TBAF (2 equiv) TFMTMS (2.5 equiv), THF, 0°C - rt (60%). vi) NaH (60% in mineral oil, 2.5 equiv), CS₂ (5 equiv), MeI (5 equiv), THF, 0°C - rt (85%). vii) TEA (5.7 equiv), AIBN (0.2 equiv), H₃PO₂ (50%, 2M), Dioxane, 110°C (83%). viii) Pd(OH)C, H₂, MeOH, rt (75%). ix) Dibenzyl diisopropyl phosphoramidite (1.2 equiv), 5-Me-1H-tetrazole (3 equiv), 30% hydrogen peroxide (6 equiv), DCM, 0°C - rt (65%).

Conclusion and Future Work

A novel synthetic route was developed for the formation of a 20-atom lipophilic chain with an ether linker and a metabolically stable trifluoromethyl terminal group. The chain was then equipped with a phosphate group and coupled to a sterically encumbered FdUMP analogue. This target compound was designed to increase selectivity and decrease toxicity. Release of the active FdUMP metabolite prevents 5-FU degradation by DPD. The added steric bulk on the nucleoside was included for the purpose of decreasing kinase activity to form di- and triphosphates from the monophosphate, decreasing misincorporation, therefore, limiting toxicity. The lipophilic chain with a metabolically stable terminal trifluoromethyl group was included in order to decrease degradation and premature release of the active drug.

Once the synthesis is complete with the nucleoside coupling, future work will include testing the compound for TS inhibition activity and HLM stability. Additionally, the prodrugs structural similarity to the TFV prodrugs would allow for hybrid formation with added lipophilic groups. As described in the previous section, the additional lipophilicity could cause association with lipoproteins. This would result in the drug being shuttled through the lymphatic system into systemic circulation, bypassing first-pass metabolism.

References

- ¹ Kingwell, K. Exploring the third dimension. *Nat. Rev. Drug Discovery*, **2009**, *8*, 931.
- ² Lovering, F.; Bikker, J.; Humblet, C. Escape from flatland: increasing saturation as an approach to improving clinical success. *J. Med. Chem.*, **2009**, *52*, 6756.
- ³ Wertjes, W. C.; Southgate, E. H.; Sarlah, D. Recent advances in chemical dearomatization of nonactivated arenes. *Chem. Soc. Rev.*, **2018**, *47*, 7996-8017.
- ⁴ Rabideau, P. W. The birch reduction of aromatic compounds. *Org. React.* **1992**, *42*, 1-334.
- ⁵ Hudlicky, T.; Olivo, H. F.; McKibben, B. Microbial oxidation of aromatics in enantiocontrolled synthesis. 3. 1 Design of amino cyclitols (exo-nitrogenous) and total synthesis of (+)-lycoridine via acylnitrosyl cycloaddition to polarized 1-halo-1, 2-cyclo-hexadienes. *J. Am. Chem. Soc.*, **1994**, *116*, 5108-5115.
- ⁶ Stanislaus, A.; Cooper, B. H. Aromatic hydrogenation catalysis: a review. *Catal. Rev.: Sci. Eng.*, **1994**, *36*, 75-123.
- ⁷ Schleyer, P. V. R.; Puhlhofer, F. Recommendations for the evaluation of aromatic stabilization energies. *Org. Lett.*, **2002**, *4*, 2873-2876.
- ⁸ Kwan, E. E.; Zeng, Y.; Besser, H. A.; Jacobsen, E. N. Concerted nucleophilic aromatic substitutions. *Nat. Chem.* **2018**, *10*, 917-923.
- ⁹ Galabov, B.; Nalbantova, D.; Schleyer, P. V. R.; Schaefer, H. F. Electrophilic aromatic substitution: new insights into an old class of reactions. *Acc. Chem. Res.* **2016**, *49*, 1191-1199.
- ¹⁰ Proctor, R. S. J.; Phipps, R. Recent advances in Minisci-type reactions. *Angew. Chem., Int. Ed.* **2019**, *58*, 13666-13699.
- ¹¹ Brodowski, M. H.; Denhart, D.; Ashraf, S.; Argentieri, S. R.; Buchman, J. H. Spiro-lactam NMDA receptor modulators and uses thereof. WO 2019/152688, Aug 8 2019.
- ¹² Shailubhai, K.; Dheer, S.; Picker, D.; Kaur, G.; Sausville, E. A.; Jacob, G. S., Atiprimod is an inhibitor of cancer cell proliferation and angiogenesis. *Journal of Experimental Therapeutics and Oncology*, **2004**, *4*, 267-279.
- ¹³ Ng, P. Y.; Davis, H.; Bair, K. W.; Millan, D. S.; Rudnitskaya, A.; Zheng, Z.; Han, B.; Barczak, N.; Lancia, D. 3-Spiro-7-hydroxamic acid tetralins as HDAC inhibitors. WO 2016/168660 A1, Oct 20 2016.
- ¹⁴ Prier, C.; Rankic, D.; MacMillan, D. Visible light photoredox catalysis with transition metal complexes: applications in organic synthesis. *Chem. Rev.* **2013**, *113*, 5322-5363.
- ¹⁵ Teegardin, K.; Day, J. I.; Chan, J.; Weaver, J. Advances in Photocatalysis: A Microreview of Visible Light Mediated Ruthenium and Iridium Catalyzed Organic Transformations. *Org. Process Res. Dev.* **2016**, *20*, 1156-1163.
- ¹⁶ Bizzarri, C.; Spuling, E.; Knoll, D. M.; Volz, D.; Brase, S. Sustainable Metal Complexes for Organic Light-Emitting Diodes (OLEDs). *Coord. Chem. Rev.* **2018**, *373*, 49-83.
- ¹⁷ Larsen, C. B.; Wenger, O. S. Photoredox Catalysis with Metal Complexes Made from Earth-Abundant Elements. *Chem. Eur. J.* **2018**, *24*, 2039-2058.

-
- ¹⁸ Zeitler, K. Metal-free Photo(redox) Catalysis. In *Visible Light Photocatalysis in Organic Chemistry*; Stephenson, C. R. J., Yoon, T. P., MacMillan, D. W. C., Eds.; Wiley-VCH: Weinheim, **2018**.
- ¹⁹ Speckmeier, E.; Fischer, T.; Zeitler, K. A toolbox approach to construct broadly applicable metal-free catalysts for photoredox chemistry: deliberate tuning of redox potentials and importance of halogens in donor-acceptor cyanoarenes. *J. Am. Chem. Soc.* **2018**, *140*, 15353-15365.
- ²⁰ McDaniel, K. A.; Flynn, A. R.; Hughes, M. E.; Vogt, D. B.; Jui, N. T. Hydroarylation of arenes via reductive radical-polar crossover. *J. Am. Chem. Soc.* **2020**, *142*, 9163-9168.
- ²¹ Fukuzumi, S.; Mochizuki, S.; Tanaka, T. Photocatalytic reduction of phenacyl halides by 9,10-dihydro-10-methylacridine: control between the reductive and oxidative quenching pathways of tris(bipyridine)ruthenium complex utilizing an acid catalysis. *J. Phys. Chem.* **1990**, *94*, 722-726.
- ²² Narayanam, J. M. R.; Tucker, J. W.; Stephenson, C. R. J. Electron-Transfer Photoredox Catalysis: Development of a Tin-Free Reductive Dehalogenation Reaction. *J. Am. Chem. Soc.* **2009**, *131*, 8756.
- ²³ Boivin, J.; Yousfi, M.; Zard, S. Z. Spirolactams by a novel ipso-radical cyclization and loss of aromaticity. *Tet. Lett.* **1997**, *38*, 5985-5988.
- ²⁴ Ibarra-Rivera, T. R.; Gamez-Montano, R.; Miranda, L. D. Efficient oxidative radical spirolactamization. *Chem. Commun.*, **2007**, 3485-3487.
- ²⁵ Diaba, F.; Montiel, J. A.; Martinez-Laporta, A.; Bonjoch, J. Dearomative radical spirocyclization from *N*-benzyltrichloroacetamides revisited using a copper(I)-mediated atom transfer reaction leading to 2-azaspiro[4.5]decanes. *Tet. Lett.* **2013**, *54*, 2619-2622.
- ²⁶ Fuentes, A.; Pineda, M.; Nagulapalli Venkata, K. Comprehension of top 200 prescribed drugs in the US as a resource for pharmacy teaching, training and practice. *Pharmacy.* **2018**, *6*, 43.
- ²⁷ Kane, S. P. The Top 200 of 2021, *ClinCalc DrugStats Database*, Version 21.1. ClinCalc: <https://clincalc.com/DrugStats/Top200Drugs.aspx>. Updated December 1, 2020.
- ²⁸ Zhou, C.; Lei, T.; Wei, X. Z.; Ye, C.; Liu, Z.; Chen, B.; Tung, C. H.; Wu, L. Z., Metal-Free, Redox-Neutral, Site-Selective Access to Heteroarylamine via Direct Radical-Radical Cross-Coupling Powered by Visible Light Photocatalysis. *J. Am. Chem. Soc.* **2020**, *142* (39), 16805-16813
- ²⁹ Nakajima, M.; Fava, E.; Loescher, S.; Jiang, Z.; Rueping, M., Photoredox-Catalyzed Reductive Coupling of Aldehydes, Ketones, and Imines with Visible Light. *Angew. Chem. Int. Ed.* **2015**, *54* (30), 8828-32.
- ³⁰ Humbel, S.; Cote, I.; Hofmann, N.; Bouquant, J., Three-Electron Binding between Carbonyl-like Compounds and Ammonia Radical Cation. Comparison with the Hydrogen Bonded Complex. *J. Am. Chem. Soc.* **1999**, *121* (23), 5507-5512
- ³¹ Tsui, E.; Metrano, A.; Tsuchiya, Y.; Knowles, R. Catalytic hydroetherification of unactivated alkenes enabled by proton-coupled electron transfer. *Angew. Chem. Int. Ed.* **2020**, *59*, 11845-11849.
- ³² Morcillo, S.; Dauncey, E.; Kim, J. H.; Douglas, J.; Sheikh, N.; Leonori, D. Photoinduced remote functionalization of amides and amines using electrophilic nitrogen radicals. *Angew. Chem. Int. Ed.* **2018**, *57*, 12945-12949.
- ³³ World Health Organization. HIV/AIDS. 17 July 2021. <https://www.who.int/news-room/fact-sheets/detail/hiv-aids>
- ³⁴ Ferris, A. L.; Hizi, A.; Showalter, S. D.; Pichuanes, S.; Babe, L.; Craik, C. S.; Hughes, S. H. Immunologic and proteolytic analysis of HIV-1 reverse transcriptase structure. *Virology*, **1990**, *175*, 456-464.

-
- ³⁵ Kirchhoff, F. HIV life cycle: Overview. In: Hope T., Stevenson M., Richman D. (eds) Encyclopedia of AIDS. 2013, Springer, New York, NY. https://doi.org/10.1007/978-1-4614-9610-6_60-1
- ³⁶ Rai, M. A.; Pannek, S.; Fichtenbaum, C. J. Emerging reverse transcriptase inhibitors for HIV-1 infection. *Expert Opin Emerg Drugs*, **2018**, *23*, 149-157.
- ³⁷ Naesens, L.; Snoeck, R.; Andrei, G.; Balzarini, J.; Neyts, J.; De Clercq, E. HPMPC (cidofovir), PMEA (adefovir) and related acyclic nucleoside phosphonate analogues: a review of their pharmacology and clinical potential in the treatment of viral infections. *Antiviral Chem and Chemother.*, **1997**, *8*, 1-23.
- ³⁸ Kakuda, T. N. Pharmacology of nucleoside and nucleotide reverse transcriptase inhibitor-induced mitochondrial toxicity. *Clin Ther.*, **2000**, *22*, 685-708.
- ³⁹ Stein, D. S.; Moore, D. H. P. Phosphorylation of nucleoside analog antiretrovirals: a review for clinicians. *Pharmacotherapy*, **2001**, *21*, 11-34.
- ⁴⁰ Johansson, N. G.; Eriksson, S. Structure-activity relationships for phosphorylation of nucleoside analogs to monophosphates by nucleoside kinases. *Acta Biochim Pol.*, **1996**, *43*, 143-160.
- ⁴¹ De Clercq, E. Potential of acyclic nucleoside phosphonates in the treatment of DNA virus and retrovirus infections. *Expert Rev Anti Infect Ther.*, **2003**, *1*, 21-43.
- ⁴² De Clercq, E.; Holy, A. Acyclic nucleoside phosphonates: a key class of antiviral drugs. *Nat Rev Drug Discov.*, **2005**, *4*, 928-940.
- ⁴³ Ng, H. H.; Stock, H.; Rausch, L.; Bunin, D.; Wang, A.; Brill, S.; Gow, J.; Mirsalis, J. C. Tenofovir Disoproxil Fumarate: toxicity, toxicokinetics, and toxicogenomics analysis after 13 weeks of oral administration in mice. *International Journal of Toxicology*, **2015**, *34*, 4-10.
- ⁴⁴ Grant, P. M.; Cotter, A. G. Tenofovir and bone health. *Curr Opin HIV AIDS*, **2016**, *11*, 326-332.
- ⁴⁵ Lee, W. A.; He, G.-X.; Eisenberg, E.; Cihlar, T.; Swaminathan, S.; Mulato, A.; Cundy, K. C. Selective intracellular activation of a novel prodrug of the human immunodeficiency virus reverse transcriptase inhibitor tenofovir leads to preferential distribution and accumulation in lymphatic tissue. *Antimicrob Agents Chemother.*, **2005**, *49*, 1898-1906.
- ⁴⁶ Shaw, J.-P.; Sueoka, C. M.; Oliyai, R.; Lee, W. A.; Arimilli, M. N.; Kim, C. U.; Cundy, K. C. Metabolism and pharmacokinetics of novel oral prodrugs of 0-[(R)-2-(phosphonomethoxy)propyl]adenine (PMPA) in dogs. *Pharm Res.*, **1997**, *14*, 1824-1829.
- ⁴⁷ Peterson, L. W.; McKenna, C. E. Prodrug approaches to improving the oral absorption of antiviral nucleotide analogues. *Expert Opinion on Drug Delivery*, **2009**, *6*, 405-420.
- ⁴⁸ Kearney, B. P.; Flaherty, J. F.; Shah, J. Tenofovir Disoproxil Fumarate. *Clin Pharmacokinet*, **2004**, *43*, 595-612.
- ⁴⁹ Ray, A. S.; Fordyce, M. W.; Hitchcock, M. J. M. Tenofovir Alafenamide: a novel prodrug of tenofovir for the treatment of human immunodeficiency virus. *Antiviral Research*, **2016**, *125*, 63-70.
- ⁵⁰ Hostetler, K. Y. Alkoxyalkyl prodrugs of acyclic nucleoside phosphonates enhance oral antiviral activity and reduce toxicity: current state of the art. *Antiviral Research*, **2009**, *82*, A84-A98.
- ⁵¹ Hecker, S. J.; Erion, M. D. Prodrugs of phosphates and phosphonates. *J. Med. Chem.*, **2008**, *51*, 2328-2345.
- ⁵² Robbins, B. L.; Srinivas, R. V.; Kim, C.; Bischofberger, N.; Fridland, A. Anti-human immunodeficiency virus activity and cellular metabolism of a potential prodrug of the acyclic nucleoside phosphonate 9-R-(2-phosphonomethoxypropyl)adenine (PMPA), bis(isopropylloxymethylcarbonyl)PMPA. *Antimicrob. Agents. Chemother.*, **1998**, *42*, 612-617.

- ⁵³ Fernandez, B.; Montoya-Ferrer, A.; Sanchez-Nino, M. D.; Izquierdo, M. C.; Poveda, J.; Sainz-Prestel, V.; Ortiz-Martin, N.; Parra-Rodriguez, A.; Selgas, R.; Ruiz-Ortega, M.; Egido, J.; Ortiz, A. Tenofovir Nephrotoxicity. *AIDS Res Treat.*, **2011**, 354908.
- ⁵⁴ Birkus, G.; Want, R.; Liu, X.; Kutty, N.; MacArthur, H.; Cihlar, T.; Gibbs, C.; Swaminathan, S.; Lee, W.; McDermott, M. Cathepsin A is the major hydrolase catalyzing the intracellular hydrolysis of the antiretroviral nucleotide phosphonoamidate prodrugs GS-7340 and GS-9131. *Antimicrob Agents Chemother.*, **2005**, *51*, 543-550.
- ⁵⁵ Mehellou, Y.; Rattan, H. S.; Balzarini, J. The prodrug technology: from the concept to the clinic. *J. Med. Chem.* **2018**, *61*, 6, 2211-2226.
- ⁵⁶ Babusis, D.; Phan, T. K.; Lee, W. A.; Watkins, W. J.; Ray, A. S. Mechanism for effective lymphoid cell and tissue loading following oral administration of nucleotide prodrug GS-7340. *Mol Pharm.*, **2013**, *10*, 459-466.
- ⁵⁷ Kim, M. J.; Kim, S.-W.; Chang, H.-H.; Kim, Y.; Jin, S.; Jung, H.; Park, J. H.; Kim, S.; Lee, J. M. Comparison of antiretroviral regimens: adverse effects and tolerability failure that cause regimen switching. *Infect. Chemother.*, **2015**, *47*, 231-238.
- ⁵⁸ Pertusati, F.; Serpi, M.; McGuigan, C. Medicinal chemistry of nucleoside phosphonate prodrugs for antiviral therapy. *Antivir Chem Chemother.*, **2012**, *14*, 181-203.
- ⁵⁹ Preissner, S. C.; Hoffmann, M. F.; Preissner, R.; Dunkel, M.; Gewiss, A.; Preissner, S. Polymorphic cytochrome P450 enzymes (CYPs) and their role in personalized therapy. *PLoS One*. **2013**, *8*(12), 1-12.
- ⁶⁰ Pribut, N.; D'Erasmus, M.; Dasari, M.; Giesler, K. E.; Iskandar, K. E.; Sharma, S. K.; Bartsch, P. W.; Raghuram, A.; Bushnev, A.; Hwang, S. S.; Burton, S. L.; Derdeyn, C. A.; Basson, A. E.; Liotta, D. C.; Miller, E. J. ω -Functionalized lipid prodrugs of HIV NtRTI Tenofovir with enhanced pharmacokinetic properties. *J. Med. Chem.*, **2021**, *64*, 12917-12937.
- ⁶¹ Ahn, H.; Park, J.-H. Liposomal delivery systems for intestinal lymphatic drug transport. *Biomater. Res.*, **2016**, *20*, 222-227.
- ⁶² Charman, W. N. A.; Stella, V. J. Estimating the maximal potential for intestinal lymphatic transport of lipophilic drug molecules. *Int. J. Pharm.*, **1986**, *34*, 175-178.
- ⁶³ Porter, C. J. H.; Travaskis, N. L.; Charman, W. N. Lipids and lipid-based formulations: optimizing the oral delivery of lipophilic drugs. *Nat Rev Drug Disc.*, **2007**, *6*, 231-248.
- ⁶⁴ Travaskis, N. L.; Kaminskas, L. M.; Porter, C. J. H. From sewer to savior – targeting the lymphatic system to promote drug exposure and activity. *Nat Rev Drug Discov.*, **2015**, *14*, 781-803.
- ⁶⁵ Dahan, A.; Duvdevani, R.; Shapiro, I.; Elmann, A.; Finkelstein, E.; Hoffman, A. The oral absorption of phospholipid prodrugs: in vivo and in vitro mechanistic investigation of trafficking of a lecithin valproic acid conjugate following oral administration. *J Control Release*. **2008**, *126*, 1-9.
- ⁶⁶ Hostetler, K. Y.; Beadle, J. R.; Trahan, J.; Aldern, K. A.; Owens, G.; Schriewer, J.; Melman, L.; Buller, R. M. Oral 1-O-octadecyl-2-O-benzyl-sn-glycero-3-cidofovir targets the lung and is effective against a lethal respiratory challenge with ectromelia virus in mice. *Antiviral Research*, **2007**, *73*, 212-218.
- ⁶⁷ Galmarini, C. M.; Mackey, J. R.; Dumontet, C. Nucleoside analogues and nucleobases in cancer treatment. *Lancet Oncol.*, **2002**, *3*, 415-424.
- ⁶⁸ Qi, J.; Zhang, Y.; Gou, Y.; Lee, P.; Wang, J.; Chen, S.; Zhou, Z.; Wu, Z.; Yang, R.; Liang, H. Multidrug delivery system based on human serum albumin for combination therapy with three anticancer agents. *Mol. Pharm.*, **2016**, *13*, 3098-3105.
- ⁶⁹ Boncel, S.; Herman, A. P.; Budniok, S.; Jedrysiak, R.; Jakobik-Kolon, A.; Skepper, J. N.; Muller, K. H.; In vitro targeting and selective killing of T47D breast cancer cells by prpurin and 5-fluorouracil anchored to magnetic CNTs: nitrene-based functionalization versus uptake, cytotoxicity, and intracellular fate. *ACS Biomater. Sci. Eng.* **2016**, *2*, 1273-1285.

-
- ⁷⁰ Zhao, J.; Ren, K.; Tang, J. Overcoming 5-FU resistance in human non-small cell lung cancer cells by the combination of 5-FU and cisplatin through the inhibition of glucose metabolism. *Tumor Biol.* **2014**, *35*, 12305-12315.
- ⁷¹ Wang, W.-B.; Yang, Y.; Zhao, Y.-P.; Zhang, T.-P.; Liao, Q.; Shu, H. Recent studies of 5-fluorouracil resistance in pancreatic cancer. *World J. Gastroenterol.*, **2014**, *20*, 15682.
- ⁷² Chen, X.-X.; Lam, K. K.-H.; Fent, Y.-B.; Xu, K.; Sze, S. C.-W.; Tang, S. C.-W.; Leung, G. P.-H.; Lee, C. K.-F.; Shi, J.; Yang, Z.-J.; Ellagitannins from pomegranate ameliorates 5-fluorouracil-induced intestinal mucositis in rats while enhancing its chemotoxicity against HT-29 colorectal cancer cells through intrinsic apoptosis induction. *J. Agric. Food Chem.*, **2018**, *66*, 7054-7064.
- ⁷³ Kanamaru, R.; Kakuta, H.; Sato, T.; Ishioka, C.; Wakui, A. The inhibitory effects of 5-fluorouracil on the metabolism of preribosomal and ribosomal RNA in L-1210 cells in vitro. *Cancer Chemother. Pharmacol.* **1986**, *17*, 43-46.
- ⁷⁴ Ghoshal, K.; Jacob, S. T. Specific inhibition of preribosomal RNA processing in extracts from the lymphosarcoma cells treated with 5-fluorouracil. *Cancer Res.*, **1994**, *54*, 632-636.
- ⁷⁵ Santi, D. V.; Hardy, L. W. Catalytic mechanism and inhibition of tRNA (uracil-5-)methyltransferase: evidence for covalent catalysis. *Biochemistry*, **1987**, *26*, 8599-8606.
- ⁷⁶ Randerath, K.; Tseng, W. C.; Harris, J. S.; Lu, L. J. Specific effects of 5-fluoropyrimidines and 5-azapyrimidines on modification of the 5 position of pyrimidines, in particular the synthesis of 5-methyluracil and 5-methylcytosine in nucleic acids. *Recent Results Cancer Res.* **1983**, *84*, 283-297.
- ⁷⁷ Malet-Marino, M.; Martino, R. Clinical studies of three oral prodrugs of 5-fluorouracil (Capecitabine, UFT, S-1): a review. *The Oncologist*, **2002**, *7*, 288-323.
- ⁷⁸ Longley, D. B.; Harkin, D. P.; Johnston, P. G. 5-Fluorouracil: mechanisms of action and clinical strategies. *Nat. Rev. Cancer*, **2003**, *3*, 330-338.
- ⁷⁹ Santi, D. V.; McHenry, C. S.; Sommer, H. Mechanism of interaction of thymidylate synthase with 5-fluorodeoxyuridylate. *Biochemistry*, **1974**, *13*, 471-481.
- ⁸⁰ Lu, Z.-H.; Zhang, R.; Diasio, R. B. Purification and characterization of dihydropyrimidine dehydrogenase from human liver. *J. Biol. Chem.*, **1992**, *267*, 17102-17109.
- ⁸¹ Baccanari, D. P.; Davis, S. T.; Knick, V. C.; Spector, T. 5-Ethynyluracil: a potent modulator of the pharmacokinetics and antitumor efficacy of 5-fluorouracil. *Pro Natl Acad Sci.*, **1993**, *90*, 11064-11068.
- ⁸² Fraile, R. J.; Baker, L. H.; Buroker, T. R.; Horwitz, J.; Vaitkevicius, V.; K. Pharmacokinetics of 5-fluorouracil administered orally, by rapid intravenous and by slow infusion. *Cancer Res.*, **1980**, *40*, 2223-2228.
- ⁸³ Diasio, R. B. The role of dihydropyrimidine dehydrogenase (DPD) modulation in 5-FU pharmacology. *Oncology*, **1998**, *12*, 23-27.
- ⁸⁴ Pasban, S.; Raissi, H.; Pakde, M.; Farzad, F. Enhance the efficiency of 5-fluorouracil targeted delivery by using a prodrug approach as a novel strategy for prolonged circulation time and improved permeation. *Int. J. Pharm.*, **2019**, *568*, 1-11.
- ⁸⁵ Kamm, Y. J. L.; Peters, G. J.; Hull, W. E.; Punt, C. J. A.; Heerschap, A. Correlation between 5-fluorouracil metabolism and treatment response in two variants of C26 murine colon carcinoma. *Br. J. Cancer*, **2003**, *89*, 754-762.
- ⁸⁶ Jiang, W.; Lu, Z.; He, Y.; Diasio, R. B. Dihydropyrimidine dehydrogenase activity in hepatocellular carcinoma: implication for 5-fluorouracil-based chemotherapy. *Clin Cancer Res.*, **1997**, *3*, 395-399.
- ⁸⁷ Hashimoto, Y.; Yoshida, Y.; Yamada, T.; Aisu, N.; Yoshimatsu, G.; Yoshimura, F.; Hasegawa, S. Current status of therapeutic drug monitoring of 5-fluorouracil prodrugs. *Anticancer Res.*, **2020**, *40*, 4655-4661.

⁸⁸ Hiller, S.; Zhuk, R.; Lidak, M.; Zidermane, A. Patent specification 1168391. *Br Patent*. **1968**, *1*, 391-395.

⁸⁹ Dasari, M.; Ma, P.; Pelly, S. C.; Sharma, S. K.; Liotta, D. C. Synthesis and biological evaluation of 5'-C-methyl nucleotide prodrugs for treating HCV infections. *Bioorg, Med. Chem. Lett.*, **2020**, *30*, 127539.

Experimental

I. General Information

I-A. General Reagent Information

Solvents used in anhydrous reactions were purified by passing over activated alumina and storing under argon. Reagents were purchased from Sigma-Aldrich, Alfa Aesar, Acros Organics, Combi-Blocks, Oakwood Chemicals, Astatech, and TCI America and used as received, unless stated otherwise. Organic solutions were concentrated under reduced pressure on a rotary evaporator using a water bath. Chromatographic purification of products was accomplished using forced-flow chromatography on 230–400 mesh silica gel. Preparative thin-layer chromatography (PTLC) separations were carried out on 1000 μm SiliCycle silica gel F-254 plates. Thin-layer chromatography (TLC) was performed on 250 μm SiliCycle silica gel F-254 plates. Visualization of the developed chromatogram was performed by fluorescence quenching or staining using KMnO_4 , p-anisaldehyde, or ninhydrin stains. All photoredox reactions were set up on the bench top and conducted under nitrogen atmosphere while subject to irradiation from blue LEDs, unless stated otherwise (LED wholesalers PAR38 Indoor Outdoor 16-Watt LED Flood Light Bulb, Blue; or Hydrofarm® PPB1002 PowerPAR LED Bulb-Blue 15W/E27 (available from Amazon)). Solvent was degassed by sonication under mild vacuum for 15 minutes. Photoredox catalysts 3DPAFIPN, 3DPA2FBN, 5CzBn, 4CzIPN, and $[\text{Ir}(\text{ppy})_2\text{dtbbpy}]\text{PF}_6$ were prepared according to literature procedures.^{1,2}

I-B. General Analytical Information

Unless otherwise noted, all yields refer to chromatographically and spectroscopically (^1H NMR) homogenous materials. New compounds were characterized by ^1H NMR, ^{13}C NMR, and MS. ^1H and ^{13}C NMR spectra were obtained from the Emory University NMR facility and recorded on a Bruker Avance III HD 600 equipped with cryo-probe (600 MHz), Bruker NEO 400 (400 MHz), INOVA 600 (600 MHz), INOVA 500 (500 MHz), INOVA 400 (400 MHz), or VNMR 400 (400 MHz) and are internally referenced to residual protio solvent signals. Data for ^1H NMR are reported as follows: chemical shift (ppm), multiplicity (s = singlet, d = doublet, t = triplet, q = quartet, m = multiplet, dd = doublet of doublets, dt = doublet of triplets, ddd = doublet of doublet of doublets, dtd = doublet of triplet of doublets, b = broad, etc.), coupling constant (Hz), integration, and assignment, when applicable. Data for decoupled ^{13}C NMR are reported in terms of chemical shift and multiplicity when applicable. Gas Chromatography Mass Spectrometry (GCMS) was performed on an Agilent 5977A mass spectrometer with an Agilent 7890A gas chromatography inlet. Liquid Chromatography Mass Spectrometry (LCMS) was performed on an Agilent 6120 mass spectrometer with an Agilent 1220 Infinity liquid chromatography inlet.

1 Speckmeier, E.; Fischer, T.; Zeitler, K. A Toolbox Approach to Construct Broadly Applicable Metal-Free Catalysts for Photoredox Chemistry: Deliberate Tuning of Redox Potentials and Importance of Halogens in Donor-Acceptor Cyanoarenes. *J. Am. Chem. Soc.* **2018**, *140*, 15354–15365.

2 Slinker, J. D.; Gorodetsky, A. A.; Lowry, M. S.; Wang, J.; Parker, S.; Rohl, R.; Bernhard, S.; Malliaras, G. G. Efficient Yellow Electroluminescence from a Single Layer of a Cyclometalated Iridium Complex. *J. Am. Chem. Soc.* **2004**, *126*, 2763–2767.

II. General Procedures

II-A. General Reductive Amination Procedure

To a round bottomed flask charged with benzaldehyde (1.0 equiv) was added MeOH (0.2 M) and primary amine. After stirring for 2-16 hours, NaBH₄ (1.5 equiv) was added slowly, and the resultant mixture was stirred until bubbling ceased. The reaction mixture was quenched with 1 M NaOH (aq) and extracted with EtOAc (3x). The combined organic layers were washed with 1 M HCl (aq), and the resulting aqueous layer was brought to pH 14 with 2 M NaOH (aq) or 50% KOH (aq) and extracted with EtOAc (3x). The combined organic layers were dried over MgSO₄ or Na₂SO₄, filtered, and concentrated under reduced pressure to afford the desired product.

II-B. General Acylation Procedure

To a round bottomed flask charged with secondary amine (1.0 equiv) was added CH₂Cl₂ (0.1 M), Et₃N (1.2 equiv), and chloroacetyl chloride (1.2 equiv). After stirring for 1-2 hours, the reaction mixture was quenched with MeOH, diluted with H₂O, and extracted with CH₂Cl₂ (3x). The combined organic layers were dried over MgSO₄ or Na₂SO₄, filtered, and concentrated under reduced pressure. The crude residue was purified on silica using the indicated solvent mixture, if necessary, to afford the desired product.

II-C. General Dearomative Spirolactamization Procedure 1

A 20 mL screw-top test tube was charged with 3DPAFIPN (16.2 mg, 0.025 mmol, 5 mol%), and substrate (0.5 mmol, 1.0 equiv). The tube was equipped with a stir bar was sealed with a PTFE/silicon septa. The atmosphere was exchanged by applying vacuum and backfilling with nitrogen (this process was conducted a total of three times). Under nitrogen atmosphere, DIPEA (0.26 mL, 1.5 mmol, 3.0 equiv) was added via syringe, followed by degassed solvent (5 mL of each MeCN and H₂O to give a 0.05 M solution). The resulting mixture was stirred at 50 °C for 16 h under irradiation by blue LEDs, unless noted otherwise. The reaction was then extracted with EtOAc (3x), dried over MgSO₄ or Na₂SO₄, and concentrated under reduced pressure. The crude residue was purified as indicated to afford the desired product.

II-D. General Dearomative Spirolactamization Procedure 2

A 20 mL screw-top test tube was charged with 3DPAFIPN (16.2 mg, 0.025 mmol, 5 mol%), and substrate (0.5 mmol, 1.0 equiv). The tube was equipped with a stir bar was sealed with a PTFE/silicon septa. The atmosphere was exchanged by applying vacuum and backfilling with nitrogen (this process was conducted a total of three times). Under nitrogen atmosphere, DIPEA (0.26 mL, 1.5 mmol, 3.0 equiv) was added via syringe, followed by degassed solvent (5 mL of each MeCN and H₂O to give a 0.05 M solution). The resulting mixture was stirred at 50 °C for 16 h under irradiation by blue LEDs, unless noted otherwise. The reaction was then extracted with EtOAc (3x), dried over MgSO₄ or Na₂SO₄, and concentrated under reduced pressure. In order to deprotect the HDH byproduct that is sometimes difficult to separate from the dearomatized product via chromatography, the crude residue was dissolved in 50% (v/v) TFA/CH₂Cl₂

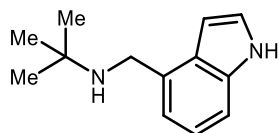
(0.1 M) for 16 hours. The reaction was quenched with saturated NaHCO_3 (aq) then extracted with EtOAc (3x), dried over MgSO_4 or Na_2SO_4 , and concentrated under reduced pressure. The crude residue was purified as indicated to afford the desired product.

III. Dearomatization Optimization Details

III-A. Optimization Procedure

An 8 mL screw-top test tube was charged with photocatalyst (0.005 mmol, 5 mol%) and *N*-benzyl-*N*-(*tert*-butyl)-2-chloroacetamide (**S39**) (24.0 mg, 0.1 mmol, 1.0 equiv). The tube was equipped with a stir bar and sealed with a PTFE/silicon septa. The atmosphere was exchanged by applying vacuum and backfilling with nitrogen (this process was conducted a total of three times). Under nitrogen atmosphere, DIPEA (52 μL , 0.3 mmol, 3 equiv) was added via syringe, followed by degassed solvent. The resulting mixture was stirred at the indicated temperature for 16 h under irradiation by blue LEDs, unless noted otherwise. The reaction was then extracted with ethyl acetate (3x) and concentrated under reduced pressure. CDCl_3 and an internal standard of dibromomethane (7 μL , 0.1 mmol) were added. The sample was analyzed by ^1H NMR ($d = 5$ s), and the integral values were used to calculate the data given in the Optimization Table.

IV. Preparation of Spirolactam Starting Materials



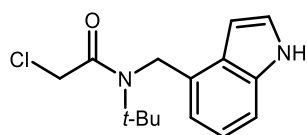
***N*-((1*H*-indol-4-yl)methyl)-2-methylpropan-2-amine (S1):**

Prepared according to General Reductive Amination Procedure. Indole-4-carboxaldehyde (435 mg, 3.0 mmol, 1.0 equiv) and *tert*-butyl amine (0.38 mL, 3.6 mmol, 1.2 equiv) were stirred in MeOH (15 mL, 0.2 M) for 16 hours. After NaBH_4 (170 mg, 4.5 mmol, 1.5 equiv) was added, the reaction was stirred for an additional 30 min. The title compound was obtained as a light-brown solid (607 mg, 100%).

^1H NMR (400 MHz, CDCl_3) δ 8.24 (br s, 1H), 7.29 (d, $J = 7.8$ Hz, 1H), 7.24 – 7.17 (m, 1H), 7.18 – 7.08 (m, 2H), 6.65 (ddd, $J = 3.2, 2.1, 1.0$ Hz, 1H), 4.04 (s, 2H), 1.25 (s, 9H) ppm.

^{13}C NMR (151 MHz, CDCl_3) δ 136.1, 133.3, 127.1, 124.0, 122.4, 119.40 110.0, 100.9, 51.0, 45.3, 29.3 ppm.

LRMS (EI) m/z : $[M]^+$ calc'd. for $\text{C}_{13}\text{H}_{18}\text{N}_2$, 202.2, found 202.2.



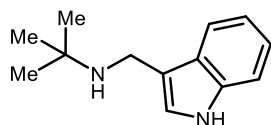
***N*-((1*H*-indol-4-yl)methyl)-*N*-(*tert*-butyl)-2-chloroacetamide (**S2**):**

Prepared according to General Acylation Procedure. *N*-((1*H*-indol-4-yl)methyl)-2-methylpropan-2-amine (**S1**) (474 mg, 2.3 mmol, 1.0 equiv), Et₃N (0.39 mL, 2.8 mmol, 1.2 equiv), and chloroacetyl chloride (0.19 mL, 2.3 mmol, 1.0 equiv) were stirred in CH₂Cl₂ (23 mL, 0.1 M) for 30 minutes. Purification on silica gel (30% EtOAc/hexanes) afforded the title compound as a light-brown solid (535 mg, 83%).

¹H NMR (400 MHz, CDCl₃) δ 8.41 (br s, 1H), 7.36 (dt, *J* = 8.2, 0.9 Hz, 1H), 7.29 (dd, *J* = 3.3, 2.4 Hz, 1H), 7.21 (dd, *J* = 8.2, 7.3 Hz, 1H), 6.98 (dq, *J* = 7.2, 1.0 Hz, 1H), 6.56 (ddd, *J* = 3.1, 2.0, 1.0 Hz, 1H), 4.92 (s, 2H), 4.01 (s, 2H), 1.51 (s, 9H) ppm.

¹³C NMR (151 MHz, CDCl₃) δ 168.0, 135.9, 130.4, 124.7, 124.7, 122.6, 116.1, 110.6, 99.9, 58.8, 46.9, 44.5, 28.5 ppm.

LRMS (EI) *m/z*: [M]⁺ calc'd. for C₁₅H₁₉ClN₂O, 278.1, found 278.1.

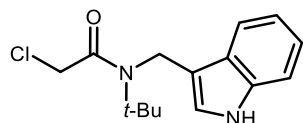
***N*-((1*H*-indol-3-yl)methyl)-2-methylpropan-2-amine (**S3**):**

Prepared according to General Reductive Amination Procedure. Indole-3-carbaldehyde (871 mg, 6.0 mmol, 1.0 equiv) and *tert*-butyl amine (0.76 mL, 7.2 mmol, 1.2 equiv) were stirred in MeOH (30 mL, 0.2 M) for 16 hours. After NaBH₄ (340 mg, 9.0 mmol, 1.5 equiv) was added, the reaction was stirred for an additional 4 hours. The title compound was obtained as an off-white solid (627 mg, 52%).

¹H NMR (600 MHz, CDCl₃) δ 8.11 (br s, 1H), 7.65 (d, *J* = 7.9 Hz, 1H), 7.35 (d, *J* = 8.1 Hz, 1H), 7.20 (t, *J* = 7.6 Hz, 1H), 7.16 (d, *J* = 2.3 Hz, 1H), 7.13 (t, *J* = 7.5 Hz, 1H), 3.96 (s, 2H), 1.25 (s, 9H) ppm.

¹³C NMR (151 MHz, CDCl₃) δ 136.6, 127.2, 122.5, 122.2, 119.6, 118.9, 115.9, 111.4, 50.8, 38.1, 29.2 ppm.

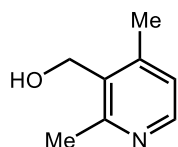
LRMS (APCI) *m/z*: [M+1]⁺ calc'd. for C₁₃H₁₈N₂, 203.2, found 203.2.

***N*-((1*H*-indol-3-yl)methyl)-*N*-(*tert*-butyl)-2-chloroacetamide (**S4**):**

Prepared according to General Acylation Procedure. *N*-((1*H*-indol-3-yl)methyl)-2-methylpropan-2-amine (**S3**) (506 mg, 2.5 mmol, 1.0 equiv), Et₃N (0.35 mL, 2.5 mmol, 1.0 equiv), and chloroacetyl chloride (0.20 mL, 2.5 mmol, 1.0 equiv) were stirred in CH₂Cl₂ (25 mL, 0.1 M) for 18 hours. Purification on silica gel (30% EtOAc/hexanes) afforded the title compound as an off-white solid (534 mg, 77%).

¹H NMR (600 MHz, C₆D₆) δ 7.55 (s, 1H), 7.41 (d, *J* = 7.8 Hz, 1H), 7.24 (t, *J* = 7.6 Hz, 1H), 7.20 – 7.14 (m, 2H), 6.51 (s, 1H), 4.35 (s, 2H), 3.80 (s, 2H), 1.39 (s, 9H) ppm.

^{13}C NMR (151 MHz, C_6D_6) δ 13C NMR (151 MHz, C_6D_6) δ 167.4, 137.2, 125.7, 123.0, 121.8, 120.1, 118.6, 114.7, 111.9, 58.1, 44.3, 41.8, 28.4 ppm.



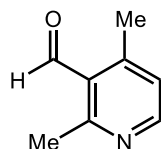
(2,4-dimethylpyridin-3-yl)methanol (S5):

Lithium aluminum hydride (4.0 M in ether, 7.5 mL, 10.0 mmol, 2.0 equiv) was added to cold, dry THF (12 mL). Ethyl 2,4-dimethylnicotinate (896.1 mg, 5.0 mmol, 1.0 equiv) was dissolved in dry THF (3 mL) and slowly added to the lithium aluminum hydride solution at 0°C. The reaction mixture was warmed to room temperature and stirred for 2 hours, then cooled to 0°C, diluted with water, quenched with 1 M NaOH (aq), filtered through a plug of celite, and extracted with EtOAc (3x). The combined organic layers were dried over Na_2SO_4 , filtered, and concentrated under reduced pressure to afford the title compound as a tan solid (519 mg, 76%).

^1H NMR (600 MHz, CDCl_3) δ 8.26 (d, $J = 5.0$ Hz, 1H), 6.96 (d, $J = 5.1$ Hz, 1H), 4.77 (s, 2H), 2.63 (s, 3H), 2.42 (s, 3H) ppm.

^{13}C NMR (151 MHz, CDCl_3) δ 157.7, 148.4, 147.0, 132.2, 124.0, 59.0, 22.4, 19.1 ppm.

LRMS (EI) m/z : $[\text{M}]^+$ calc'd. for $\text{C}_8\text{H}_{11}\text{NO}$, 137.1, found 137.0.



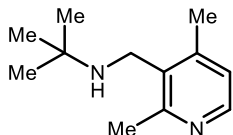
2,4-dimethylnicotinaldehyde (S6):

(2,4-dimethylpyridin-3-yl)methanol (S5) (478.8 mg, 3.5 mmol, 1.0 equiv), and manganese dioxide (1520 mg, 20.0 mmol, 5.0 equiv) were dissolved in CH_2Cl_2 (32 mL, 0.15 M) and refluxed at 40°C for 18 hours. The reaction mixture was cooled to room temperature and filtered through a plug of celite. Purification on silica gel (20-50% EtOAc/hexanes) afforded the title compound as a brown solid (263 mg, 56%).

^1H NMR (600 MHz, CDCl_3) δ 10.64 (s, 1H), 8.47 (d, $J = 5.1$ Hz, 1H), 7.06 (d, $J = 5.2$ Hz, 1H), 2.83 (s, 3H), 2.61 (s, 3H) ppm.

^{13}C NMR (151 MHz, CDCl_3) δ 192.7, 160.9, 152.2, 150.1, 128.6, 125.3, 23.3, 20.4 ppm.

LRMS (EI) m/z : $[\text{M}]^+$ calc'd. for $\text{C}_8\text{H}_9\text{NO}$, 135.1, found 135.0.



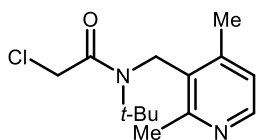
***N*-((2,4-dimethylpyridin-3-yl)methyl)-2-methylpropan-2-amine (S7):**

Prepared according to General Reductive Amination Procedure. 2,4-dimethylnicotinaldehyde (**S6**) (237 mg, 1.8 mmol, 1.0 equiv) and *tert*-butyl amine (0.28 mL, 2.6 mmol, 1.5 equiv) were stirred in MeOH (9 mL, 0.2 M) for 16 hours. After NaBH₄ (100 mg, 2.6 mmol, 1.5 equiv) was added, the reaction was stirred for an additional 1 hour. The title compound was obtained as a white solid (316 mg, 94%).

¹H NMR (600 MHz, CDCl₃) δ 8.22 (d, J = 5.0 Hz, 1H), 6.92 (d, J = 5.0 Hz, 1H), 3.72 (s, 2H), 2.61 (s, 3H), 2.38 (s, 3H), 1.20 (s, 9H) ppm.

¹³C NMR (151 MHz, CDCl₃) δ 157.2, 147.3, 146.4, 132.7, 123.7, 50.7, 40.4, 28.9, 22.1, 18.9 ppm.

LRMS (EI) m/z: [M]⁺ calc'd. for C₁₂H₂₀N₂, 192.2, found 192.2.



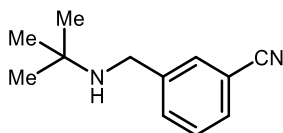
***N*-(*tert*-butyl)-2-chloro-*N*-((2,4-dimethylpyridin-3-yl)methyl)acetamide (S8):**

Prepared according to General Acylation Procedure. *N*-((2,4-dimethylpyridin-3-yl)methyl)-2-methylpropan-2-amine (**S7**) (289 mg, 1.5 mmol, 1.0 equiv), Et₃N (0.23 mL, 1.7 mmol, 1.1 equiv), and chloroacetyl chloride (0.13 mL, 1.7 mmol, 1.1 equiv) were stirred in THF (15 mL, 0.1 M) for 3 hours. The title compound was afforded as a white solid (148 mg, 37%).

¹H NMR (600 MHz, CDCl₃) δ 8.28 (d, J = 5.0 Hz, 1H), 6.94 (d, J = 4.9 Hz, 1H), 4.69 (s, 2H), 4.15 (s, 2H), 2.59 (s, 3H), 2.38 (s, 3H), 1.38 (s, 9H) ppm.

¹³C NMR (151 MHz, CDCl₃) δ 168.6, 155.9, 147.6, 145.4, 130.9, 125.2, 59.4, 46.0, 44.9, 28.4, 23.9, 20.5 ppm.

LRMS (EI) m/z: [M]⁺ calc'd. for C₁₄H₂₁ClN₂O, 268.1, found 268.1.



3-((*tert*-butylamino)methyl)benzonitrile (S9):

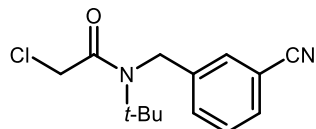
Prepared according to General Reductive Amination Procedure. 3-formylbenzonitrile (525 mg, 4.0 mmol, 1.0 equiv) and *tert*-butyl amine (0.73 mL, 4.8 mmol, 1.2 equiv) were stirred in MeOH (20 mL, 0.2 M) for

12 hours. After NaBH₄ (227 mg, 6.0 mmol, 1.5 equiv) was added, the reaction was stirred for an additional 2 hours. The title compound was obtained as a clear oil (694 mg, 92%).

¹H NMR (600 MHz, CDCl₃) δ 7.65 (s, 1H), 7.56 (d, J = 8.3 Hz, 1H), 7.47 (d, J = 7.7 Hz, 1H), 7.37 (t, J = 7.7 Hz, 1H), 3.73 (s, 2H), 1.14 (s, 9H) ppm.

¹³C NMR (151 MHz, CDCl₃) δ 143.4, 132.7, 131.8, 130.5, 129.1, 119.1, 112.3, 50.9, 46.5, 29.2 ppm.

LRMS (EI) m/z: [M]⁺ calc'd. for C₁₂H₁₆N₂, 188.1, found 188.2.



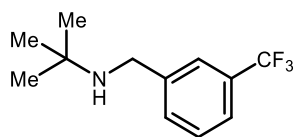
***N*-(*tert*-butyl)-2-chloro-*N*-(3-cyanobenzyl)acetamide (S10):**

Prepared according to General Acylation Procedure. 3-((*tert*-butylamino)methyl)benzotrile (S9) (377 mg, 2.0 mmol, 1.0 equiv), Et₃N (0.31 mL, 2.2 mmol, 1.1 equiv), and chloroacetyl chloride (0.18 mL, 2.2 mmol, 1.1 equiv) were stirred in CH₂Cl₂ (20 mL, 0.1 M) for 3 hours. The title compound was afforded as a tan solid (526 mg, 99%).

¹H NMR (600 MHz, CDCl₃) δ 7.59 (d, J = 7.6 Hz, 1H), 7.54 – 7.49 (m, 2H), 7.47 (d, J = 7.7 Hz, 1H), 4.69 (s, 2H), 3.92 (s, 2H), 1.43 (s, 9H) ppm.

¹³C NMR (151 MHz, CDCl₃) δ 167.7, 140.7, 131.4, 130.1, 130.0, 129.2, 118.5, 113.5, 59.1, 48.4, 44.0, 28.6 ppm.

LRMS (EI) m/z: [M]⁺ calc'd. for C₁₄H₁₇ClN₂O, 264.1, found 264.1.



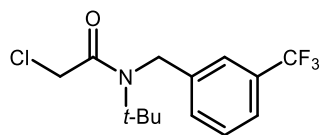
2-methyl-*N*-(3-(trifluoromethyl)benzyl)propan-2-amine (S11):

Prepared according to General Reductive Amination Procedure. 3-(trifluoromethyl)benzaldehyde (0.54 mL, 4.0 mmol, 1.0 equiv) and *tert*-butyl amine (0.50 mL, 4.8 mmol, 1.2 equiv) were stirred in MeOH (20 mL, 0.2 M) for 26 hours. After NaBH₄ (227 mg, 6.0 mmol, 1.5 equiv) was added, the reaction was stirred for an additional 30 min. The title compound was obtained as a light-yellow oil (590 mg, 86%).

¹H NMR (400 MHz, CDCl₃) δ 7.62 (s, 1H), 7.54 (d, J = 7.3 Hz, 1H), 7.49 (d, J = 7.5 Hz, 1H), 7.44 – 7.39 (m, 1H), 3.79 (s, 2H), 1.18 (s, 9H) ppm.

¹³C NMR (151 MHz, CDCl₃) 142.5, 131.7, 130.7 (q, ²J_{C-F} = 32.1 Hz), 128.8, 125.0 (q, ³J_{C-F} = 3.9 Hz), 124.3 (q, ¹J_{C-F} = 272.2 Hz), 123.7 (q, ³J_{C-F} = 3.9 Hz), 50.9, 46.8, 29.2 ppm.

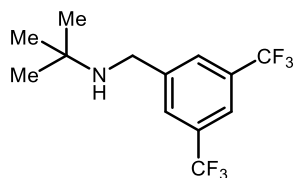
LRMS (EI) m/z: [M]⁺ calc'd. for C₁₂H₁₆F₃N, 231.1, found 231.2.



***N*-(*tert*-butyl)-2-chloro-*N*-(3-(trifluoromethyl)benzyl)acetamide (S12):**

Prepared according to General Acylation Procedure. 2-methyl-*N*-(3-(trifluoromethyl)benzyl)propan-2-amine (S11) (490 mg, 3.0 mmol, 1.0 equiv), Et₃N (0.50 mL, 3.6 mmol, 1.2 equiv), and chloroacetyl chloride (0.29 mL, 3.6 mmol, 1.2 equiv) were stirred in CH₂Cl₂ (30 mL, 0.1 M) for 1 hour. The title compound afforded as a light-yellow solid (685 mg, 95%).

¹H NMR (600 MHz, CDCl₃) δ 7.57 (d, J = 7.7 Hz, 1H), 7.52 (t, J = 7.7 Hz, 1H), 7.47 (s, 1H), 7.42 (d, J = 7.6 Hz, 1H), 4.73 (s, 2H), 3.94 (s, 2H), 1.46 (s, 9H) ppm. ¹H NMR spectrum is consistent with reported values.³



***N*-(3,5-bis(trifluoromethyl)benzyl)-2-methylpropan-2-amine (S13):**

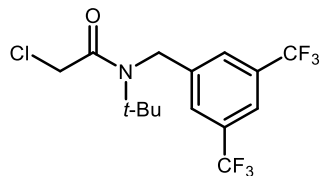
Prepared according to General Reductive Amination Procedure. 3,5-bis(trifluoromethyl)benzaldehyde (0.66 mL, 4.0 mmol, 1.0 equiv) and *tert*-butyl amine (0.50 mL, 4.8 mmol, 1.2 equiv) were stirred in MeOH (20 mL, 0.2 M) for 17 hours. After NaBH₄ (227 mg, 6.0 mmol, 1.5 equiv) was added, the reaction was stirred for an additional 30 min. The title compound was obtained as a colorless oil (164 mg, 14%).

¹H NMR (400 MHz, CDCl₃) δ 7.84 (s, 2H), 7.74 (s, 1H), 3.86 (s, 2H), 1.18 (s, 9H) ppm.

¹³C NMR (151 MHz, CDCl₃) δ 131.6 (q, ²J_{C-F} = 33.1 Hz), 128.6, 123.6 (q, ¹J_{C-F} = 272.5 Hz), 121.0, 51.4, 46.5, 29.2 ppm.

LRMS (EI) m/z: [M]⁺ calc'd. for C₁₃H₁₅F₆N, 299.1, found 299.1.

3 Yanagita, H.; Urano, E.; Matsumoto, K.; Ichikawa, R.; Takaesu, Y.; Ogata, M.; Murakami, T.; Wu, H.; Chiba, J.; Komano, J.; Hoshino, T. Structural and biochemical study on the inhibitory activity of derivatives of 5-nitro-furan-2-carboxylic acid for RNase H function of HIV-1 reverse transcriptase. *Bioorg. Med. Chem.* **2011**, *19*, 816-825.



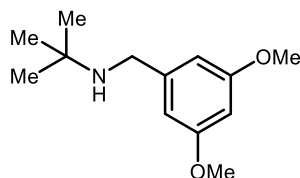
***N*-(3,5-bis(trifluoromethyl)benzyl)-*N*-(*tert*-butyl)-2-chloroacetamide (S14):**

Prepared according to General Acylation Procedure. *N*-(3,5-bis(trifluoromethyl)benzyl)-2-methylpropan-2-amine (**S13**) (157 mg, 0.52 mmol, 1.0 equiv), Et₃N (84 μ L, 0.62 mmol, 1.2 equiv), and chloroacetyl chloride (49 μ L, 0.62 mmol, 1.2 equiv) were stirred in CH₂Cl₂ (5 mL, 0.1 M) for 1 hour. The title compound afforded as a light-yellow solid (180 mg, 92%).

¹H NMR (600 MHz, CDCl₃) δ 7.83 (s, 1H), 7.69 (s, 2H), 4.80 (s, 2H), 3.92 (s, 2H), 1.45 (s, 9H) ppm.

¹³C NMR (151 MHz, CDCl₃) δ 167.8, 142.0, 132.8 (q, ²J_{C-F} = 33.5 Hz), 125.9 (q, ³J_{C-F} = 3.8 Hz), 123.2 (q, ¹J_{C-F} = 272.9 Hz), 121.8 (hept, ³J_{C-F} = 3.8 Hz), 59.2, 48.6, 43.8, 28.6 ppm.

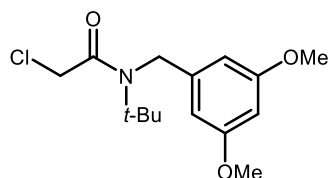
LRMS (EI) *m/z*: [M]⁺ calc'd. for C₁₅H₁₆ClF₆NO, 375.1, found 375.1.



***N*-(3,5-dimethoxybenzyl)-2-methylpropan-2-amine (S15):**

Prepared according to General Reductive Amination Procedure. 3,5-dimethoxybenzaldehyde (665 mg, 4.0 mmol, 1.0 equiv) and *tert*-butyl amine (0.50 mL, 4.8 mmol, 1.2 equiv) were stirred in MeOH (20 mL, 0.2 M) for 2 hours. After NaBH₄ (227 mg, 6.0 mmol, 1.5 equiv) was added, the reaction was stirred for an additional 1 hour. The title compound was obtained as a white solid (701 mg, 78%).

¹H NMR (400 MHz, CDCl₃) δ 6.51 (d, *J* = 2.1 Hz, 2H), 6.34 (t, *J* = 2.3 Hz, 1H), 3.79 (s, 6H), 3.67 (s, 2H), 1.17 (s, 9H) ppm. ¹H NMR is consistent with reported values.⁴

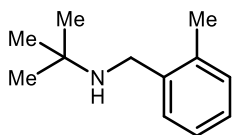


4 Padwa, A.; Kuethe, J. T. Additive and Vinylogous Pummerer Reactions of Amido Sulfoxides and Their Use in the Preparation of Nitrogen Containing Heterocycles. *J. Org. Chem.* **1998**, *63*, 4256-4268.

***N*-(*tert*-butyl)-2-chloro-*N*-(3,5-dimethoxybenzyl)acetamide (S16):**

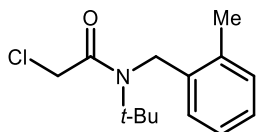
Prepared according to General Acylation Procedure. *N*-(3,5-dimethoxybenzyl)-2-methylpropan-2-amine (S15) (670 mg, 3.0 mmol, 1.0 equiv), Et₃N (0.50 mL, 3.6 mmol, 1.2 equiv), and chloroacetyl chloride (0.29 mL, 3.6 mmol, 1.2 equiv) were stirred in CH₂Cl₂ (30 mL, 0.1 M) for 1 hour. The title compound was obtained as a light-brown solid (899 mg, 100%).

¹H NMR (400 MHz, CDCl₃) δ 6.36 (t, J = 2.2 Hz, 1H), 6.34 (d, J = 2.2 Hz, 2H), 4.59 (d, J = 0.8 Hz, 2H), 3.97 (s, 2H), 3.78 (s, 6H), 1.47 (s, 9H) ppm. ¹H NMR spectrum is consistent with reported values.⁵

**2-methyl-*N*-(2-methylbenzyl)propan-2-amine (S17):**

Prepared according to General Reductive Amination Procedure. 2-methylbenzaldehyde (0.46 mL, 4.0 mmol, 1.0 equiv) and *tert*-butyl amine (0.73 mL, 4.8 mmol, 1.2 equiv) were stirred in MeOH (20 mL, 0.2 M) for 3 hours. After NaBH₄ (227 mg, 6.0 mmol, 1.5 equiv) was added, the reaction was stirred for an additional 2 hours. The title compound was obtained as a white solid (546 mg, 77%).

¹H NMR (400 MHz, cdcl₃) δ 7.33 – 7.24 (m, 1H), 7.21 – 7.11 (m, 3H), 3.70 (s, 2H), 2.37 (s, 3H), 1.20 (s, 9H) ppm. ¹H NMR spectrum is consistent with reported values.⁶

***N*-(*tert*-butyl)-2-chloro-*N*-(2-methylbenzyl)acetamide (S18):**

Prepared according to General Acylation Procedure. 2-methyl-*N*-(2-methylbenzyl)propan-2-amine (S17) (319 mg, 1.8 mmol, 1.0 equiv), Et₃N (0.28 mL, 2.0 mmol, 1.1 equiv), and chloroacetyl chloride (0.16 mL, 2.0 mmol, 1.1 equiv) were stirred in CH₂Cl₂ (18 mL, 0.1 M) for 3.5 hours, which afforded the title compound as a white solid (401 mg, 88%).

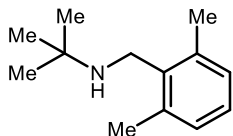
¹H NMR (600 MHz, CDCl₃) δ 7.25 – 7.15 (m, 4H), 4.54 (s, 2H), 3.89 (s, 2H), 2.29 (s, 3H), 1.46 (s, 9H) ppm.

5 Hamada, T.; Okuno, Y.; Ohmori, M.; Nishi, T.; Yonemitsu, O. Photochemical Synthesis of 1,2,3,4-Tetrahydroisoquinolin-3-ones and Oxindoles from *N*-Chloroacetyl Derivatives of Benzylamines and Anilines. Role of Intramolecular Exciplex Formation and *cis* Conformation of Amide Bonds. *Chem. Pharm. Bull.* **1981**, *29*, 128-136.

6 Franchi, P.; Casati, C.; Mezzina, E.; Lucarini, M. Kinetic control of the direction of inclusion of nitroxide cyclodextrines. *Org. Biomol. Chem.*, **2011**, *9*, 6396-6401.

^{13}C NMR (151 MHz, CDCl_3) δ 167.8, 136.3, 134.3, 130.7, 127.3, 127.3, 126.7, 124.6, 58.6, 46.7, 44.1, 28.3, 19.1 ppm.

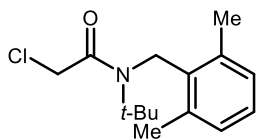
LRMS (EI) m/z : $[M]^+$ calc'd. for $\text{C}_{14}\text{H}_{20}\text{ClNO}$, 253.1, found 253.2.



***N*-(2,6-dimethylbenzyl)-2-methylpropan-2-amine (S19):**

Prepared according to General Reductive Amination Procedure. 2,6-dimethylbenzaldehyde (537 mg, 4.0 mmol, 1.0 equiv) and *tert*-butyl amine (1.20 mL, 8.0 mmol, 2.0 equiv) were stirred in MeOH (20 mL, 0.2 M) for 6 hours. After NaBH_4 (227 mg, 6.0 mmol, 1.5 equiv) was added, the reaction was stirred for an additional 1.5 hours. The title compound was obtained as a white solid (708 mg, 93%).

^1H NMR (600 MHz, CDCl_3) δ 7.07 – 6.98 (m, 3H), 3.72 (s, 2H), 2.39 (s, 6H), 1.45 (s, 1H), 1.21 (s, 9H). ^1H NMR spectrum is consistent with reported values.⁷



***N*-(*tert*-butyl)-2-chloro-*N*-(2,6-dimethylbenzyl)acetamide (S20):**

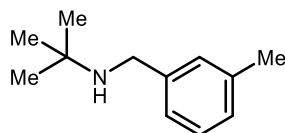
Prepared according to General Acylation Procedure. *N*-(2,6-dimethylbenzyl)-2-methylpropan-2-amine (S19) (574 mg, 3.0 mmol, 1.0 equiv), Et_3N (0.46 mL, 3.3 mmol, 1.1 equiv), and chloroacetyl chloride (0.26 mL, 3.3 mmol, 1.1 equiv) were stirred in CH_2Cl_2 (30 mL, 0.1 M) for 14 hours, which afforded the title compound as a yellow solid (654 mg, 81%).

^1H NMR (600 MHz, CDCl_3) δ 7.08 (t, $J = 7.5$ Hz, 1H), 7.00 (d, $J = 7.5$ Hz, 2H), 4.65 (s, 2H), 4.11 (s, 2H), 2.36 (s, 6H), 1.39 (s, 9H) ppm.

^{13}C NMR (151 MHz, CDCl_3) δ 168.6, 136.0, 134.8, 130.1, 127.4, 59.5, 46.8, 45.2, 28.3, 28.3, 21.1 ppm.

LRMS (EI) m/z : $[M]^+$ calc'd. for $\text{C}_{15}\text{H}_{22}\text{ClNO}$, 267.1, found 267.1.

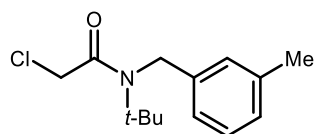
7 Franchi, P.; Casati, C.; Mezzina, E.; Lucarini, M. Kinetic control of the direction of inclusion of nitroxide cyclodextrines. *Org. Biomol. Chem.*, **2011**, *9*, 6396-6401.



2-methyl-*N*-(3-methylbenzyl)propan-2-amine (S21):

Prepared according to General Reductive Amination Procedure. 3-methylbenzaldehyde (0.71 mL, 6.0 mmol, 1.0 equiv) and *tert*-butyl amine (1.10 mL, 7.2 mmol, 1.2 equiv) were stirred in MeOH (30 mL, 0.2 M) for 15 hours. After NaBH₄ (340 mg, 9.0 mmol, 1.5 equiv) was added, the reaction was stirred for an additional 2 hours. The title compound was obtained as a light-yellow oil (990 mg, 93%).

¹H NMR (400 MHz, CDCl₃) δ 7.23 – 7.10 (m, 3H), 7.04 (d, *J* = 7.5 Hz, 1H), 3.69 (s, 2H), 2.34 (d, *J* = 0.7 Hz, 3H), 1.18 (s, 9H) ppm. ¹H NMR spectrum is consistent with reported values.⁸



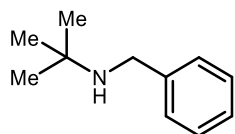
***N*-(*tert*-butyl)-2-chloro-*N*-(3-methylbenzyl)acetamide (S22):**

Prepared according to General Reductive Amination Procedure. 2-methyl-*N*-(3-methylbenzyl)propan-2-amine (S21) (443 mg, 2.5 mmol, 1.0 equiv) Et₃N (0.38 mL, 2.8 mmol, 1.1 equiv), and chloroacetyl chloride (0.22 mL, 2.8 mmol, 1.1 equiv) were stirred in CH₂Cl₂ (25 mL, 0.1 M) for 1 hour, which afforded the title compound as a white solid (593 mg, 94%).

¹H NMR (600 MHz, CDCl₃) δ 7.21 (t, *J* = 7.5 Hz, 1H), 7.04 (d, *J* = 7.6 Hz, 1H), 6.97 (s, 1H), 6.96 (d, *J* = 8.5 Hz, 1H), 4.59 (s, 2H), 3.95 (s, 2H), 2.31 (s, 3H), 1.42 (s, 9H) ppm.

¹³C NMR (151 MHz, CDCl₃) δ 167.5, 138.7, 138.4, 128.9, 128.1, 126.0, 122.3, 77.4, 77.2, 77.0, 58.6, 48.6, 44.2, 28.3, 21.4 ppm.

LRMS (EI) *m/z*: [M]⁺ calc'd. for C₁₄H₂₀ClNO, 253.1, found 253.2.

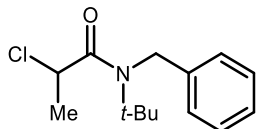


***N*-benzyl-2-methylpropan-2-amine (S23):**

⁸ Jankowski, K.; Harvey, R. A general one-pot, three-component mono *N*-alkylation of amines and amine derivatives in lithium perchlorate/diethyl ether solution. *Synthesis*, **2005**, *4*, 627-633.

Prepared according to General Reductive Amination Procedure. Benzaldehyde (1.02 mL, 10.0 mmol, 1.0 equiv) and *tert*-butyl amine (1.26 mL, 12.0 mmol, 1.2 equiv) were stirred in MeOH (50 mL, 0.2 M) for 4 hours. After NaBH₄ (567 mg, 15.0 mmol, 1.5 equiv) was added, the reaction was stirred for an additional 1 hour. The title compound was obtained as a clear oil (1061 mg, 100%).

¹H NMR (400 MHz, cdcl₃) δ 7.38 – 7.28 (m, 4H), 7.25 – 7.20 (m, 1H), 3.73 (s, 2H), 1.18 (s, 9H) ppm. ¹H NMR spectrum is consistent with reported values.⁹



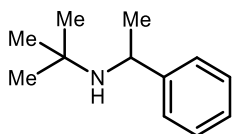
N-benzyl-N-(*tert*-butyl)-2-chloropropanamide (S24):

Prepared according to General Acylation Procedure. *N*-benzyl-2-methylpropan-2-amine (**S23**) (264 mg, 1.6 mmol, 1.0 equiv), Et₃N (0.26 mL, 1.9 mmol, 1.2 equiv), and 2-chloropropionyl chloride (0.18 mL, 1.9 mmol, 1.2 equiv) were stirred in CH₂Cl₂ (16 mL, 0.1 M) for 1 hour. Purification on silica gel (10% EtOAc/hexanes) afforded the title compound as a white solid (276 mg, 68%).

¹H NMR (600 MHz, CDCl₃) δ 7.38 (t, J = 7.7 Hz, 2H), 7.28 (t, J = 7.4 Hz, 1H), 7.17 (d, J = 7.2 Hz, 2H), 4.82 (d, J = 18.9 Hz, 1H), 4.62 (d, J = 18.9 Hz, 1H), 4.32 (q, J = 6.4 Hz, 1H), 1.60 (d, J = 6.4 Hz, 3H), 1.45 (s, 9H) ppm.

¹³C NMR (151 MHz, CDCl₃) δ 170.5, 139.2, 129.1, 127.3, 125.3, 58.5, 52.1, 48.3, 28.4, 21.4 ppm.

LRMS (EI) m/z: [M]⁺ calc'd. for C₁₄H₂₀ClNO, 253.1, found 253.2.

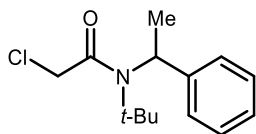


2-methyl-N-(1-phenylethyl)propan-2-amine (S25):

To a round bottomed flask charged with (1-bromoethyl)benzene (0.41 mL, 3.0 mmol, 1.0 equiv) was added MeCN (15 mL, 0.2 M), *tert*-butylamine (0.38 mL, 3.6 mmol, 1.2 equiv), and K₂CO₃ (829 mg, 6.0 mmol, 2.0 equiv). The resulting suspension was heated at reflux for 16 hours. After cooling to room temperature, the reaction was quenched with H₂O and extracted with EtOAc (3x). The combined organic layers were washed with 1 M HCl (aq), and the resulting aqueous layer was brought to pH 14 with 2 M NaOH (aq) extracted with CH₂Cl₂ (3x). The combined organic layers were dried over MgSO₄, filtered, and concentrated under reduced pressure to afford the title compound as a colorless oil (363 mg, 68%).

9 Niu, Z.; Zhang, W.; Lan, P. C.; Aguila, B.; Ma, S. Promoting frustrated lewis pairs for heterogeneous chemoselective hydrogenation via the tailored pore environment within metal-organic frameworks. *Angew. Chem. Int. Ed.* **2019**, *58*, 7420-7424.

$^1\text{H NMR}$ (400 MHz, CDCl_3) δ 7.41 – 7.33 (m, 2H), 7.33 – 7.23 (m, 2H), 7.23 – 7.14 (m, 1H), 3.95 (q, $J = 6.7$ Hz, 1H), 1.31 (d, $J = 6.7$ Hz, 3H), 1.02 (s, 9H) ppm. $^1\text{H NMR}$ spectrum is consistent with reported values.¹⁰



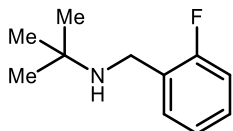
***N*-(*tert*-butyl)-2-chloro-*N*-(1-phenylethyl)acetamide (S26):**

Prepared according to General Acylation Procedure. 2-methyl-*N*-(1-phenylethyl)propan-2-amine (**S25**) (266 mg, 1.5 mmol, 1.0 equiv), Et_3N (0.25 mL, 1.8 mmol, 1.2 equiv), and chloroacetyl chloride (0.14 mL, 1.8 mmol, 1.2 equiv) were stirred in CH_2Cl_2 (15 mL, 0.1 M) for 4 hours. Purification on silica gel (30% EtOAc /hexanes) afforded the title compound as a light-yellow oil (292 mg, 77%).

$^1\text{H NMR}$ (600 MHz, CDCl_3) δ 7.38 (dd, $J = 8.3, 7.2$ Hz, 2H), 7.33 – 7.26 (m, 3H), 5.13 (q, $J = 7.0$ Hz, 1H), 3.76 (d, $J = 12.7$ Hz, 1H), 3.45 (d, $J = 11.9$ Hz, 1H), 1.79 (d, $J = 7.1$ Hz, 3H), 1.56 (s, 9H) ppm.

$^{13}\text{C NMR}$ (151 MHz, CDCl_3) δ 169.0, 143.1, 129.3, 127.3, 125.6, 60.0, 53.0, 44.7, 29.4, 21.0 ppm.

LRMS (EI) m/z : $[\text{M}]^+$ calc'd. for $\text{C}_{14}\text{H}_{20}\text{ClNO}$, 253.1, found 253.1.



***N*-(2-fluorobenzyl)-2-methylpropan-2-amine (S27):**

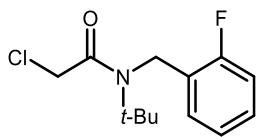
Prepared according to General Reductive Amination Procedure. 2-fluorobenzaldehyde (0.42 mL, 4.0 mmol, 1.0 equiv) and *tert*-butyl amine (0.73 mL, 4.8 mmol, 1.2 equiv) were stirred in MeOH (20 mL, 0.2 M) for 3 hours. After NaBH_4 (227 mg, 4.8 mmol, 1.5 equiv) was added, the reaction was stirred for an additional 1.5 hours. The title compound was obtained as a clear oil (508 mg, 70%).

$^1\text{H NMR}$ (600 MHz, CDCl_3) δ 7.39 (td, $J = 7.6, 1.8$ Hz, 1H), 7.21 (tdd, $J = 7.5, 5.2, 1.8$ Hz, 1H), 7.09 (td, $J = 7.5, 1.2$ Hz, 1H), 7.01 (ddd, $J = 9.8, 8.2, 1.2$ Hz, 1H), 3.78 (s, 2H), 1.19 (s, 9H) ppm.

$^{13}\text{C NMR}$ (151 MHz, CDCl_3) δ 161.3 (d, $^1J_{\text{C-F}} = 245.0$ Hz), 130.6 (d, $^3J_{\text{C-F}} = 4.9$ Hz), 128.6 (d, $^3J_{\text{C-F}} = 7.9$ Hz), 128.5, 124.3 (d, $^4J_{\text{C-F}} = 3.5$ Hz), 115.4 (d, $^2J_{\text{C-F}} = 21.9$ Hz), 51.0, 40.9 (d, $^3J_{\text{C-F}} = 3.5$ Hz), 29.3 ppm.

LRMS (EI) m/z : $[\text{M}]^+$ calc'd. for $\text{C}_{11}\text{H}_{16}\text{FN}$, 181.1, found 181.2.

10 Cliffe, I. A.; Crossley, R.; Shepherd, R. G. Sterically Hindered Lithium Dialkylamides; A Novel Synthesis of Lithium Dialkylamides from *N-t*-Alkyl-*N*-benzylideneamines and the Isolation of Highly Hindered *s*-Alkyl-*t*-alkylamines. *Synthesis* **1985**, *12*, 1138-1140.



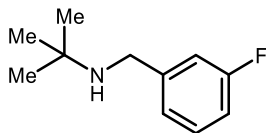
***N*-(*tert*-butyl)-2-chloro-*N*-(2-fluorobenzyl)acetamide (S28):**

Prepared according to General Acylation Procedure. *N*-(2-fluorobenzyl)-2-methylpropan-2-amine (S27) (399 mg, 2.0 mmol, 1.0 equiv), Et₃N (0.31 mL, 2.2 mmol, 1.1 equiv), and chloroacetyl chloride (0.16 mL, 2.0 mmol, 1.1 equiv) were stirred in CH₂Cl₂ (20 mL, 0.1 M) for 3 hours. Purification on silica gel (30% EtOAc/hexanes) afforded the title compound as a white solid (473 mg, 92%).

¹H NMR (600 MHz, CDCl₃) δ 7.29 (dtd, *J* = 7.4, 6.3, 5.2, 1.8 Hz, 1H), 7.23 (t, *J* = 7.2 Hz, 1H), 7.21 – 7.15 (t, *J* = 7.2 Hz, 1H), 7.08 (ddd, *J* = 10.3, 8.2, 1.2 Hz, 1H), 4.69 (s, 2H), 3.98 (s, 2H), 1.46 (s, 9H) ppm.

¹³C NMR (151 MHz, CDCl₃) δ 167.77, 159.79 (d, ¹*J*_{C-F} = 245.8 Hz), 129.21 (d, ³*J*_{C-F} = 7.9 Hz), 127.06 (d, ³*J*_{C-F} = 3.8 Hz), 125.87 (d, ²*J*_{C-F} = 13.9 Hz), 124.74 (d, ⁴*J*_{C-F} = 3.8 Hz), 115.80 (d, ²*J*_{C-F} = 20.8 Hz), 58.89, 44.15, 42.99 (d, ³*J*_{C-F} = 5.9 Hz), 28.40.

LRMS (EI) *m/z*: [M]⁺ calc'd. for C₁₃H₁₇ClFNO, 257.1, found 257.1.



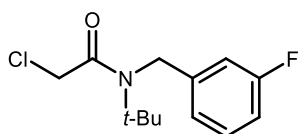
***N*-(3-fluorobenzyl)-2-methylpropan-2-amine (S29):**

Prepared according to General Reductive Amination Procedure. 3-Fluorobenzaldehyde (0.42 mL, 4.0 mmol, 1.0 equiv) and *tert*-butyl amine (0.50 mL, 4.8 mmol, 1.2 equiv) were stirred in MeOH (20 mL, 0.2 M) for 3 hours. After NaBH₄ (227 mg, 6.0 mmol, 1.5 equiv) was added, the reaction was stirred for an additional 14 hours. The title compound was obtained as a white solid (633 mg, 87%).

¹H NMR (400 MHz, CDCl₃) δ 7.30 – 7.23 (m, 1H), 7.19 – 7.10 (m, 2H), 6.96 – 6.88 (m, 1H), 3.75 (s, 2H), 1.20 (s, 9H) ppm.

¹³C NMR (151 MHz, CDCl₃) δ 163.1 (d, ¹*J*_{C-F} = 245.6 Hz), 130.0 (d, ³*J*_{C-F} = 8.3 Hz), 124.3, 122.4 (d, ⁴*J*_{C-F} = 2.9 Hz), 115.7 (d, ²*J*_{C-F} = 21.4 Hz), 114.1 (d, ²*J*_{C-F} = 21.2 Hz), 64.7, 46.7, 28.9 ppm.

LRMS (EI) *m/z*: [M]⁺ calc'd. for C₁₁H₁₆FN, 181.1, found 181.0.



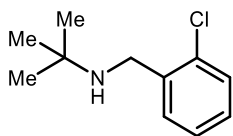
***N*-(*tert*-butyl)-2-chloro-*N*-(3-fluorobenzyl)acetamide (S30):**

Prepared according to General Acylation Procedure. *N*-(3-fluorobenzyl)-2-methylpropan-2-amine (**S29**) (544 mg, 3.0 mmol, 1.0 equiv), Et₃N (0.50 mL, 3.6 mmol, 1.2 equiv), and chloroacetyl chloride (0.29 mL, 3.6 mmol, 1.2 equiv) were stirred in CH₂Cl₂ (30 mL, 0.1 M) for 2 hours. Purification on silica gel (10-20% EtOAc/hexanes) afforded the title compound as a white solid (601 mg, 78%).

¹H NMR (400 MHz, CDCl₃) δ 7.35 (td, *J* = 8.0, 5.8 Hz, 1H), 7.03 – 6.95 (m, 2H), 6.95 – 6.87 (m, 1H), 4.65 (s, 2H), 3.95 (s, 2H), 1.45 (s, 9H) ppm.

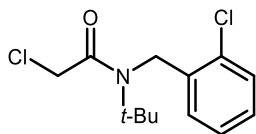
¹³C NMR (151 MHz, CDCl₃) δ 167.7, 163.5 (d, ¹*J*_{C-F} = 247.7 Hz), 141.7 (d, ³*J*_{C-F} = 6.6 Hz), 130.9 (d, ³*J*_{C-F} = 8.3 Hz), 121.1 (d, ⁴*J*_{C-F} = 2.8 Hz), 114.6 (d, ²*J*_{C-F} = 21.1 Hz), 112.7 (d, ²*J*_{C-F} = 22.3 Hz), 59.0, 48.6 (d, ⁴*J*_{C-F} = 2.0 Hz), 44.2, 28.6 ppm.

LRMS (EI) *m/z*: [M]⁺ calc'd. for C₁₃H₁₇ClFNO, 257.1, found 257.1.

***N*-(2-chlorobenzyl)-2-methylpropan-2-amine (S31):**

Prepared according to General Reductive Amination Procedure. 2-chlorobenzaldehyde (0.45 mL, 4.0 mmol, 1.0 equiv) and *tert*-butyl amine (0.73 mL, 4.8 mmol, 1.2 equiv) were stirred in MeOH (20 mL, 0.2 M) for 3 hours. After NaBH₄ (227 mg, 6.0 mmol, 1.5 equiv) was added, the reaction was stirred for an additional 4 hours. The title compound was obtained as a clear oil (515 mg, 65%).

¹H NMR (600 MHz, CDCl₃) δ 7.45 (dd, *J* = 7.5, 1.7 Hz, 1H), 7.33 (dd, *J* = 7.9, 1.4 Hz, 1H), 7.22 (td, *J* = 7.5, 1.4 Hz, 1H), 7.17 (td, *J* = 7.6, 1.8 Hz, 1H), 3.82 (s, 2H), 1.20 (s, 9H) ppm. ¹H NMR spectrum is consistent with reported values.¹¹

***N*-(*tert*-butyl)-2-chloro-*N*-(2-chlorobenzyl)acetamide (S32):**

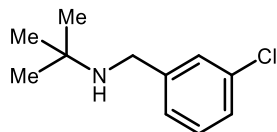
Prepared according to General Acylation Procedure. *N*-(2-chlorobenzyl)-2-methylpropan-2-amine (**S31**) (395 mg, 2.0 mmol, 1.0 equiv), Et₃N (0.31 mL, 2.2 mmol, 1.1 equiv), and chloroacetyl chloride (0.18 mL, 2.2 mmol, 1.1 equiv) were stirred in CH₂Cl₂ (20 mL, 0.1 M) for 3.5 hours. Purification on silica gel (10-20% EtOAc/hexanes) afforded the title compound as a light yellow oil (435 mg, 79%).

11 Franchi, P.; Casati, C.; Mezzina, E.; Lucarini, M. Kinetic control of the direction of inclusion of nitroxide cyclodextrines. *Org. Biomol. Chem.*, **2011**, *9*, 6396-6401.

$^1\text{H NMR}$ (600 MHz, CDCl_3) δ 7.40 (d, $J = 8.0$ Hz, 1H), 7.32 (t, $J = 7.5$ Hz, 1H), 7.29 – 7.23 (m, 2H), 4.67 (s, 2H), 3.92 (s, 2H), 1.46 (s, 9H) ppm.

$^{13}\text{C NMR}$ (151 MHz, CDCl_3) δ 167.8, 136.0, 132.1, 130.1, 128.9, 127.5, 126.8, 59.0, 47.0, 44.1, 28.4 ppm.

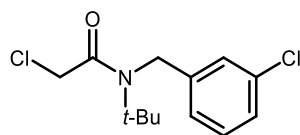
LRMS (EI) m/z : $[\text{M}]^+$ calc'd. for $\text{C}_{13}\text{H}_{17}\text{Cl}_2\text{NO}$, 273.1, found 273.1.



***N*-(3-chlorobenzyl)-2-methylpropan-2-amine (S33):**

Prepared according to General Reductive Amination Procedure. 3-chlorobenzaldehyde (0.45 mL, 4.0 mmol, 1.0 equiv) and *tert*-butyl amine (0.73 mL, 4.8 mmol, 1.2 equiv) were stirred in MeOH (20 mL, 0.2 M) for 4.5 hours. After NaBH_4 (227 mg, 6.0 mmol, 1.5 equiv) was added, the reaction was stirred for an additional 1.5 hours. The title compound was obtained as a light-yellow oil (744 mg, 94%).

$^1\text{H NMR}$ (400 MHz, CDCl_3) δ 7.36 (s, 1H), 7.24 – 7.14 (m, 3H), 3.70 (s, 2H), 1.17 (s, 9H) ppm. $^1\text{H NMR}$ spectrum is consistent with reported values.¹²



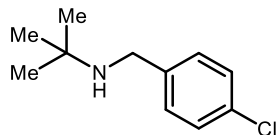
***N*-(*tert*-butyl)-2-chloro-*N*-(3-chlorobenzyl)acetamide (S34):**

Prepared according to General Acylation Procedure. *N*-(3-chlorobenzyl)-2-methylpropan-2-amine (**S33**) (395 mg, 2.0 mmol, 1.0 equiv), Et_3N (0.15 mL, 2.2 mmol, 1.1 equiv), and chloroacetyl chloride (0.18 mL, 2.2 mmol, 1.1 equiv) were stirred in CH_2Cl_2 (20 mL, 0.1 M) for 3.5 hours, which afforded the title compound as a white solid (436 mg, 72%).

$^1\text{H NMR}$ (400 MHz, CDCl_3) δ 7.36 – 7.23 (m, 2H), 7.19 (s, 1H), 7.09 (d, $J = 7.8$ Hz, 1H), 4.64 (s, 2H), 3.95 (s, 2H), 1.45 (s, 9H) ppm.

$^{13}\text{C NMR}$ (101 MHz, CDCl_3) δ 167.6, 140.9, 135.2, 130.4, 127.8, 125.7, 123.5, 58.9, 48.4, 44.0, 28.4 ppm.

LRMS (EI) m/z : $[\text{M}]^+$ calc'd. for $\text{C}_{13}\text{H}_{17}\text{Cl}_2\text{NO}$, 273.1, found 273.1.



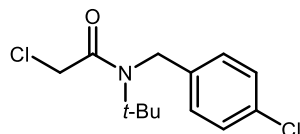
N-(4-chlorobenzyl)-2-methylpropan-2-amine (S35):

Prepared according to General Reductive Amination Procedure. 4-Chlorobenzaldehyde (562 mg, 4.0 mmol, 1.0 equiv) and *tert*-butyl amine (0.50 mL, 4.8 mmol, 1.2 equiv) were stirred in MeOH (20 mL, 0.2 M) for 17 hours. After NaBH₄ (227 mg, 6.0 mmol, 1.5 equiv) was added, the reaction was stirred for an additional 30 min. The title compound was obtained as a white solid (676 mg, 85%).

¹H NMR (600 MHz, CDCl₃) δ 7.29 – 7.26 (m, 4H), 3.70 (s, 2H), 1.17 (s, 9H) ppm.

¹³C NMR (151 MHz, CDCl₃) δ 140.2, 132.6, 129.8, 128.6, 51.0, 46.7, 29.3 ppm.

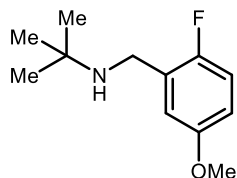
LRMS (EI) m/z: [M]⁺ calc'd. for C₁₁H₁₆ClN, 197.1, found 197.1.



N-(*tert*-butyl)-2-chloro-N-(4-chlorobenzyl)acetamide (S36):

Prepared according to General Acylation Procedure. *N*-(4-chlorobenzyl)-2-methylpropan-2-amine (S35) (593 mg, 3.0 mmol, 1.0 equiv), Et₃N (0.50 mL, 3.6 mmol, 1.2 equiv), and chloroacetyl chloride (0.29 mL, 3.6 mmol, 1.2 equiv) were stirred in CH₂Cl₂ (30 mL, 0.1 M) for 1 hour. The title compound was obtained as a yellow oil (823 mg, 100%).

¹H NMR (400 MHz, CDCl₃) δ 7.38 (d, J = 8.5 Hz, 2H), 7.17 (d, J = 8.7 Hz, 2H), 4.65 (s, 2H), 3.97 (s, 2H), 1.46 (s, 9H) ppm. ¹H NMR spectrum is consistent with reported values.¹³



N-(2-fluoro-5-methoxybenzyl)-2-methylpropan-2-amine (S37):

Prepared according to General Reductive Amination Procedure. 2-fluoro-5-methoxybenzaldehyde (0.25 mL, 2.0 mmol, 1.0 equiv) and *tert*-butyl amine (0.41 mL, 2.4 mmol, 1.2 equiv) were stirred in MeOH (4 mL,

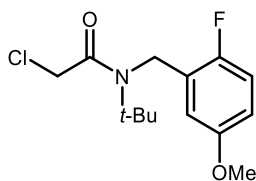
13 Pedroni, J.; Boghi, M.; Saget, T.; Cramer, N. Access to β-Lactams by Enantioselective Palladium(0)-Catalyzed C(sp³)—H Alkylation. *Angew. Chem. Int. Ed.* **2014**, *53*, 9064-9067.

0.5 M) for 14 hours. After NaBH₄ (114 mg, 3.0 mmol, 1.5 equiv) was added, the reaction was stirred for an additional 1 hour. The title compound was obtained as a light-yellow oil (386 mg, 46%).

¹H NMR (400 MHz, CDCl₃) δ 6.95 – 6.86 (m, 2H), 6.69 (ddd, J = 8.9, 4.0, 3.2 Hz, 1H), 3.75 (s, 3H), 3.72 (s, 2H), 1.17 (s, 9H) ppm.

¹³C NMR (101 MHz, CDCl₃) δ 155.8 (d, ⁴J_{C-F} = 2.0 Hz), 155.5 (d, ¹J_{C-F} = 237.4 Hz), 129.1 (d, ²J_{C-F} = 16.8 Hz), 115.7 (d, ²J_{C-F} = 23.8 Hz), 115.4 (d, ³J_{C-F} = 4.7 Hz), 113.2 (d, ³J_{C-F} = 8.2 Hz), 55.8, 50.9, 41.0 (d, ³J_{C-F} = 2.9 Hz), 29.1 ppm.

LRMS (EI) m/z: [M]⁺ calc'd. for C₁₂H₁₈FNO, 211.1, found 211.2.



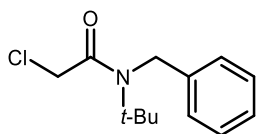
N-(tert-butyl)-2-chloro-N-(2-fluoro-5-methoxybenzyl)acetamide (S38):

Prepared according to General Acylation Procedure. *N*-(2-fluoro-5-methoxybenzyl)-2-methylpropan-2-amine (**S37**) (211 mg, 1.0 mmol, 1.0 equiv), Et₃N (0.15 mL, 1.1 mmol, 1.1 equiv), and chloroacetyl chloride (0.09 mL, 1.1 mmol, 1.1 equiv) were stirred in CH₂Cl₂ (10 mL, 0.1 M) for 4.5 hours, which afforded the title compound as a tan solid (263 mg, 91%).

¹H NMR (400 MHz, CDCl₃) δ 6.99 (t, J = 9.1 Hz, 1H), 6.80 – 6.72 (m, 1H), 6.76 – 6.70 (m, 1H), 4.64 (s, 2H), 3.98 (s, 2H), 3.76 (s, 3H), 1.46 (s, 9H) ppm.

¹³C NMR (101 MHz, CDCl₃) δ 167.8, 156.4 (d, ⁴J_{C-F} = 2.0 Hz), 154.0 (d, ¹J_{C-F} = 238.2 Hz), 126.8 (d, ²J_{C-F} = 15.7 Hz), 116.4 (d, ²J_{C-F} = 22.9 Hz), 113.3 (d, ³J_{C-F} = 7.9 Hz), 112.6 (d, ³J_{C-F} = 3.8 Hz), 58.9, 55.9, 44.1, 43.2 (d, ³J_{C-F} = 5.1 Hz), 28.4 ppm.

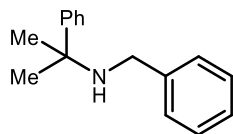
LRMS (EI) m/z: [M]⁺ calc'd. for C₁₄H₁₉ClFNO₂, 287.1, found 287.1.



N-benzyl-N-(tert-butyl)-2-chloroacetamide (S39):

Prepared according to General Acylation Procedure. *N*-benzyl-2-methylpropan-2-amine (**S23**) (688 mg, 4.2 mmol, 1.0 equiv), Et₃N (0.64 mL, 4.6 mmol, 1.1 equiv), and chloroacetyl chloride (0.37 mL, 4.6 mmol, 1.1 equiv) were stirred in CH₂Cl₂ (42 mL, 0.1 M) for 3.5 hours. The title compound was afforded as a white solid (946 mg, 99%).

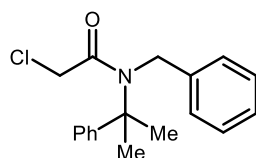
¹H NMR (400 MHz, cdCl₃) δ 7.38 (t, J = 7.4 Hz, 2H), 7.29 (t, J = 7.3 Hz, 1H), 7.20 (d, J = 6.9 Hz, 2H), 4.66 (s, 2H), 3.98 (s, 2H), 1.46 (s, 9H) ppm. ¹H NMR spectrum is consistent with reported values.¹⁴



N-benzyl-2-phenylpropan-2-amine (S40):

Prepared according to General Reductive Amination Procedure. Benzaldehyde (0.20 mL, 2.0 mmol, 1.0 equiv) and 2-phenylpropan-2-amine (0.35 mL, 2.4 mmol, 1.2 equiv) were stirred in MeOH (10 mL, 0.2 M) for 14 hours. After NaBH₄ (114 mg, 3.0 mmol, 1.5 equiv) was added, the reaction was stirred for an additional 2 hours. The title compound was obtained as a clear oil (414 mg, 92%).

¹H NMR (600 MHz, CDCl₃) δ 7.49 (d, J = 7.7 Hz, 2H), 7.32 (t, J = 7.6 Hz, 2H), 7.28 – 7.22 (m, 4H), 7.21 – 7.15 (m, 2H), 3.44 (s, 2H), 1.49 (s, 6H) ppm. ¹H NMR spectrum is consistent with reported values.¹⁵



N-benzyl-2-chloro-N-(2-phenylpropan-2-yl)acetamide (S41):

Prepared according to General Acylation Procedure. N-benzyl-2-phenylpropan-2-amine (**S40**) (225 mg, 1.0 mmol, 1.0 equiv), Et₃N (0.15 mL, 1.1 mmol, 1.1 equiv), and chloroacetyl chloride (0.09 mL, 1.1 mmol, 1.1 equiv) were stirred in CH₂Cl₂ (10 mL, 0.1 M) for 16 hours. Purification on silica gel (10% EtOAc/hexanes) afforded the title compound as a white solid (138 mg, 46%).

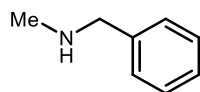
¹H NMR (600 MHz, CDCl₃) δ 7.40 (t, J = 7.5 Hz, 2H), 7.32 (dd, J = 9.4, 5.9 Hz, 7H), 7.22 (hept, J = 4.2 Hz, 1H), 4.92 (s, 2H), 3.89 (s, 2H), 1.70 (s, 6H) ppm.

¹³C NMR (151 MHz, CDCl₃) δ 167.9, 148.1, 138.7, 129.2, 128.7, 127.7, 126.8, 126.4, 124.4, 63.1, 49.5, 43.7, 29.4 ppm.

LRMS (EI) m/z: [M]⁺ calc'd. for C₁₈H₂₀ClNO, 301.1, found 301.1.

14 Pedroni, J.; Boghi, M.; Saget, T.; Cramer, N. Access to β-Lactams by Enantioselective Palladium(0)-Catalyzed C(sp³)-H Alkylation. *Angew. Chem. Int. Ed.* **2014**, *126*, 9210-9213.

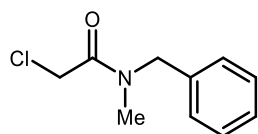
15 Milburn, R. R.; Snieckus, V. *ortho*-Anisylsufonyl as a protecting group for secondary amines: mild Ni⁰-catalyzed hydrodesulfonylation. *Angew. Chem. Int. Ed.* **2004**, *43*, 892-893.



***N*-methyl-1-phenylmethanamine (S42):**

Prepared according to General Reductive Amination Procedure. Benzaldehyde (0.41 mL, 4.0 mmol, 1.0 equiv) and methanamine (0.37 mL, 4.8 mmol, 1.2 equiv) were stirred in MeOH (20 mL, 0.2 M) for 2 hours. After NaBH₄ (227 mg, 6.0 mmol, 1.5 equiv) was added, the reaction was stirred for an additional 30 min. The title compound was obtained as a white solid (479 mg, 99%).

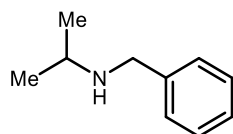
¹H NMR (400 MHz, CDCl₃) δ 7.36 – 7.30 (m, 4H), 7.29 – 7.22 (m, 1H), 3.75 (s, 2H), 2.46 (s, 3H), 1.59 (s, 1H) ppm. ¹H NMR spectrum is consistent with reported values.¹⁶



***N*-benzyl-2-chloro-*N*-methylacetamide (S43):**

Prepared according to General Acylation Procedure. *N*-methyl-1-phenylmethanamine (**S42**) (364 mg, 3.0 mmol, 1.0 equiv), Et₃N (0.46 mL, 3.3 mmol, 1.1 equiv), and chloroacetyl chloride (0.26 mL, 1.1 mmol, 1.1 equiv) were stirred in CH₂Cl₂ (30 mL, 0.1 M) for 30 min. Purification on silica gel (10-30% EtOAc/hexanes) afforded the title compound as a clear oil (401 mg, 68%).

¹H NMR (600 MHz, CDCl₃) δ 7.40 – 7.26 (m, 3H), 7.26 – 7.24 (m, 1H), 7.19 (d, J = 7.5 Hz, 1H), 4.60 (s, 2H), 4.12 (d, J = 22.3 Hz, 2H), 2.99 (d, J = 16.5 Hz, 3H) ppm. ¹H NMR spectrum is consistent with reported values.¹⁷



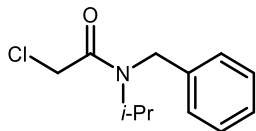
***N*-benzylpropan-2-amine (S44):**

16 Ji, P.; Manna, K.; Lin, Z.; Feng, X.; Urban, A.; Song, Y.; Lin, W. Single-site cobalt catalysts at new Zr₁₂(μ₃-O)₈(μ₃-OH)₈(μ₂-OH)₆ metal-organic framework nodes for highly active e hydrogenation of nitroarenes, nitriles and isocyanides. *J. Am. Chem. Soc.* **2017**, *139*, 7004-7011.

17 Pedroni, J.; Boghi, M.; Saget, T.; Cramer, N. Access to β-Lactams by Enantioselective Palladium(0)-Catalyzed C(sp³)-H Alkylation. *Angew. Chem. Int. Ed.* **2014**, *126*, 9210-9213.

Prepared according to General Reductive Amination Procedure. Benzaldehyde (0.41 mL, 4.0 mmol, 1.0 equiv) and propan-2-amine (0.39 mL, 4.8 mmol, 1.2 equiv) were stirred in MeOH (20 mL, 0.2 M) for 2 hours. After NaBH₄ (227 mg, 6.0 mmol, 1.5 equiv) was added, the reaction was stirred for an additional 30 min. The title compound was obtained as a yellow solid (557 mg, 93%).

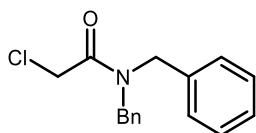
¹H NMR (400 MHz, CDCl₃) δ 7.32 (d, J = 4.4 Hz, 4H), 7.26 – 7.22 (m, 1H), 3.78 (s, 2H), 2.85 (h, J = 6.2 Hz, 1H), 1.10 (d, J = 6.2 Hz, 6H) ppm. ¹H NMR spectrum is consistent with reported values.¹⁸



N-benzyl-2-chloro-N-isopropylacetamide (S45):

Prepared according to General Acylation Procedure. *N*-benzylpropan-2-amine (**S44**) (448 mg, 3.0 mmol, 1.0 equiv), Et₃N (0.46 mL, 3.3 mmol, 1.1 equiv), and chloroacetyl chloride (0.26 mL, 3.3 mmol, 1.1 equiv) were stirred in CH₂Cl₂ (30 mL, 0.1 M) for 30 min. Purification on silica gel (10-30% EtOAc/hexanes) afforded the title compound as a clear oil (414 mg, 61%). Mixture of rotamers (H* denotes major rotamer and H denotes minor rotamer).

¹H NMR (600 MHz, CDCl₃) δ 7.36 (t, J = 7.6 Hz, 2(H+H*)), 7.29 (t, J = 7.7 Hz, 4(H+H*)), 7.22 (t, J = 8.1 Hz, 4(H+H*)), 4.79 (spt, J = 6.8 Hz, 1H*), 4.54 (m, 4(H+H*)), 4.22 (spt, J = 6.8 Hz, 1H), 4.20 (s, 2H*), 3.91 (s, 2H), 1.20 (d, J = 6.6 Hz, 3H), 1.15 (d, J = 6.8 Hz, 3H*) ppm. ¹H NMR spectrum is consistent with reported values.¹⁹



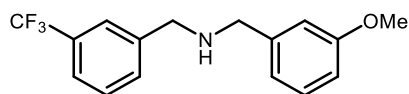
N,N-dibenzyl-2-chloroacetamide (S46):

Prepared according to General Acylation Procedure. Dibenzylamine (0.22 mL, 2.0 mmol, 1.0 equiv), Et₃N (0.31 mL, 2.2 mmol, 1.1 equiv), and chloroacetyl chloride (0.18 mL, 2.2 mmol, 1.1 equiv) were stirred in CH₂Cl₂ (20 mL, 0.1 M) for 20 min. Purification on silica gel (10-30% EtOAc/hexanes) afforded the title compound as a clear oil. (307 mg, 56%).

18 Rauser, M.; Eckert, R.; Gerbershagen, M.; Niggemann, M. Catalyst-free reductive coupling of aromatic and aliphatic nitro compounds with organohalides. *Angew. Chem. Int. Ed.* **2019**, *58*, 6713-6717.

19 Pedroni, J.; Boghi, M.; Saget, T.; Cramer, N. Access to β-Lactams by Enantioselective Palladium(0)-Catalyzed C(sp³)-H Alkylation. *Angew. Chem. Int. Ed.* **2014**, *126*, 9210-9213.

$^1\text{H NMR}$ (400 MHz, CDCl_3) δ 7.42 – 7.27 (m, 6H), 7.23 (d, $J = 6.4$ Hz, 2H), 7.18 – 7.15 (d, $J = 6.4$ Hz, 2H), 4.62 (s, 2H), 4.52 (s, 2H), 4.15 (s, 2H). $^1\text{H NMR}$ spectrum is consistent with reported values.²⁰



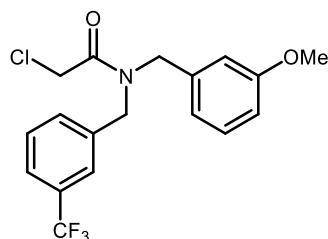
***N*-(3-methoxybenzyl)-1-(3-(trifluoromethyl)phenyl)methanamine (S47):**

Prepared according to General Reductive Amination Procedure. 3-(trifluoromethyl)benzaldehyde (0.54 mL, 4.0 mmol, 1.0 equiv) and (3-methoxyphenyl)methanamine (0.77 mL, 6.0 mmol, 1.5 equiv) were stirred in MeOH (20 mL, 0.2 M) for 22 hours. After NaBH_4 (227 mg, 6.0 mmol, 1.5 equiv) was added, the reaction was stirred for an additional 1 hour. The title compound was obtained as a clear oil (1181 mg, 100%).

$^1\text{H NMR}$ (600 MHz, CDCl_3) δ 7.64 (s, 1H), 7.53 (dd, $J = 17.3, 7.7$ Hz, 2H), 7.44 (t, $J = 7.7$ Hz, 1H), 7.26 (t, $J = 7.8$ Hz, 1H), 6.95 – 6.90 (m, 2H), 6.82 (dd, $J = 7.6, 2.2$ Hz, 1H), 3.86 (s, 2H), 3.82 (s, 3H), 3.80 (s, 2H), 1.66 (s, 1H) ppm.

$^{13}\text{C NMR}$ (151 MHz, CDCl_3) δ 160.0, 141.9, 141.6, 131.6, 130.9 (q, $^2J_{\text{C-F}} = 32.1$ Hz), 129.6, 129.0, 125.0 (q, $^3J_{\text{C-F}} = 3.8$ Hz), 124.4 (q, $^1J_{\text{C-F}} = 272.4$ Hz), 124.0 (q, $^3J_{\text{C-F}} = 3.8$ Hz), 120.6, 113.8, 112.8, 55.4, 53.3, 52.7 ppm.

LRMS (EI) m/z : $[\text{M}]^+$ calc'd. for $\text{C}_{16}\text{H}_{16}\text{F}_3\text{NO}$, 295.1, found 295.1.



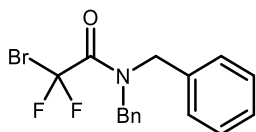
2-chloro-*N*-(3-methoxybenzyl)-*N*-(3-(trifluoromethyl)benzyl)acetamide (S48):

Prepared according to General Acylation Procedure. *N*-(3-methoxybenzyl)-1-(3-(trifluoromethyl)phenyl)methanamine (**S47**) (886 mg, 3.0 mmol, 1.0 equiv), Et_3N (0.46 mL, 3.3 mmol, 1.1 equiv), and chloroacetyl chloride (0.26 mL, 3.3 mmol, 1.1 equiv) were stirred in CH_2Cl_2 (30 mL, 0.1 M) for 4.5 hours. Purification on silica gel (10-20% EtOAc/hexanes) afforded the title compound as a clear oil (728 mg, 65%). Mixture of rotamers (* denotes major rotamer # denotes minor isomer).

$^1\text{H NMR}$ (600 MHz, CDCl_3) δ 7.57 (dd, $J = 28.6, 7.5$ Hz, 1H), 7.53 – 7.36 (m, 3H), 7.27 (dt, $J = 34.8, 7.9$ Hz, 1H), 6.85 (ddd, $J = 14.4, 8.4, 2.6$ Hz, 1H), 6.79 – 6.68 (m, 2H), 4.69 – 4.47 (m, 4H), 4.15 (m, 2H), 3.79 (s, 3H) ppm.

¹³C NMR (151 MHz, CDCl₃) δ 167.6*, 167.4[#], 160.5*, 160.2[#], 137.7*, 137.7[#], 137.1*, 137.1[#], 131.7*, 131.2^(**#) (q, ²J_{C-F} = 32.3 Hz), 130.5*, 130.0[#], 129.9[#], 130.0[#], 129.5*, 125.1[#] (q, ³J_{C-F} = 3.0 Hz), 125.0* (q, ³J_{C-F} = 4.0 Hz), 124.7* (q, ³J_{C-F} = 3.8 Hz), 123.6[#] (q, ³J_{C-F} = 3.5 Hz), 120.6[#], 118.8*, 113.7[#], 113.6[#], 113.5*, 112.5*, 55.5*, 55.4[#], 51.0*, 50.3[#], 48.8[#], 48.7*, 41.4^(**#) ppm.

LRMS (EI) m/z: [M]⁺ calc'd. for C₁₈H₁₇F₃NO₂, 371.1, found 371.2.



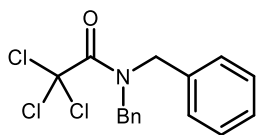
***N,N*-dibenzyl-2-bromo-2,2-difluoroacetamide (S49):**

An oven-dried reaction vial was cooled under N₂. Dibenzylamine (0.19 mL, 1.0 mmol, 1.0 equiv), ethyl bromodifluoroacetate (0.15 mL, 1.2 mmol, 1.2 equiv), and La(OTf)₃ (59 mg, 0.1 mmol, 10 mol %) were added sequentially. The reaction was stirred for 20 hours then quenched with 1 M HCl (aq), extracted with EtOAc (3x), filtered through a plug of silica with EtOAc, and concentrated under reduced pressure. The crude residue was purified on silica gel (20% EtOAc/hexanes) to afford the title compound as a white solid (104 mg, 29%).

¹H NMR (400 MHz, CDCl₃) δ 7.43 – 7.29 (m, 6H), 7.19 (ddd, J = 7.4, 5.5, 1.6 Hz, 4H), 4.63 (s, 2H), 4.55 (s, 2H) ppm.

¹³C NMR (151 MHz, CDCl₃) δ 160.1 (t, ²J_{C-F} = 26.3 Hz), 135.5, 134.8, 129.2, 129.1, 128.4, 128.4, 128.2, 127.5, 111.3 (t, ¹J_{C-F} = 315.1 Hz), 50.6 (t, ⁴J_{C-F} = 3.8 Hz), 48.8 ppm.

LRMS (EI) m/z: [M]⁺ calc'd. for C₁₆H₁₄BrF₂NO, 353.0, found 353.1.

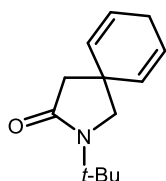


***N,N*-dibenzyl-2,2,2-trichloroacetamide (S50):**

Prepared according to General Acylation Procedure. Dibenzylamine (0.66 mL, 3.3 mmol, 1.1 equiv), Et₃N (0.46 mL, 3.3 mmol, 1.1 equiv), and trichloroacetyl chloride (0.33 mL, 3.0 mmol, 1.0 equiv) were stirred in CH₂Cl₂ (30 mL, 0.1 M) for 23 hours. Purification on silica gel (0-10% EtOAc/hexanes) afforded the title compound as a white solid (654 mg, 64%).

$^1\text{H NMR}$ (400 MHz, CDCl_3) δ 7.43 – 7.30 (m, 6H), 7.24 (d, $J = 6.9$ Hz, 2H), 7.16 (d, $J = 6.9$ Hz, 2H), 4.91 (s, 2H), 4.58 (s, 2H) ppm. $^1\text{H NMR}$ spectrum is consistent with reported values.²¹

V. Preparation of Spirolactam Products



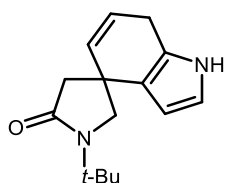
2-(*tert*-butyl)-2-azaspiro[4.5]deca-6,9-dien-3-one (10):

Prepared according to General Dearomative Spirolactamization Procedure 1 using *N*-benzyl-*N*-(*tert*-butyl)-2-chloroacetamide (**S39**) (120 mg, 0.5 mmol, 1.0 equiv), 3DPAFIPN (16.2 mg, 0.025 mmol, 5 mol%), DIPEA (0.26 mL, 1.5 mmol, 3.0 equiv), and 50% $\text{H}_2\text{O}/\text{MeCN}$ (10 mL, 0.05 M). Purification on silica gel (10% EtOAc/hexanes) afforded the title compound as a white solid (103 mg, 73%).

$^1\text{H NMR}$ (600 MHz, CDCl_3) δ 5.77 (dt, $J = 10.1, 3.3$ Hz, 2H), 5.66 (dt, $J = 10.3, 2.1$ Hz, 2H), 3.28 (s, 2H), 2.63 (p, $J = 2.7$ Hz, 2H), 2.31 (s, 2H), 1.38 (s, 9H) ppm.

$^{13}\text{C NMR}$ (151 MHz, CDCl_3) δ 173.7, 130.3, 124.7, 58.8, 54.1, 48.0, 36.4, 27.9, 26.4 ppm.

LRMS (EI) m/z : $[\text{M}]^+$ calc'd. for $\text{C}_{13}\text{H}_{19}\text{NO}$, 205.2, found 205.2.



1'-(*tert*-butyl)-1,7-dihydrospiro[indole-4,3'-pyrrolidin]-5'-one (13):

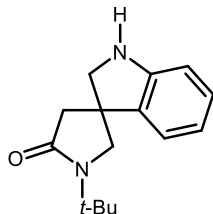
Prepared according to General Dearomative Spirolactamization Procedure 1 using *N*-((1*H*-indol-4-yl)methyl)-*N*-(*tert*-butyl)-2-chloroacetamide (**S2**) (139 mg, 0.5 mmol, 1.0 equiv), 3DPAFIPN (16.2 mg, 0.025 mmol, 5 mol%), DIPEA (0.26 mL, 1.5 mmol, 3.0 equiv), and 50% $\text{H}_2\text{O}/\text{MeCN}$ (10 mL, 0.05 M). Purification on silica gel (0-10% acetone/ CH_2Cl_2) afforded the title compound as a yellow oil (96.3 mg, 79%).

21 Diaba, F.; Montiel, J.A.; Martínez-Laporta, A.; Bonjoch, J. Dearomative radical spirocyclization from *N*-benzyltrichloroacetamides revisited using a copper(I)-mediated atom transfer reaction leading to 2-azaspiro[4.5]decanes. *Tetrahedron Lett.* **2013**, 54, 2619-2622.

¹H NMR (400 MHz, CDCl₃) δ 7.91 (s, 1H), 6.72 (dd, J = 3.0, 2.4 Hz, 1H), 6.16 (t, J = 2.7 Hz, 1H), 5.86 (dt, J = 10.0, 3.0 Hz, 1H), 5.81 (dt, J = 10.0, 1.8 Hz, 1H), 3.59 (d, J = 9.6 Hz, 1H), 3.44 (d, J = 9.7 Hz, 1H), 3.28 – 3.22 (m, 2H), 2.64 (d, J = 16.4 Hz, 1H), 2.48 (d, J = 16.5 Hz, 1H), 1.43 (s, 9H) ppm.

¹³C NMR (151 MHz, CDCl₃) δ 174.1, 132.4, 124.1, 122.6, 120.9, 117.3, 104.4, 59.9, 54.2, 48.7, 37.3, 28.0, 24.1 ppm.

LRMS (EI) m/z: [M]⁺ calc'd. for C₁₅H₂₀N₂O, 244.2, found 244.2.



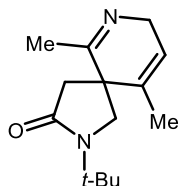
1'-(*tert*-butyl)spiro[indoline-3,3'-pyrrolidin]-5'-one (14):

Prepared according to General Dearomative Spirolactamization Procedure 1 using *N*-((1*H*-indol-3-yl)methyl)-*N*-(*tert*-butyl)-2-chloroacetamide (**S4**) (56 mg, 0.2 mmol, 1.0 equiv), 3DPAFIPN (6.5 mg, 0.01 mmol, 5 mol%), DIPEA (0.10 mL, 0.6 mmol, 3.0 equiv), cyclohexanethiol (1.2 μL, 0.01 mmol, 5 mol%), and 50% H₂O/MeCN (4 mL, 0.05 M). Purification on silica gel (10-50% EtOAc/hexanes) afforded the title compound as a yellow oil (34.4 mg, 70%).

¹H NMR (600 MHz, CDCl₃) δ 7.15 (d, J = 7.4 Hz, 1H), 7.14 – 7.08 (m, 1H), 6.83 – 6.77 (m, 1H), 6.71 (d, J = 7.8 Hz, 1H), 3.63 (d, J = 9.8 Hz, 1H), 3.58 (d, J = 9.1 Hz, 1H), 3.51 (d, J = 9.1 Hz, 1H), 3.49 (d, J = 9.8 Hz, 1H), 2.80 (d, J = 16.7 Hz, 1H), 2.52 (d, J = 16.7 Hz, 1H), 1.42 (s, 9H) ppm.

¹³C NMR (151 MHz, CDCl₃) δ 173.6, 150.4, 133.3, 128.8, 122.4, 119.9, 110.5, 60.2, 57.7, 54.4, 45.6, 45.5, 28.0 ppm.

LRMS (EI) m/z: [M]⁺ calc'd. for C₁₅H₂₀N₂O, 244.2, found 244.2.



2-(*tert*-butyl)-6,10-dimethyl-2,7-diazaspiro[4.5]deca-6,9-dien-3-one (15):

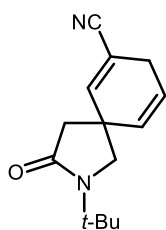
Prepared according to General Dearomative Spirolactamization Procedure 1 using *N*-(*tert*-butyl)-2-chloro-*N*-((2,4-dimethylpyridin-3-yl)methyl)acetamide (**S8**) (26.9 mg, 0.1 mmol, 1.0 equiv), 3DPAFIPN (3.2 mg,

0.005 mmol, 5 mol%), DIPEA (0.05 mL, 0.3 mmol, 3.0 equiv), and 50% H₂O/MeCN (2 mL, 0.05 M). Purification on silica gel (20-100% EtOAc/hexanes) afforded the title compound as a white solid (23 mg, 97%).

¹H NMR (600 MHz, CDCl₃) δ 5.55 (dq, J = 3.1, 1.5 Hz, 1H), 4.16 – 4.08 (m, 2H), 3.49 (d, J = 10.9 Hz, 1H), 3.42 (d, J = 10.9 Hz, 1H), 2.55 (d, J = 9.6 Hz, 2H), 2.06 (d, J = 1.8 Hz, 3H), 1.73 (t, J = 1.8 Hz, 3H), 1.42 (s, 9H) ppm.

¹³C NMR (151 MHz, CDCl₃) δ 172.97, 166.99, 131.70, 121.38, 77.37, 77.16, 76.95, 54.70, 54.21, 50.26, 41.56, 39.06, 27.71, 22.25, 18.14.

LRMS (EI) m/z: [M]⁺ calc'd. for C₁₄H₂₂N₂O, 234.2, found 234.2.



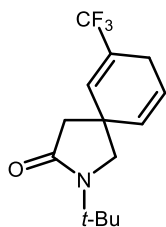
2-(tert-butyl)-3-oxo-2-azaspiro[4.5]deca-6,9-diene-7-carbonitrile (16):

Prepared according to General Dearomative Spirolactamization Procedure 2 using N-(tert-butyl)-2-chloro-N-(3-cyanobenzyl)acetamide (**S10**) (132.4 mg, 0.5 mmol, 1.0 equiv), 3DPAFIPN (16.2 mg, 0.025 mmol, 5 mol%), DIPEA (0.26 mL, 1.5 mmol, 3.0 equiv), and 50% H₂O/MeCN (10 mL, 0.05 M). Purification on silica gel (0-30% EtOAc/hexanes) afforded the title compound as a yellow solid (73 mg, 63%).

¹H NMR (600 MHz, CDCl₃) δ 6.50 (q, J = 2.0 Hz, 1H), 5.77 (dt, J = 10.3, 3.4 Hz, 1H), 5.67 (dq, J = 10.2, 2.2 Hz, 1H), 3.33 (q, J = 12 Hz, 2H), 2.85 (dq, J = 3.4, 1.7 Hz, 2H), 2.35 (d, J = 1.6 Hz, 2H), 1.37 (s, 9H) ppm.

¹³C NMR (151 MHz, CDCl₃) δ 172.0, 145.4, 145.4, 128.8, 122.6, 122.6, 118.5, 110.8, 57.3, 54.4, 46.7, 37.6, 27.8, 27.8, 27.8, 27.8, 27.7 ppm.

LRMS (EI) m/z: [M]⁺ calc'd. for C₁₄H₁₈N₂O, 230.1, found 230.2.



2-(tert-butyl)-7-(trifluoromethyl)-2-azaspiro[4.5]deca-6,9-dien-3-one (17):

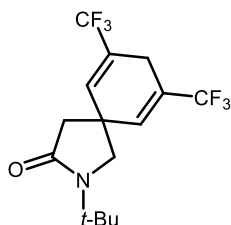
Prepared according to General Dearomative Spirolactamization Procedure 2 using N-(tert-butyl)-2-chloro-N-(3-(trifluoromethyl)benzyl)acetamide (**S12**) (120 mg, 0.5 mmol, 1.0 equiv), 3DPAFIPN (16.2 mg, 0.025

mmol, 5 mol%), DIPEA (0.26 mL, 1.5 mmol, 3.0 equiv), and 50% H₂O/MeCN (10 mL, 0.05 M). Purification on silica gel (10-20% EtOAc/hexanes) afforded the title compound as a yellow solid (75 mg, 55%).

¹H NMR (400 MHz, CDCl₃) δ 6.26 (p, J = 1.7 Hz, 1H), 5.83 (dt, J = 10.1, 3.4 Hz, 1H), 5.70 (dq, J = 10.0, 2.1 Hz, 1H), 3.36 (d, J = 10.1 Hz, 1H), 3.33 (d, J = 10.3 Hz, 1H), 2.84 – 2.77 (m, 2H), 2.38 (s, 2H), 1.40 (s, 9H) ppm.

¹³C NMR (151 MHz, CDCl₃) δ 72.7, 132.1 (q, ³J_{C-F} = 5.6 Hz), 129.2, 126.6 (q, ²J_{C-F} = 31.2 Hz), 123.5 (q, ¹J_{C-F} = 272.1 Hz), 122.8, 57.7, 54.4, 47.0, 37.0, 27.9, 23.7 ppm.

LRMS (EI) m/z: [M]⁺ calc'd. for C₁₄H₁₈F₃NO, 273.1, found 273.1.



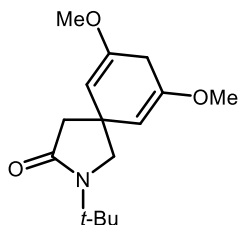
2-(tert-butyl)-7,9-bis(trifluoromethyl)-2-azaspiro[4.5]deca-6,9-dien-3-one (18):

Prepared according to General Dearomative Spirolactamization Procedure 1 using *N*-(3,5-bis(trifluoromethyl)benzyl)-*N*-(tert-butyl)-2-chloroacetamide (**S14**) (174 mg, 0.46 mmol, 1.0 equiv), 3DPAFIPN (14.9 mg, 0.023 mmol, 5 mol%), DIPEA (0.24 mL, 1.38 mmol, 3.0 equiv), and 50% H₂O/MeCN (9 mL, 0.05 M). Purification on silica gel (10% EtOAc/hexanes) afforded the title compound as a yellow solid (103 mg, 66%).

¹H NMR (400 MHz, CDCl₃) δ 6.30 (p, J = 1.8 Hz, 2H), 3.41 (s, 2H), 2.97 (s, 2H), 2.45 (s, 2H), 1.41 (s, 9H) ppm.

¹³C NMR (151 MHz, CDCl₃) δ 171.6, 131.2 (q, ³J_{C-F} = 5.4 Hz), 125.4 (q, ²J_{C-F} = 31.8 Hz), 123.0 (q, ¹J_{C-F} = 272.4 Hz), 56.7, 54.7, 46.1, 37.8, 27.8, 21.4 ppm.

LRMS (EI) m/z: [M]⁺ calc'd. for C₁₅H₁₇F₆NO, 341.1, found 341.2.



2-(tert-butyl)-7,9-dimethoxy-2-azaspiro[4.5]deca-6,9-dien-3-one (19):

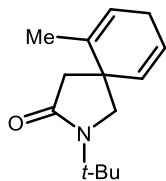
Prepared according to General Dearomative Spirolactamization Procedure 1 using *N*-(3,5-dimethoxybenzyl)-2-methylpropan-2-amine (**S16**) (60 mg, 0.2 mmol, 1.0 equiv), 3DPAFIPN (6.5 mg, 0.01 mmol, 5 mol%), DIPEA (0.10 mL, 0.6 mmol, 3.0 equiv), and 50% H₂O/MeCN (4 mL, 0.05 M). Purification by

preparatory TLC (20% acetone/hexanes eluent) afforded the title compound as an off-white solid (28 mg, 54%).

$^1\text{H NMR}$ (600 MHz, C_6D_6) δ 4.45 (t, $J = 1.3$ Hz, 2H), 3.13 (s, 6H), 3.03 (s, 2H), 2.95 (qt, $J = 8.0, 1.3$ Hz, 2H), 2.35 (s, 2H), 1.40 (s, 9H) ppm.

$^{13}\text{C NMR}$ (151 MHz, C_6D_6) δ 173.3, 152.9, 98.4, 60.1, 54.0, 53.6, 49.5, 39.4, 32.0, 28.0 ppm.

LRMS (EI) m/z : $[\text{M}]^+$ calc'd. for $\text{C}_{15}\text{H}_{23}\text{NO}_3$, 265.2, found 265.1.



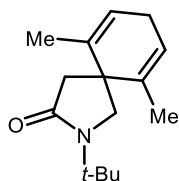
2-(tert-butyl)-6-methyl-2-azaspiro[4.5]deca-6,9-dien-3-one (20):

Prepared according to General Dearomative Spirolactamization Procedure 1 using *N*-(tert-butyl)-2-chloro-*N*-(2-methylbenzyl)acetamide (**S18**) (126.6 mg, 0.5 mmol, 1.0 equiv), 3DPAFIPN (16.2 mg, 0.025 mmol, 5 mol%), DIPEA (0.26 mL, 1.5 mmol, 3.0 equiv), and 50% $\text{H}_2\text{O}/\text{MeCN}$ (10 mL, 0.05 M). Purification on silica gel (5-10% acetone/hexanes) afforded the title compound as a yellow oil (72 mg, 66%).

$^1\text{H NMR}$ (600 MHz, CDCl_3) δ 5.70 (dtd, $J = 9.8, 3.3, 1.5$ Hz, 1H), 5.57 (dt, $J = 9.9, 2.1$ Hz, 1H), 5.46 (tt, $J = 3.4, 1.6$ Hz, 1H), 3.45 (d, $J = 10.2$ Hz, 1H), 3.21 (d, $J = 10.2$ Hz, 1H), 2.59 (tq, $J = 3.7, 1.9$ Hz, 2H), 2.49 (d, $J = 17.1$ Hz, 1H), 2.23 (d, $J = 17.1$ Hz, 1H), 1.72 (q, $J = 1.8$ Hz, 3H), 1.37 (s, 9H) ppm.

$^{13}\text{C NMR}$ (151 MHz, CDCl_3) δ 173.7, 134.7, 131.9, 123.6, 121.6, 57.4, 54.2, 45.8, 37.9, 27.8, 27.0, 19.0 ppm.

LRMS (EI) m/z : $[\text{M}]^+$ calc'd. for $\text{C}_{14}\text{H}_{21}\text{NO}$, 219.2, found 219.2.



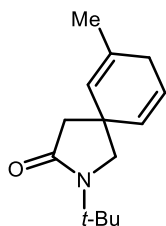
2-(tert-butyl)-6,10-dimethyl-2-azaspiro[4.5]deca-6,9-dien-3-one (21):

Prepared according to General Dearomative Spirolactamization Procedure 1 using *N*-(tert-butyl)-2-chloro-*N*-(2,6-dimethylbenzyl)acetamide (**S20**) (133.9 mg, 0.5 mmol, 1.0 equiv), 3DPAFIPN (16.2 mg, 0.025 mmol, 5 mol%), DIPEA (0.26 mL, 1.5 mmol, 3.0 equiv), and 50% $\text{H}_2\text{O}/\text{MeCN}$ (10 mL, 0.05 M). Purification on silica gel (10-15% acetone/hexanes) afforded the title compound as a yellow oil (98 mg, 84%).

$^1\text{H NMR}$ (600 MHz, CDCl_3) δ 5.47 (t, $J = 3.5$ Hz, 2H), 3.39 (s, 2H), 2.59 (tt, $J = 3.7, 1.9$ Hz, 2H), 2.47 (s, 2H), 1.75 – 1.72 (m, 6H), 1.41 (s, 9H) ppm.

$^{13}\text{C NMR}$ (151 MHz, CDCl_3) δ 174.1, 134.8, 121.3, 55.6, 54.5, 42.5, 39.8, 27.8, 27.3, 18.9 ppm.

LRMS (EI) m/z: [M]⁺ calc'd. for C₁₅H₂₃NO, 233.2, found 233.3.



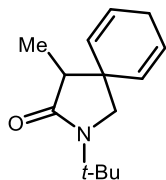
2-(tert-butyl)-7-methyl-2-azaspiro[4.5]deca-6,9-dien-3-one (22):

Prepared according to General Dearomative Spirolactamization Procedure 1 using *N*-(tert-butyl)-2-chloro-*N*-(3-methylbenzyl)acetamide (**S22**) (126.9 mg, 0.5 mmol, 1.0 equiv), 3DPAFIPN (16.2 mg, 0.025 mmol, 5 mol%), DIPEA (0.26 mL, 1.5 mmol, 3.0 equiv), and 50% H₂O/MeCN (10 mL, 0.05 M). Purification on silica gel (10-20% EtOAc/hexanes) afforded the title compound as a yellow oil (65 mg, 59%).

¹H NMR (600 MHz, CDCl₃) δ 5.74 (dt, J = 10.0, 3.3 Hz, 1H), 5.65 (dq, J = 10.0, 2.1 Hz, 1H), 5.35 (s, 1H), 3.24 (s, 2H), 2.54 – 2.50 (m, 2H), 2.26 (s, 2H), 1.69 (s, 3H), 1.37 (s, 9H) ppm.

¹³C NMR (151 MHz, CDCl₃) δ 173.8, 132.1, 130.2, 125.0, 124.3, 58.7, 54.0, 47.9, 37.6, 31.2, 27.9, 23.2 ppm.

LRMS (EI) m/z: [M]⁺ calc'd. for C₁₄H₂₁NO, 219.2, found 219.3.



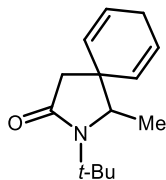
2-(tert-butyl)-4-methyl-2-azaspiro[4.5]deca-6,9-dien-3-one (23):

Prepared according to General Dearomative Spirolactamization Procedure 1 using *N*-benzyl-*N*-(tert-butyl)-2-chloropropanamide (**S24**) (127 mg, 0.5 mmol, 1.0 equiv), 3DPAFIPN (16.2 mg, 0.025 mmol, 5 mol%), DIPEA (0.26 mL, 1.5 mmol, 3.0 equiv), and 50% H₂O/MeCN (10 mL, 0.05 M). Purification on silica gel (2-3% acetone/hexanes) afforded the title compound as an off-white solid (94 mg, 85%).

¹H NMR (400 MHz, CDCl₃) δ 5.93 – 5.81 (m, 2H), 5.55 (dq, J = 9.6, 1.9 Hz, 1H), 5.48 (dq, J = 10.0, 2.1 Hz, 1H), 3.24 (d, J = 9.7 Hz, 1H), 3.19 (d, J = 9.8 Hz, 1H), 2.70 – 2.62 (m, 1H), 2.24 (q, J = 7.3 Hz, 1H), 1.38 (s, 9H), 0.94 (d, J = 7.3 Hz, 3H) ppm.

¹³C NMR (151 MHz, CDCl₃) δ 175.9, 130.0, 127.2, 127.0, 125.8, 56.6, 53.9, 49.3, 41.9, 27.9, 26.8, 9.7 ppm.

LRMS (EI) m/z: [M]⁺ calc'd. for C₁₄H₂₁NO, 219.2, found 219.2.



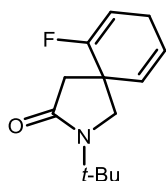
2-(tert-butyl)-1-methyl-2-azaspiro[4.5]deca-6,9-dien-3-one (24):

Prepared according to General Dearomative Spirolactamization Procedure 2 using *N*-(tert-butyl)-2-chloro-*N*-(1-phenylethyl)acetamide (**S26**) (254 mg, 1.0 mmol, 1.0 equiv), 3DPAFIPN (32.4 mg, 0.05 mmol, 5 mol%), DIPEA (0.52 mL, 3.0 mmol, 3.0 equiv), and 50% H₂O/MeCN (20 mL, 0.05 M). Purification on silica gel (10-20% EtOAc/hexanes) afforded the title compound as a yellow solid (89.7 mg, 41%).

¹H NMR (400 MHz, CDCl₃) δ 5.88 (dtd, J = 10.3, 3.4, 1.7 Hz, 1H), 5.81 (dq, J = 10.2, 2.0 Hz, 1H), 5.72 (dtd, J = 10.2, 3.3, 1.7 Hz, 1H), 5.60 (dq, J = 10.3, 2.1 Hz, 1H), 3.49 (q, J = 6.5 Hz, 1H), 2.64 (m, 2H), 2.51 (d, J = 16.6 Hz, 1H), 2.11 (d, J = 16.6 Hz, 1H), 1.43 (s, 9H), 1.20 (d, J = 6.4 Hz, 3H) ppm.

¹³C NMR (151 MHz, CDCl₃) δ 73.0, 131.3, 127.9, 127.0, 123.3, 64.9, 54.2, 45.5, 40.2, 28.4, 26.7, 17.7 ppm.

LRMS (EI) m/z: [M]⁺ calc'd. for C₁₄H₂₁NO, 219.2, found 219.2.



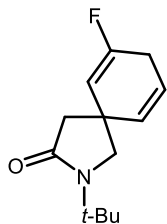
2-(tert-butyl)-6-fluoro-2-azaspiro[4.5]deca-6,9-dien-3-one (25):

Prepared according to General Dearomative Spirolactamization Procedure 1 using *N*-(tert-butyl)-2-chloro-*N*-(2-fluorobenzyl)acetamide (**S28**) (128.6 mg, 0.5 mmol, 1.0 equiv), 3DPAFIPN (16.2 mg, 0.025 mmol, 5 mol%), DIPEA (0.26 mL, 1.5 mmol, 3.0 equiv), and 50% H₂O/MeCN (10 mL, 0.05 M). Purification on silica gel (0-20% EtOAc/hexanes) afforded the title compound as a yellow solid (81 mg, 72%).

¹H NMR (600 MHz, CDCl₃) δ 5.72 – 5.64 (m, 2H), 5.33 (dt, J = 17.5, 3.9 Hz, 1H), 3.71 (d, J = 9.8 Hz, 1H), 3.27 (d, J = 9.9 Hz, 1H), 2.83 – 2.77 (m, 3H), 2.25 (d, J = 16.7 Hz, 1H), 1.40 (d, J = 0.8 Hz, 9H) ppm.

¹³C NMR (151 MHz, CDCl₃) δ 172.6, 158.4 (d, ¹J_{C-F} = 254.7 Hz), 130.2 (d, ³J_{C-F} = 6.4 Hz), 123.2 (d, ⁴J_{C-F} = 2.7 Hz), 101.7 (d, ²J_{C-F} = 17.2 Hz), 55.4, 54.4, 43.6, 37.8 (d, ²J_{C-F} = 23.2 Hz), 27.8, 26.4 (d, ³J_{C-F} = 7.0 Hz) ppm.

LRMS (EI) m/z: [M]⁺ calc'd. for C₁₃H₁₈FNO, 223.1, found 223.2.



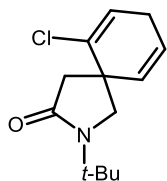
2-(tert-butyl)-7-fluoro-2-azaspiro[4.5]deca-6,9-dien-3-one (26):

Prepared according to General Dearomative Spirolactamization Procedure 2 using *N*-(tert-butyl)-2-chloro-*N*-(3-fluorobenzyl)acetamide (**S30**) (129 mg, 0.5 mmol, 1.0 equiv), 3DPAFIPN (16.2 mg, 0.025 mmol, 5 mol%), DIPEA (0.26 mL, 1.5 mmol, 3.0 equiv), and 50% H₂O/MeCN (10 mL, 0.05 M). Purification on silica gel (10-20% EtOAc/hexanes) afforded the title compound as a yellow solid (84.7 mg, 76%).

¹H NMR (600 MHz, CDCl₃) δ 5.69 (ddt, *J* = 9.9, 7.8, 3.3 Hz, 1H), 5.64 (ddq, *J* = 9.8, 3.7, 1.9 Hz, 1H), 5.24 (dq, *J* = 17.0, 1.5 Hz, 1H), 3.34 (dd, *J* = 9.9, 1.1 Hz, 1H), 3.32 (d, *J* = 9.9 Hz, 1H), 2.86 – 2.82 (m, 2H), 2.36 (d, *J* = 1.0 Hz, 1H), 2.35 (d, *J* = 16.6 Hz, 1H), 1.39 (s, 9H) ppm.

¹³C NMR (151 MHz, CDCl₃) δ 173.2, 158.5 (d, ¹*J*_{C-F} = 256.0 Hz), 130.5 (d, ⁴*J*_{C-F} = 2.8 Hz), 121.9 (d, ³*J*_{C-F} = 10.6 Hz), 106.3 (d, ²*J*_{C-F} = 15.0 Hz), 58.4 (d, ⁴*J*_{C-F} = 2.6 Hz), 54.2, 47.6 (d, ⁴*J*_{C-F} = 2.0 Hz), 39.5 (d, ³*J*_{C-F} = 7.8 Hz), 27.9, 27.2 (d, ²*J*_{C-F} = 26.4 Hz) ppm.

LRMS (EI) *m/z*: [M]⁺ calc'd. for C₁₃H₁₈FNO, 223.1, found 223.2.



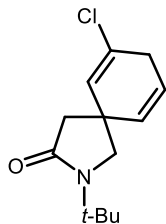
2-(tert-butyl)-6-chloro-2-azaspiro[4.5]deca-6,9-dien-3-one (27):

Prepared according to General Dearomative Spirolactamization Procedure 1 using *N*-(tert-butyl)-2-chloro-*N*-(2-chlorobenzyl)acetamide (**S32**) (137.1 mg, 0.5 mmol, 1.0 equiv), 3DPAFIPN (16.2 mg, 0.025 mmol, 5 mol%), DIPEA (0.26 mL, 1.5 mmol, 3.0 equiv), and 50% H₂O/MeCN (10 mL, 0.05 M). Purification on silica gel (5-10% acetone/hexanes) afforded the title compound as a yellow oil (57 mg, 47%).

¹H NMR (600 MHz, CDCl₃) δ 5.93 (t, *J* = 3.7 Hz, 1H), 5.75 – 5.67 (m, 2H), 3.79 (d, *J* = 10.1 Hz, 1H), 3.27 (d, *J* = 10.1 Hz, 1H), 2.92 (d, *J* = 17.0 Hz, 1H), 2.79 (dq, *J* = 4.0, 2.4, 2.0 Hz, 2H), 2.27 (d, *J* = 16.9 Hz, 1H), 1.41 (s, 9H) ppm.

¹³C NMR (151 MHz, CDCl₃) δ 172.8, 134.4, 130.9, 124.8, 122.0, 56.82, 54.5, 45.2, 40.4, 28.5, 27.8 ppm.

LRMS (EI) *m/z*: [M]⁺ calc'd. for C₁₃H₁₈ClNO, 239.1, found 239.2.



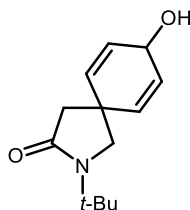
2-(*tert*-butyl)-7-chloro-2-azaspiro[4.5]deca-6,9-dien-3-one (28):

Prepared according to General Dearomative Spirolactamization Procedure 1 using *N*-(*tert*-butyl)-2-chloro-*N*-(3-chlorobenzyl)acetamide (**S34**) (137.1 mg, 0.5 mmol, 1.0 equiv), 3DPAFIPN (16.2 mg, 0.025 mmol, 5 mol%), DIPEA (0.26 mL, 1.5 mmol, 3.0 equiv), and 50% H₂O/MeCN (10 mL, 0.05 M). Purification on silica gel (10% EtOAc/hexanes) afforded the title compound as a yellow solid (84 mg, 70%).

¹H NMR (600 MHz, CDCl₃) δ 5.78 (q, *J* = 1.8 Hz, 1H), 5.69 (dt, *J* = 10.0, 3.3 Hz, 1H), 5.63 (dq, *J* = 10.0, 2.0 Hz, 1H), 3.30 (dd, *J* = 18.0, 12.0 Hz, 2H), 2.89 (dt, *J* = 3.4, 2.0 Hz, 2H), 2.33 (d, *J* = 1.9 Hz, 2H), 1.36 (s, 9H) ppm.

¹³C NMR (151 MHz, CDCl₃) δ 173.0, 131.0, 129.4, 127.2, 123.4, 57.9, 54.3, 47.1, 40.0, 33.6, 27.8 ppm.

LRMS (EI) *m/z*: [M]⁺ calc'd. for C₁₃H₁₈ClNO, 239.1, found 239.2.



2-(*tert*-butyl)-8-hydroxy-2-azaspiro[4.5]deca-6,9-dien-3-one (29):

Prepared according to General Dearomative Spirolactamization Procedure 1 using *N*-(*tert*-butyl)-2-chloro-*N*-(4-chlorobenzyl)acetamide (**S36**) (137 mg, 0.5 mmol, 1.0 equiv), 3DPAFIPN (16.2 mg, 0.025 mmol, 5 mol%), DIPEA (0.26 mL, 1.5 mmol, 3.0 equiv), and 50% H₂O/MeCN (10 mL, 0.05 M). Purification on silica gel (50-75% EtOAc/hexanes) afforded the title compound (72.2 mg, 65%, 1:1 d.r.).

Diastereomer 1 (elutes first, 36.2 mg, yellow solid):

¹H NMR (400 MHz, CDCl₃) δ 5.93 (dq, *J* = 10.3, 3.0 Hz, 2H), 5.88 (dd, *J* = 10.3, 1.3 Hz, 2H), 4.54 (s, 1H), 3.33 (s, 2H), 2.32 (s, 2H), 1.39 (s, 9H) ppm.

¹³C NMR (101 MHz, CDCl₃) δ 173.0, 132.9, 128.1, 62.3, 56.5, 54.3, 46.2, 37.2, 27.9 ppm.

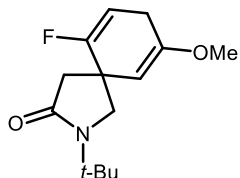
LRMS (APCI) *m/z*: [M+1]⁺ calc'd. for C₁₃H₂₀NO₂, 222.1, found 222.2.

Diastereomer 2 (elutes second, 36.0 mg, yellow solid):

¹H NMR (400 MHz, CDCl₃) δ 5.94 (dq, J = 10.3, 3.1 Hz, 2H), 5.87 (dq, J = 10.2, 1.5 Hz, 2H), 4.51 (s, 1H), 3.28 (s, 2H), 2.37 (s, 2H), 1.39 (s, 9H) ppm.

¹³C NMR (101 MHz, CDCl₃) δ 173.2, 132.9, 128.2, 62.2, 57.0, 54.3, 45.7, 37.2, 27.9 ppm.

LRMS (APCI) m/z: [M+1]⁺ calc'd. for C₁₃H₂₀NO₂, 222.1, found 222.2.



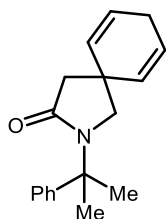
2-(tert-butyl)-6-fluoro-9-methoxy-2-azaspiro[4.5]deca-6,9-dien-3-one (30):

Prepared according to General Dearomative Spirolactamization Procedure 1 using *N*-(tert-butyl)-2-chloro-*N*-(2-fluoro-5-methoxybenzyl)acetamide (**S38**) (143.9 mg, 0.5 mmol, 1.0 equiv), 3DPAFIPN (16.2 mg, 0.025 mmol, 5 mol%), DIPEA (0.26 mL, 1.5 mmol, 3.0 equiv), and 50% H₂O/MeCN (10 mL, 0.05 M). Purification on silica gel (10-20% EtOAc/hexanes) afforded the title compound as a yellow oil (88 mg, 69%).

¹H NMR (600 MHz, C₆D₆) δ 4.86 (dt, J = 16.1, 3.7 Hz, 1H), 4.36 (d, J = 7.3 Hz, 1H), 3.52 (dd, J = 9.6, 1.0 Hz, 1H), 3.01 (s, 3H), 2.95 (d, J = 9.6 Hz, 1H), 2.87 (d, J = 16.5 Hz, 1H), 2.61 – 2.48 (m, 2H), 2.23 (d, J = 16.5 Hz, 1H), 1.32 (s, 9H) ppm.

¹³C NMR (151 MHz, C₆D₆) δ 172.0, 159.1 (d, ¹J_{C-F} = 254.5 Hz), 153.3 (d, ⁴J_{C-F} = 2.8 Hz), 99.8 (d, ²J_{C-F} = 20.1 Hz), 98.5 (d, ³J_{C-F} = 7.4 Hz), 56.39, 54.2, 44.7, 38.8 (d, ²J_{C-F} = 23.8 Hz), 28.3 (d, ³J_{C-F} = 8.2 Hz), 27.7 ppm.

LRMS (EI) m/z: [M]⁺ calc'd. for C₁₄H₂₀FNO₂, 253.2, found 253.2.



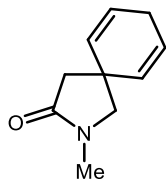
2-(2-phenylpropan-2-yl)-2-azaspiro[4.5]deca-6,9-dien-3-one (S51):

Prepared according to General Dearomative Spirolactamization Procedure 1 using *N*-benzyl-2-chloro-*N*-(2-phenylpropan-2-yl)acetamide (**S41**) (121 mg, 0.4 mmol, 1.0 equiv), 3DPAFIPN (13.0 mg, 0.020 mmol, 5 mol%), DIPEA (0.21 mL, 1.2 mmol, 3.0 equiv), and 50% H₂O/MeCN (8 mL, 0.05 M). Purification on silica gel (10-20% EtOAc/hexanes) afforded the title compound as a white solid (63 mg, 59%).

¹H NMR (600 MHz, CDCl₃) δ 7.37 – 7.28 (m, 4H), 7.23 (tt, J = 6.6, 2.1 Hz, 1H), 5.78 (dt, J = 10.3, 3.3 Hz, 2H), 5.70 (dt, J = 10.3, 2.1 Hz, 2H), 3.22 (s, 2H), 2.63 (dh, J = 7.4, 2.2 Hz, 2H), 2.36 (s, 2H), 1.75 (s, 6H) ppm.

¹³C NMR (151 MHz, CDCl₃) δ 173.5, 146.7, 130.2, 128.5, 126.9, 125.2, 124.8, 59.6, 59.0, 47.9, 36.7, 27.9, 26.4.

LRMS (EI) m/z: [M]⁺ calc'd. for C₁₈H₂₁NO, 267.2, found 267.1.

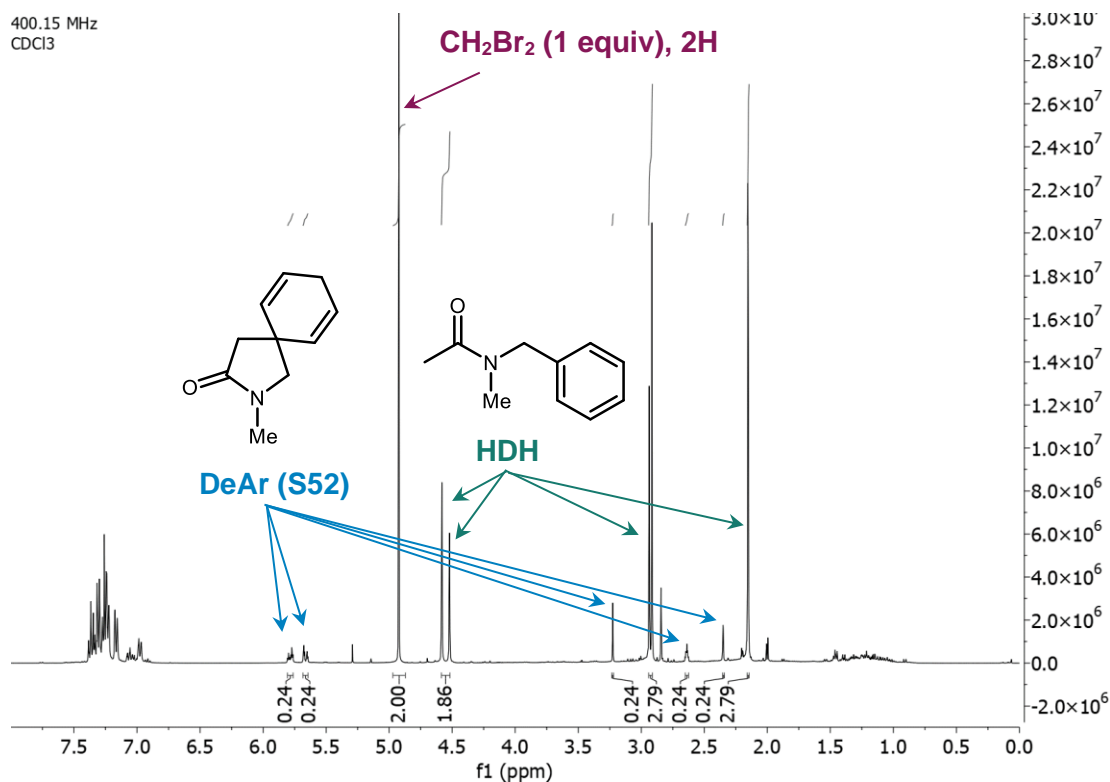


2-methyl-2-azaspiro[4.5]deca-6,9-dien-3-one (S52):

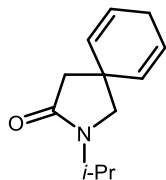
Prepared according to General Dearomative Spirolactamization Procedure 1 using *N*-benzyl-2-chloro-*N*-methylacetamide (**S43**) (20 mg, 0.1 mmol, 1.0 equiv), 3DPAFIPN (3.2 mg, 0.005 mmol, 5 mol%), DIPEA (52 μ L, 0.3 mmol, 3.0 equiv), and 50% H₂O/MeCN (2 mL, 0.05 M). CDCl₃ and an internal standard of dibromomethane (7 μ L, 0.1 mmol) were added to the crude residue. The sample was analyzed by ¹H NMR (*d* = 5 s), and the integral values were used to calculate the yield of the title compound (12%) and the hydrodehalogenation byproduct (93%). ¹H NMR spectrum of HDH byproduct is consistent with reported values.²²

Characteristic peaks

¹H NMR (400 MHz, CDCl₃) δ 5.82 – 5.75 (m, 2H), 5.66 (dt, *J* = 10.3, 2.0 Hz, 2H), 3.23 (s, 2H), 2.84 (t, *J* = 0.8 Hz, 3H), 2.64 (ddd, *J* = 5.4, 3.4, 2.0 Hz, 2H), 2.35 (d, *J* = 0.9 Hz, 2H) ppm.



22 Rauser, M.; Ascheberg, A.; Niggemann, M. Direct Reductive *N*-Functionalization of Aliphatic Nitro Compounds. *Chem. Eur. J.* **2018**, *24*, 3970-3974.

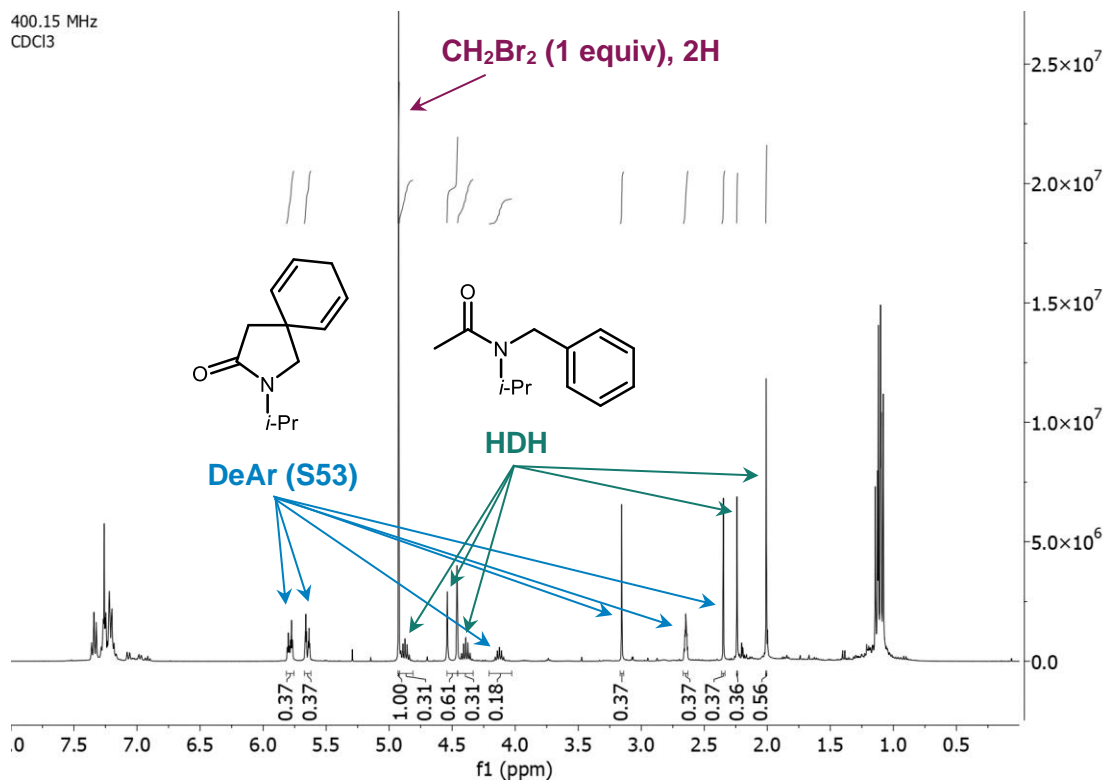


2-isopropyl-2-azaspiro[4.5]deca-6,9-dien-3-one (S53):

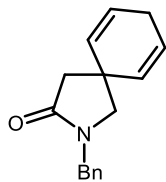
Prepared according to General Dearomative Spirolactamization Procedure 1 using *N*-benzyl-2-chloro-*N*-isopropylacetamide (**S45**) (23 mg, 0.1 mmol, 1.0 equiv), 3DPAFIPN (3.2 mg, 0.005 mmol, 5 mol%), DIPEA (52 μ L, 0.3 mmol, 3.0 equiv), and 50% H₂O/MeCN (2 mL, 0.05 M). CDCl₃ and an internal standard of dibromomethane (7 μ L, 0.1 mmol) were added to the crude residue. The sample was analyzed by ¹H NMR ($d = 5$ s), and the integral values were used to calculate the yield of the title compound (37%) and the hydrodehalogenation byproduct (61%). ¹H NMR spectrum of HDH byproduct is consistent with reported values.²³

Characteristic peaks

¹H NMR (400 MHz, CDCl₃) δ 5.86 – 5.74 (m, 2H), 5.65 (dt, $J = 10.4, 2.0$ Hz, 2H), 4.12 (p, $J = 6.7$ Hz, 1H), 3.15 (s, 2H), 2.65 (tt, $J = 3.4, 2.0$ Hz, 2H), 2.35 (s, 2H) ppm.



23 Rauser, M.; Ascheberg, A.; Niggemann, M. Direct Reductive *N*-Functionalization of Aliphatic Nitro Compounds. *Chem. Eur. J.* **2018**, *24*, 3970-3974.

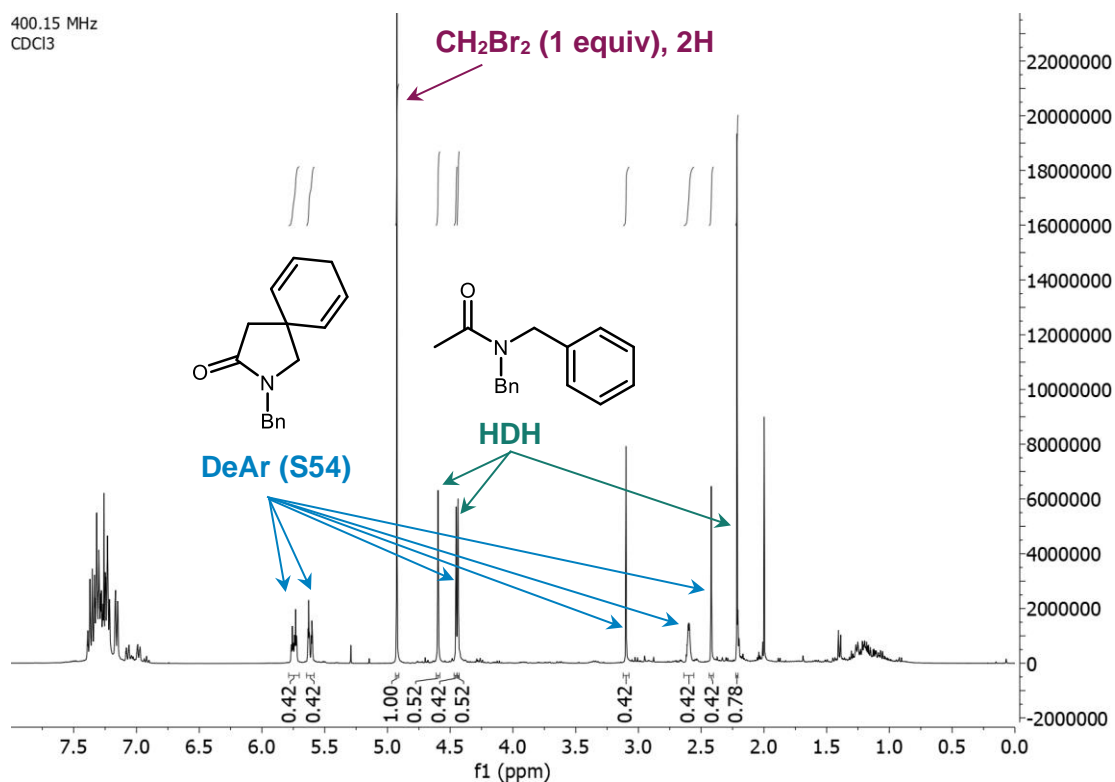


2-benzyl-2-azaspiro[4.5]deca-6,9-dien-3-one (S54):

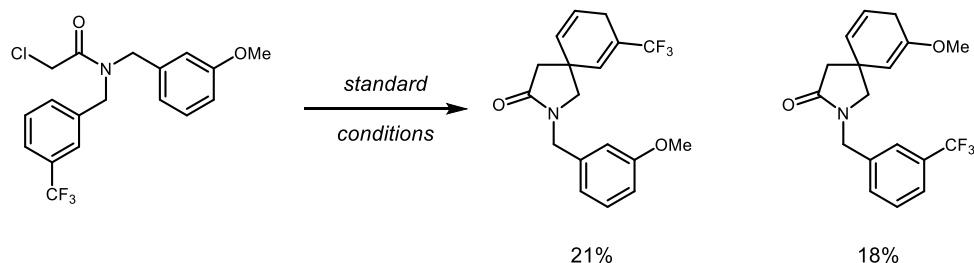
Prepared according to General Dearomative Spirolactamization Procedure 1 using *N,N*-dibenzyl-2-chloroacetamide (**S46**) (27 mg, 0.1 mmol, 1.0 equiv), 3DPAFIPN (3.2 mg, 0.005 mmol, 5 mol%), DIPEA (52 μ L, 0.3 mmol, 3.0 equiv), and 50% H₂O/MeCN (2 mL, 0.05 M). CDCl₃ and an internal standard of dibromomethane (7 μ L, 0.1 mmol) were added to the crude residue. The sample was analyzed by ¹H NMR (*d* = 5 s), and the integral values were used to calculate the yield of the title compound (42%) and the hydrodehalogenation byproduct (52%). ¹H NMR spectrum of HDH byproduct is consistent with reported values.²⁴

Characteristic peaks

¹H NMR (400 MHz, CDCl₃) δ 5.77 – 5.69 (m, 2H), 5.61 (dt, *J* = 10.4, 2.0 Hz, 2H), 4.45 (s, 2H), 3.10 (s, 2H), 2.60 (dtt, *J* = 4.1, 3.3, 2.1 Hz, 2H), 2.42 (s, 2H) ppm.



24 Zhou, S.; Junge, K.; Addis, D.; Das, S.; Beller, M. A Convenient and General Iron-Catalyzed Reduction of Amides to Amines. *Angew. Chem. Int. Ed.* **2009**, *48*, 9507-9510.



2-(3-methoxybenzyl)-7-(trifluoromethyl)-2-azaspiro[4.5]deca-6,9-dien-3-one (S55) and 7-methoxy-2-(3-(trifluoromethyl)benzyl)-2-azaspiro[4.5]deca-6,9-dien-3-one (S56):

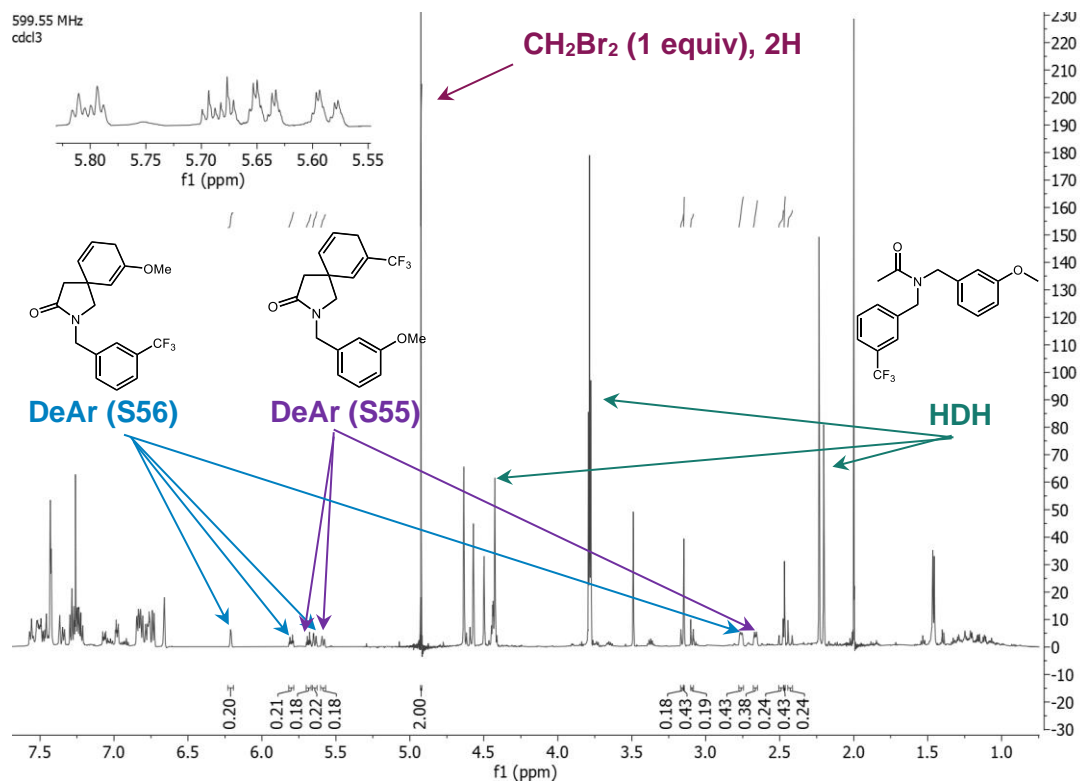
Prepared according to General Dearomative Spirolactamization Procedure 1 using 2-chloro-*N*-(3-methoxybenzyl)-*N*-(3-(trifluoromethyl)benzyl)acetamide (**S47**) (37.0 mg, 0.1 mmol, 1.0 equiv), 3DPAFIPN (3.2 mg, 0.005 mmol, 5 mol%), DIPEA (52 μ L, 0.3 mmol, 3.0 equiv), and 50% H₂O/MeCN (2 mL, 0.05 M). CDCl₃ and an internal standard of dibromomethane (7 μ L, 0.1 mmol) were added to the crude residue. The sample was analyzed by ¹H NMR ($d = 5$ s), and the integral values were used to calculate the yield of the title compounds (21%, 18%) and the hydrodehalogenation byproduct (50%).

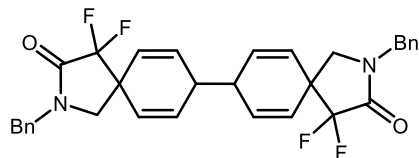
S55 (characteristic peaks):

¹H NMR (600 MHz, cdcl₃) δ 5.69 (dt, $J = 10.0, 3.4$ Hz, 1H), 5.59 (dq, $J = 9.9, 2.1$ Hz, 1H), 3.16 (d, $J = 10.0$ Hz, 1H), 3.09 (d, $J = 9.8$ Hz, 1H), 2.66 (dddt, $J = 7.7, 3.1, 2.0, 1.0$ Hz, 2H), 2.49 (d, $J = 16.7$ Hz, 1H), 2.43 (d, $J = 16.9$ Hz, 1H) ppm.

S56 (characteristic peaks):

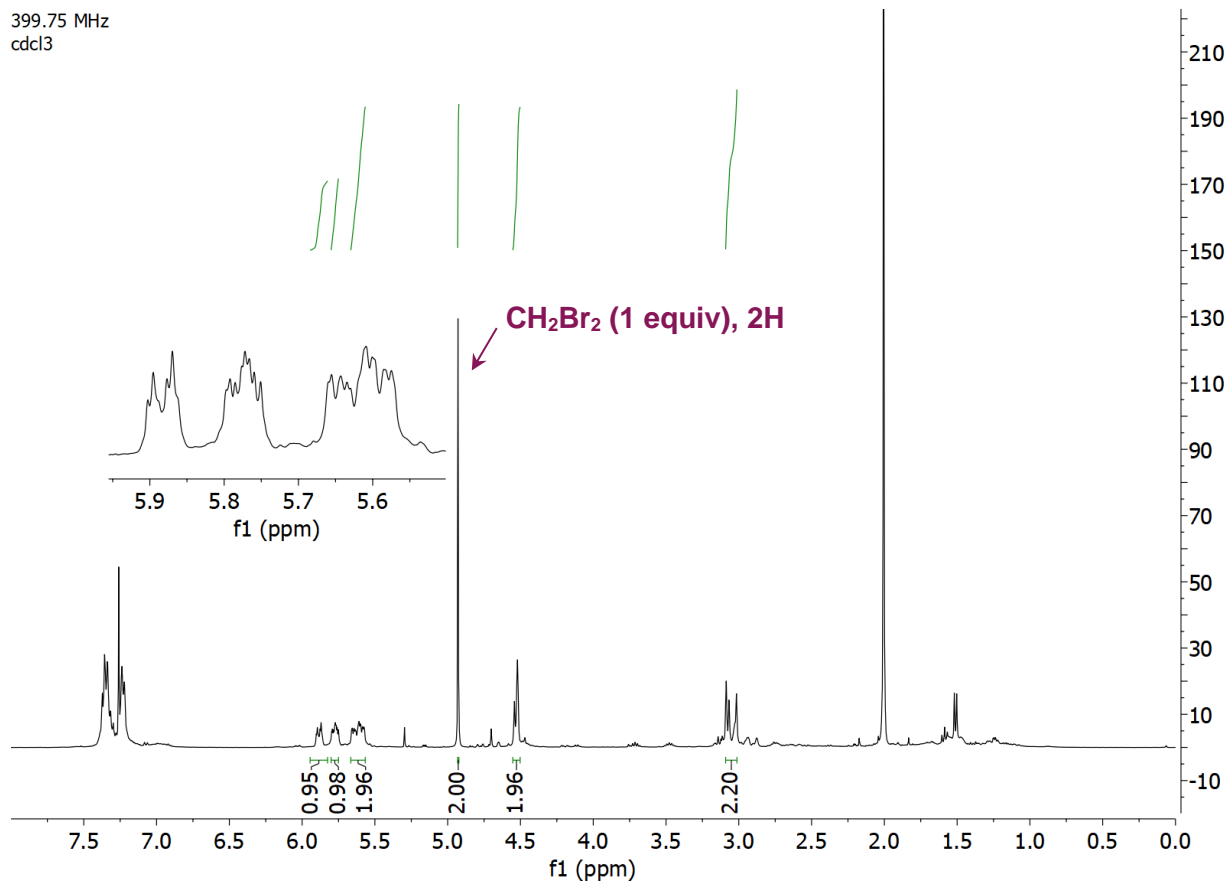
¹H NMR (600 MHz, cdcl₃) δ 6.21 (s, 1H), 5.80 (dt, $J = 10.1, 3.5$ Hz, 1H), 5.64 (dq, $J = 10.0, 2.0$ Hz, 1H), 3.15 (s, 2H), 2.78 – 2.74 (m, 2H), 2.47 (s, 2H) ppm.

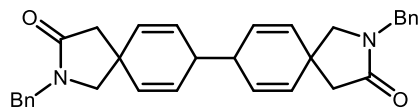




2,2'-dibenzyl-4,4',4'-tetrafluoro-2,2'-diazabicyclo[8,8']deca-6,6',9,9'-tetraene-3,3'-dione (S57):

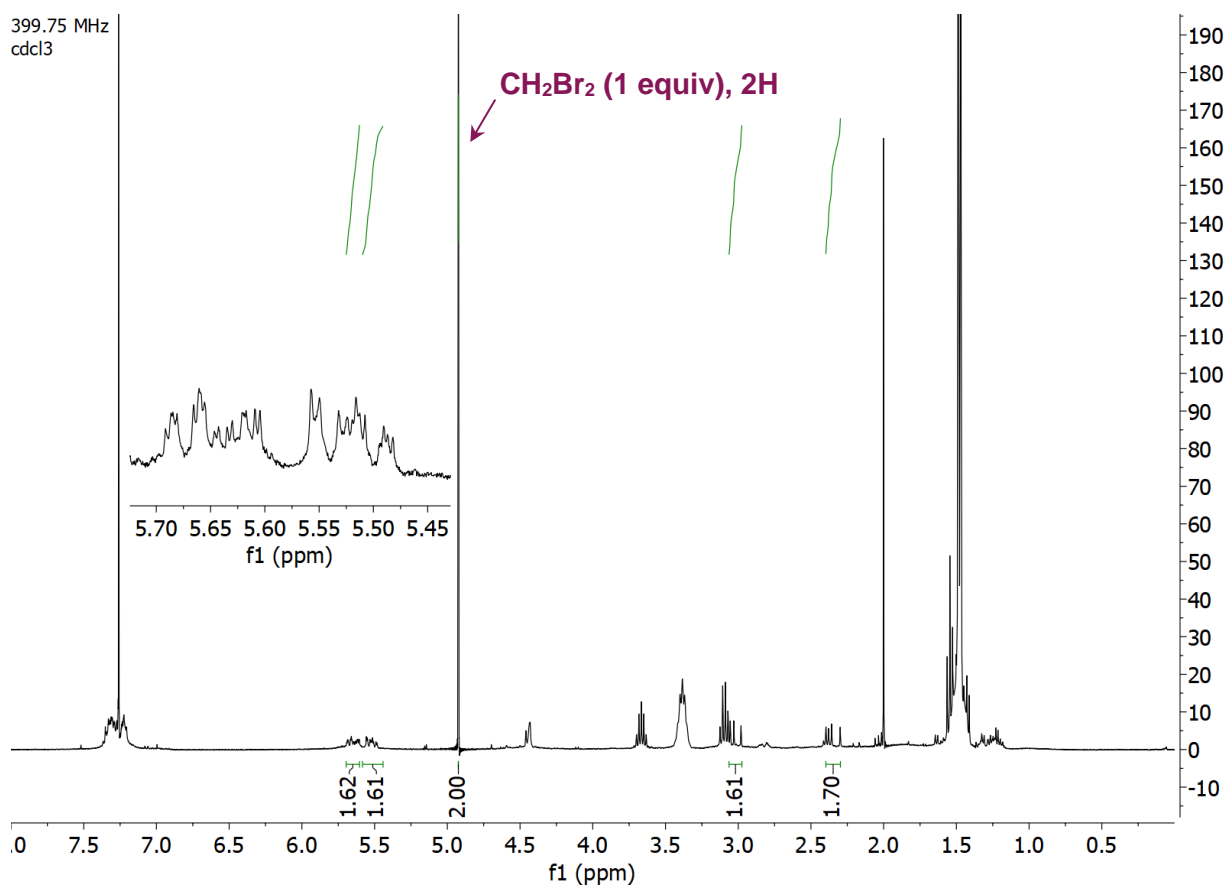
Prepared according to General Dearomative Spirolactamization Procedure 1 using *N,N*-dibenzyl-2-bromo-2,2-difluoroacetamide (**S49**) (35.4 mg, 0.1 mmol, 1.0 equiv), 3DPAFIPN (3.2 mg, 0.005 mmol, 5 mol%), DIPEA (52 μ L, 0.3 mmol, 3.0 equiv), and 50% H₂O/MeCN (2 mL, 0.05 M). CDCl₃ and an internal standard of dibromomethane (7 μ L, 0.1 mmol) were added to the crude residue. The sample was analyzed by ¹H NMR (d = 5 s), and the integral values were used to calculate the yield of the title compound (98%).



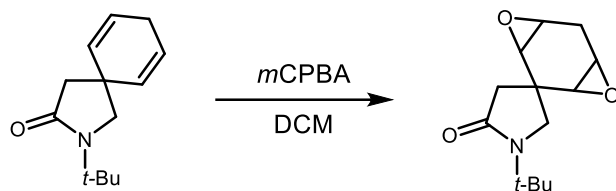


2,2'-dibenzyl-2,2'-diazabicyclo[4.5]decane-6,6',9,9'-tetraene-3,3'-dione (S58):

Prepared according to General Dearomatic Spirolactamization Procedure 1 using *N,N*-dibenzyl-2,2,2-trichloroacetamide (**S50**) (34.3 mg, 0.1 mmol, 1.0 equiv), 3DPAFIPN (3.2 mg, 0.005 mmol, 5 mol%), DIPEA (52 μ L, 0.3 mmol, 3.0 equiv), and 50% H₂O/MeCN (2 mL, 0.05 M). CDCl₃ and an internal standard of dibromomethane (7 μ L, 0.1 mmol) were added to the crude residue. The sample was analyzed by ¹H NMR (d = 5 s), and the integral values were used to calculate the yield of the title compound (81%).

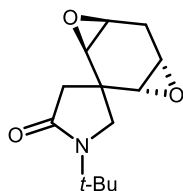


VI. Spirolactam Derivatization



1-(*tert*-butyl)-4',8'-dioxaspiro[pyrrolidine-3,2'-tricyclo[5.1.0.0^{3,5}]octan]-5-one (**31**):

To an reaction vial charged with 2-(*tert*-butyl)-2-azaspiro[4.5]deca-6,9-dien-3-one (**10**) (62 mg, 0.3 mmol, 1.0 equiv) cooled to 0 °C was added CH₂Cl₂ (6 mL, 0.05 M) and *m*CPBA (75%, 172 mg, 0.75 mmol, 2.5 equiv). The resulting solution was allowed to stir at 23 °C for 17 hours. The precipitate was filtered and washed with CH₂Cl₂ and 1 M NaOH (aq). The filtrate was extracted with CH₂Cl₂ (3x), washed with brine, dried over MgSO₄, and concentrated under reduced pressure. The crude residue was purified on silica gel (10-50% acetone/hexanes) to yield the title compound (57.0 mg, 82%, 5:6:1 d.r.; diastereomers 2 and 3 isolated as a mixture).

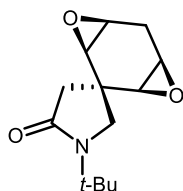


Diastereomer 1 (elutes first, 23.8 mg, white solid): (1'*R*,3'*R*,5'*S*,7'*S*)-1-(*tert*-butyl)-4',8'-dioxaspiro[pyrrolidine-3,2'-tricyclo[5.1.0.0^{3,5}]octan]-5-one:

¹H NMR (400 MHz, CDCl₃) δ 3.68 (d, *J* = 10.5 Hz, 1H), 3.37 (d, *J* = 10.5 Hz, 1H), 3.18 (tq, *J* = 4.0, 1.8 Hz, 2H), 2.94 (dt, *J* = 5.8, 2.9 Hz, 2H), 2.71 (d, *J* = 17.0 Hz, 1H), 2.42 (d, *J* = 16.9 Hz, 1H), 2.34 (t, *J* = 2.3 Hz, 2H), 1.43 (s, 9H) ppm.

¹³C NMR (151 MHz, CDCl₃) δ 172.8, 56.5, 55.9, 54.5, 52.4, 51.0, 50.8, 41.6, 34.8, 27.9, 23.9 ppm.

LRMS (EI) *m/z*: [M]⁺ calc'd. for C₁₃H₁₉NO₃, 237.1, found 237.1.

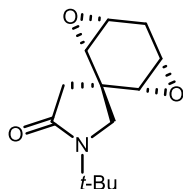


Diastereomer 2 (elutes second, 29.0 mg, white solid): (1'*R*,3'*r*,3'*S*,5'*R*,7'*S*)-1-(*tert*-butyl)-4',8'-dioxaspiro[pyrrolidine-3,2'-tricyclo[5.1.0.0^{3,5}]octan]-5-one one:

$^1\text{H NMR}$ (400 MHz, CDCl_3) δ 3.78 (s, 2H), 3.23 (ddd, $J = 4.1, 2.9, 1.2$ Hz, 2H), 3.05 – 3.01 (m, 2H), 2.76 (dt, $J = 17.3, 1.3$ Hz, 1H), 2.43 (s, 2H), 2.24 (dt, $J = 17.3, 3.0$ Hz, 1H), 1.44 (s, 9H) ppm.

$^{13}\text{C NMR}$ (151 MHz, CDCl_3) δ 172.0, 55.8, 54.7, 53.1, 51.3, 41.0, 34.4, 27.9, 23.0 ppm.

LRMS (EI) m/z : $[\text{M}]^+$ calc'd. for $\text{C}_{13}\text{H}_{19}\text{NO}_3$, 237.1, found 237.1.

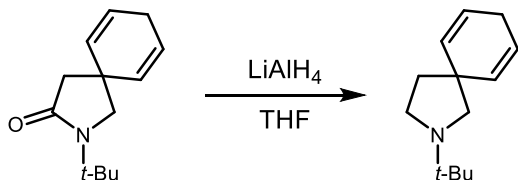


Diastereomer 3 (elutes second, 5.1 mg, white solid): (1'R,3s,3'S,5'R,7'S)-1-(tert-butyl)-4',8'-dioxaspiro[pyrrolidine-3,2'-tricyclo[5.1.0.0^{3,5}]octan]-5-one one (characteristic peaks):

$^1\text{H NMR}$ (400 MHz, CDCl_3) δ 3.43 (s, 2H), 3.20 (ddd, $J = 3.9, 2.9, 1.2$ Hz, 2H), 3.01 – 2.99 (m, 2H), 2.79 (s, 2H), 2.21 (dt, $J = 17.2, 3.0$ Hz, 2H), 1.43 (s, 9H) ppm.

$^{13}\text{C NMR}$ (151 MHz, CDCl_3) δ 172.8, 56.0, 54.5, 52.0, 41.6, 34.2, 27.9 ppm.

LRMS (EI) m/z : $[\text{M}]^+$ calc'd. for $\text{C}_{13}\text{H}_{19}\text{NO}_3$, 237.1, found 237.2.



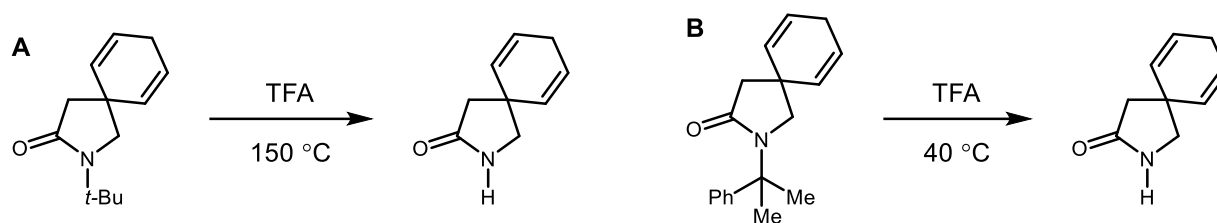
2-(tert-butyl)-2-azaspiro[4.5]deca-6,9-diene (32):

To an oven-dried reaction vial charged with 2-(tert-butyl)-2-azaspiro[4.5]deca-6,9-dien-3-one (**10**) (20.5 mg, 0.1 mmol, 1.0 equiv) was added THF (1 mL, 0.1 M). The solution was cooled to 0 °C and LiAlH_4 (1 M in THF, 0.25 mL, 0.25 mmol, 2.5 equiv) was added dropwise. The resulting solution was allowed to warm to 23 °C and stir for 20 hours. The reaction was cooled to 0 °C and diluted with Et_2O . Then 0.01 mL H_2O , 0.01 mL 15% NaOH (aq), and 0.03 mL H_2O were added sequentially, and the resulting solution was stirred for 15 minutes at 23 °C. Anhydrous MgSO_4 was added and the resulting suspension was stirred for an additional 15 minutes. After filtration and concentration under reduced pressure, the title compound was obtained as a white solid (19.1 mg, 100%).

$^1\text{H NMR}$ (600 MHz, C_6D_6) δ 5.83 (dt, $J = 10.4, 2.1$ Hz, 2H), 5.60 (dt, $J = 10.2, 3.3$ Hz, 2H), 2.66 (t, $J = 7.0$ Hz, 2H), 2.63 (s, 2H), 2.49 (tt, $J = 3.5, 2.1$ Hz, 2H), 1.75 (t, $J = 7.0$ Hz, 2H), 1.00 (s, 9H) ppm.

$^{13}\text{C NMR}$ (151 MHz, C_6D_6) δ 134.2, 122.0, 60.8, 52.0, 45.6, 42.1, 41.3, 26.8, 26.2 ppm.

LRMS (EI) m/z : $[\text{M}]^+$ calc'd. for $\text{C}_{13}\text{H}_{21}\text{N}$, 191.2, found 191.2.



2-azaspiro[4.5]deca-6,9-dien-3-one (**33**):

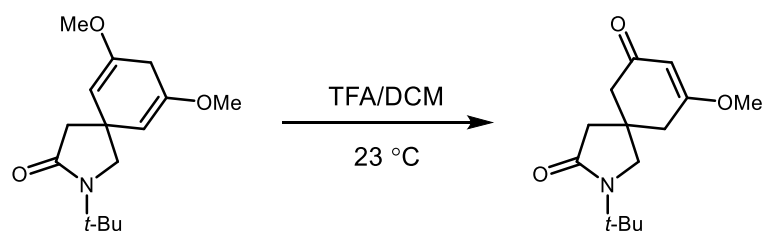
Procedure A: Dissolved 2-(*tert*-butyl)-2-azaspiro[4.5]deca-6,9-dien-3-one (**10**) (20.5 mg, 0.1 mmol, 1.0 equiv) in TFA (4 mL). The reaction was heated to 150 °C in a pressure tube. After 16 hours, quenched with 1 M NaOH (aq), extracted with CH₂Cl₂ (3x) and concentrated under reduced pressure. The crude residue was purified on silica gel (10-100% ethyl acetate/hexanes) to yield the title compound as a tan solid (14.9 mg, 100%).

Procedure B: Dissolved 2-(2-phenylpropan-2-yl)-2-azaspiro[4.5]deca-6,9-dien-3-one (**S51**) (57.8 mg, 0.22 mmol, 1.0 equiv) in TFA (1 mL). The reaction was heated to 40 °C. After 2 hours, quenched with 1 M NaOH (aq), extracted with CH₂Cl₂ (3x) and concentrated under reduced pressure. The crude residue was purified on silica gel (20-100% ethyl acetate/hexanes) to yield the title compound as a tan solid (19.0 mg, 59%).

¹H NMR (600 MHz, CDCl₃) δ 6.55 (s, 1H), 5.78 (dt, J = 10.4, 3.3 Hz, 2H), 5.72 (dt, J = 10.4, 2.0 Hz, 2H), 3.24 (s, 2H), 2.64 (tt, J = 3.5, 1.9 Hz, 2H), 2.28 (s, 2H) ppm.

¹³C NMR (151 MHz, CDCl₃) δ 177.3, 130.1, 124.7, 55.4, 45.3, 39.9, 26.3 ppm.

LRMS (EI) m/z: [M]⁺ calc'd. for C₉H₁₁NO, 149.1, found 149.1.



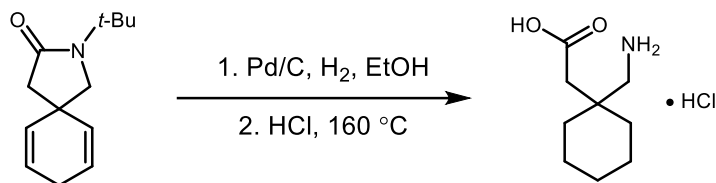
2-(*tert*-butyl)-9-methoxy-2-azaspiro[4.5]dec-8-ene-3,7-dione (**S59**):

Dissolved 2-(*tert*-butyl)-7,9-dimethoxy-2-azaspiro[4.5]deca-6,9-dien-3-one (**19**) (2.8 mg, 0.011 mmol) in CH₂Cl₂ (0.5 mL) and added TFA (0.1 mL). After 18 hours, quenched with saturated NaHCO₃ (aq), extracted with EtOAc (3x) and concentrated under reduced pressure to obtain the title compound as a yellow oil (2.7 mg, 100%).

¹H NMR (400 MHz, CDCl₃) δ 5.48 (s, 1H), 3.75 (s, 3H), 3.34 (s, 2H), 2.60 – 2.43 (m, 4H), 2.47 (s, 2H), 1.39 (s, 9H) ppm.

¹³C NMR (151 MHz, CDCl₃) δ 197.6, 176.6, 174.2, 102.2, 56.7, 56.5, 55.3, 47.2, 44.9, 40.0, 36.2, 27.9 ppm.

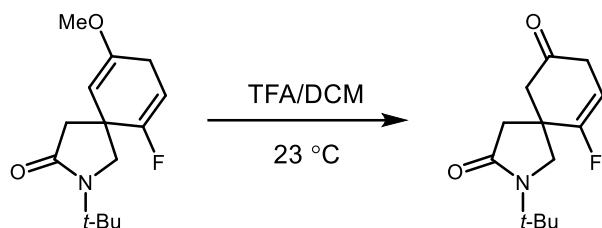
LRMS (EI) m/z: $[M]^+$ calc'd. for $C_{14}H_{21}NO_3$, 251.2, found 251.2.



2-(1-(aminomethyl)cyclohexyl)acetic acid hydrochloride (34):

Dissolved 2-(tert-butyl)-2-azaspiro[4.5]deca-6,9-dien-3-one (**10**) (102.6 mg, 0.50 mmol, 1.0 equiv) in methanol (20 mL, 0.025 M). Added palladium (5% on carbon, wet basis, 5 mg), and evacuated and backfilled with hydrogen. After 16 hours, the reaction mixture was filtered through a plug of celite to afford a white solid, which was added to a microwave vial with hydrochloric acid (37% in water, 5 mL), and microwaved at 160°C for 16 hours. The resulting reaction mixture was extracted with CH₂Cl₂ (X4) and Et₂O (X1). The aqueous phase was azeotroped with acetonitrile under reduced pressure. The resulting white solid was sonicated in Et₂O and vacuum filtered to afford the title compound as a white solid (103 mg, 52%).

¹H NMR (600 MHz, D₂O) δ 3.12 (s, 2H), 2.56 (s, 2H), 1.57 – 1.35 (m, 10H) ppm. ¹H NMR spectrum is consistent with reported values.²⁵



2-(tert-butyl)-10-fluoro-2-azaspiro[4.5]dec-9-ene-3,7-dione (35):

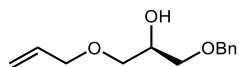
Dissolved 2-(tert-butyl)-6-fluoro-9-methoxy-2-azaspiro[4.5]deca-6,9-dien-3-one (**30**) (6.0 mg, 0.024 mmol) in CH₂Cl₂ (1.0 mL) and added TFA (0.2 mL). After 16 hours, quenched with 1M NaOH (aq), extracted with DCM (3x) and concentrated under reduced pressure to obtain the title compound as a yellow oil (5.7 mg, 100%).

¹H NMR (400 MHz, CDCl₃) δ 5.40 (dt, J = 15.5, 3.9 Hz, 1H), 3.58 (dt, J = 10.0, 0.8 Hz, 1H), 3.21 (dt, J = 10.1, 0.6 Hz, 1H), 3.05 (ddd, J = 20.9, 5.5, 3.6 Hz, 1H), 2.93 (d, J = 16.6 Hz, 1H), 2.89 (dt, J = 20.9, 4.6 Hz, 1H), 2.77 – 2.62 (m, 2H), 2.19 (d, J = 16.6 Hz, 1H), 1.38 (s, 9H) ppm.

¹³C NMR (101 MHz, CDCl₃) δ 204.6 (d, ⁴J_{C-F} = 2.5 Hz), 171.8, 158.6 (d, ¹J_{C-F} = 260.1 Hz), 101.8 (d, ²J_{C-F} = 22.2 Hz), 54.6, 53.4 (d, ³J_{C-F} = 1.5 Hz), 50.0 (d, ³J_{C-F} = 5.3 Hz), 42.2 (d, ³J_{C-F} = 2.5 Hz), 40.6 (d, ²J_{C-F} = 23.9 Hz), 37.4 (d, ³J_{C-F} = 8.1 Hz), 27.8 ppm.

LRMS (EI) m/z: $[M]^+$ calc'd. for $C_{13}H_{18}FNO_2$, 239.1, found 239.2.

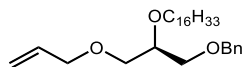
VII. Preparation of TFV Prodrugs



Rac-(2R)-1-allyloxy-3-benzyloxy-propan-2-ol (55):

To a 100 mL flame dried round bottom flask with a stir bar was added rac-(2R)-2-(benzyloxymethyl)oxirane (0.80 mL, 5.22 mmol), anhydrous DCM (20 mL) and allyl alcohol (3.55 mL, 52.23 mmol) under argon. boron trifluoride etherate (0.17 mL, 1.31 mmol) and the reaction stirred at rt for 1 h. The reaction mixture was then concentrated. Flash chromatography (12 g silica, 0-40% ethyl acetate in hexanes) afforded the product rac-(2R)-1-allyloxy-3-benzyloxy-propan-2-ol (878.7 mg, 3.9531 mmol, 75.688 % yield) as a clear oil.

$^1\text{H NMR}$ (600 MHz, CDCl_3) δ 7.37 – 7.27 (m, 5H), 5.90 (ddt, $J = 17.3, 10.4, 5.7$ Hz, 1H), 5.27 (dq, $J = 17.2, 1.6$ Hz, 1H), 5.19 (dq, $J = 10.4, 1.4$ Hz, 1H), 4.56 (s, 2H), 4.55 (d, $J = 3.4$ Hz, 1H), 4.01 (dt, $J = 5.7, 1.4$ Hz, 2H), 3.58 – 3.46 (m, 4H). $^1\text{H NMR}$ spectrum is consistent with reported values.²⁶



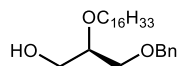
[rac-(2R)-3-allyloxy-2-hexadecoxy-propoxy]methylbenzene (56):

To a flame dried 100 mL round bottom flask with a stir bar was added sodium hydride (537.58 mg, 13.44 mmol) (60% dispersion in mineral oil) and anhydrous DMF (15 mL) under argon. A separate solution of rac-(2R)-1-allyloxy-3-benzyloxy-propan-2-ol (853.70 mg, 3.84 mmol) in anhydrous DMF (5 mL) was then transferred to the reaction dropwise and the mixture stirred for 10 minutes. 1-bromohexadecane (2.40 mL, 7.85 mmol) was added and the reaction stirred at rt overnight (22 h). The reaction was quenched with 1 M HCl and extracted with DCM (3x). The combined organic phases were washed with brine, dried over anhydrous sodium sulfate, and concentrated in vacuo. Flash chromatography (24 g silica, 0-10% ethyl acetate in hexanes) afforded the product [rac-(2R)-3-allyloxy-2-hexadecoxy-propoxy]methylbenzene (1358.3 mg, 3.0407 mmol, 79.2 % yield) as a clear oil.

$^1\text{H NMR}$ (600 MHz, CDCl_3) δ 7.36 – 7.32 (m, 5H), 5.94 – 5.83 (m, 1H), 5.26 (dt, $J = 17.3, 1.5$ Hz, 1H), 5.17 (dt, $J = 10.4, 1.5$ Hz, 1H), 4.56 (s, 2H), 4.16 (dd, $J = 5.6, 1.4$ Hz, 1H), 4.00 (dq, $J = 5.6, 1.4$ Hz, 2H), 3.64 – 3.49

26 Ainge, G. D.; Parlane, N. A.; Denis, M.; Dyer, B. S.; Haerer, A.; Hayman, C. M.; Larsen, D. S.; Painter, G. F. Phosphatidylinositol Mannoside Ether Analogues: Syntheses and Interleukin-12-inducing properties. *J. Org. Chem.*, **2007**, *72*, 5291-5296.

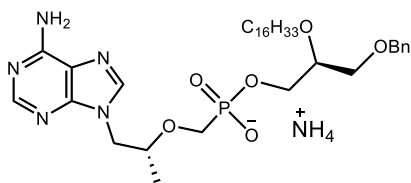
(m, 6H), 1.57 (p, $J = 7.2$ Hz, 2H), 1.35 – 1.23 (m, 26H), 0.88 (td, $J = 7.1, 2.2$ Hz, 3H). ^1H NMR spectrum is consistent with reported values. ^1H NMR spectrum is consistent with reported values.²⁶



rac-(2R)-3-benzyloxy-2-hexadecoxy-propan-1-ol (52):

To a 100 mL flame dried round bottom flask with a stir bar was added [(2R)-3-allyloxy-2-hexadecoxy-propoxy]methylbenzene (638.80 mg, 1.43 mmol) and dissolved in anhydrous Methanol (10 mL) under argon. Tetrakis triphenylphosphine Palladium (115.00 mg, 0.1 mmol) was added and the reaction stirred for 5 minutes. potassium carbonate (829.20 mg, 6. mmol) was then added and the reaction was refluxed at 75 °C for 7 hours. The reaction mixture was then concentrated in vacuo, diluted with 2 N HCl, and extracted with DCM (3x). The combined organic layers were washed with brine, dried over anhydrous sodium sulfate, and concentrated in vacuo. Flash chromatography (12 g silica, 0-30% ethyl acetate in hexanes) afforded the product rac-(2R)-3-benzyloxy-2-hexadecoxy-propan-1-ol (431.3 mg, 1.0606 mmol, 74.171 % yield) as a yellow oil.

^1H NMR (600 MHz, CDCl_3) δ 7.37 – 7.27 (m, 5H), 4.54 (d, $J = 3.2$ Hz, 2H), 3.74 (ddd, $J = 10.7, 6.9, 3.3$ Hz, 1H), 3.66 – 3.48 (m, 6H), 2.08 (ddd, $J = 7.0, 5.5, 1.8$ Hz, 1H), 1.57 (dtd, $J = 8.7, 6.8, 3.8$ Hz, 4H), 1.25 (d, $J = 4.0$ Hz, 26H), 0.88 (t, $J = 6.9$ Hz, 3H). ^1H NMR spectrum is consistent with reported values.²⁶



ammonium;[(1R)-2-(6-aminopurin-9-yl)-1-methyl-ethoxy]methyl-[(2S)-3-benzyloxy-2-hexadecoxy-propoxy]phosphinate (53):

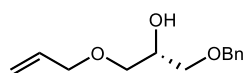
To a 10 mL schlenk tube with a stir bar was added [(1R)-2-(6-aminopurin-9-yl)-1-methyl-ethoxy]methylphosphonic acid (85.52 mg, 0.3 mmol), dicyclohexylcarbodiimide (81.91 mg, 0.4 mmol), and (2R)-3-benzyloxy-2-hexadecoxy-propan-1-ol (100.90 mg, 0.25 mmol) dissolved in NMP (1.7 mL) under argon. DMAP (3.03 mg, 0.02 mmol) was added and the reaction was heated to 100 °C and stirred overnight (21 h). The reaction was then cooled to rt and a few drops of water were added to cause precipitation. The precipitate was filtered off and the filtrate was concentrated in vacuo. Flash chromatography of the filtrate (12 g silica, 100% DCM - 100% DCM:MeOH:NH4OH 80:20:3) afforded the product ammonium;[(1R)-2-(6-aminopurin-9-yl)-1-methyl-ethoxy]methyl-[(2S)-3-benzyloxy-2-hexadecoxy-propoxy]phosphinate (29.8 mg, 0.0430 mmol, 17.333 % yield) as a white solid.

$^1\text{H NMR}$ (500 MHz, CD_3OD) δ 8.33 (s, 1H), 8.20 (s, 1H), 7.32 – 7.26 (m, 4H), 7.25 – 7.20 (m, 1H), 4.50 (s, 2H), 4.40 – 4.32 (m, 1H), 4.20 (dd, $J = 14.4, 6.4$ Hz, 1H), 3.95 – 3.82 (m, 2H), 3.73 (dd, $J = 12.8, 9.4$ Hz, 1H), 3.65 – 3.55 (m, 2H), 3.54 – 3.46 (m, 4H), 1.53 – 1.44 (m, 2H), 1.35 – 1.23 (m, 28H), 1.12 (d, $J = 6.2$ Hz, 3H), 0.89 (t, 3H).

$^{13}\text{C NMR}$ (151 MHz, CD_3OD) δ 127.9, 127.3, 48.0, 47.9, 47.7, 47.6, 47.5, 47.3, 47.2, 29.4, 29.4, 29.3.

$^{31}\text{P NMR}$ (243 MHz, CD_3OD) δ 16.6.

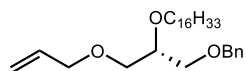
HRMS (ESI+) $[\text{M}+\text{H}]$ calc. for $\text{C}_{35}\text{H}_{57}\text{O}_6\text{N}_5\text{P}$, 674.40519, observed, 674.4056.



rac-(2S)-1-allyloxy-3-benzyloxy-propan-2-ol (58):

To a 100 mL flame dried round bottom flask with a stir bar was added rac-(2S)-2-(benzyloxymethyl)oxirane (0.70 mL, 4.57 mmol), anhydrous DCM (20 mL) and allyl alcohol (3.11 mL, 45.7 mmol) under argon. boron trifluoride etherate (0.17 mL, 1.31 mmol) and the reaction stirred at rt for 1 h. The reaction mixture was then concentrated. Flash chromatography (12 g silica, 0-40% ethyl acetate in hexanes) afforded the product rac-(2S)-1-allyloxy-3-benzyloxy-propan-2-ol (1015 mg, 4.5663 mmol, 99.919 % yield) as a clear oil.

$^1\text{H NMR}$ (500 MHz, CDCl_3) δ 7.40 – 7.28 (m, 5H), 5.90 (ddt, $J = 17.3, 10.4, 5.7$ Hz, 1H), 5.30 (dq, $J = 17.2, 1.6$ Hz, 1H), 5.19 (dq, $J = 10.4, 1.4$ Hz, 1H), 4.56 (s, 2H), 4.55 (d, $J = 3.4$ Hz, 1H), 4.01 (dt, $J = 5.7, 1.4$ Hz, 2H), 3.58 – 3.46 (m, 4H). $^1\text{H NMR}$ spectrum is consistent with reported values.²⁷



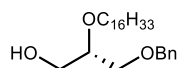
[rac-(2S)-3-allyloxy-2-hexadecoxy-propoxy]methylbenzene (59):

To a flame dried 100 mL round bottom flask with a stir bar was added sodium hydride (639.97 mg, 16. mmol) (60% dispersion in mineral oil) and anhydrous DMF (15 mL) under argon. A separate solution of rac-(2S)-1-allyloxy-3-benzyloxy-propan-2-ol (1015.00 mg, 4.57 mmol) in anhydrous DMF (5 mL) was then transferred to the reaction dropwise and the mixture stirred for 10 minutes. 1-bromohexadecane (2.80 mL, 9.16 mmol) was added and the reaction stirred overnight (18 h). The reaction was then quenched with 1 M HCl and extracted with DCM (3x). The combined organic phases were washed with

27 Van der Es, D.; Groenia, N. A.; Laverde, D.; Overkleeft, H. S.; Huebner, J.; van der Marel, G. A.; Codee, J. D. C. Synthesis of E. faecium wall teichoic acid fragments. *Bioorg. Med. Chem.* **2016**, *24*, 3893-3907.

water and brine, dried over anhydrous sodium sulfate, and concentrated in vacuo. Flash chromatography (24 g silica, 0-10% ethyl acetate in hexanes) afforded the product [rac-(2S)-3-allyloxy-2-hexadecoxy-propoxy]methylbenzene (1127.6 mg, 2.5242 mmol, 55.279 % yield) as a clear oil.

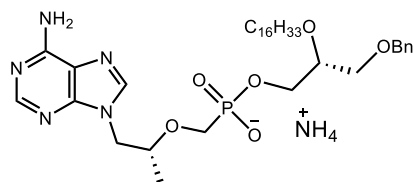
$^1\text{H NMR}$ (600 MHz, CDCl_3) δ 7.34 (d, $J = 4.7$ Hz, 3H), 7.28 (ddd, $J = 6.1, 3.7, 2.3$ Hz, 2H), 5.93 – 5.85 (m, 1H), 5.26 (dq, $J = 17.2, 1.7$ Hz, 1H), 5.19 – 5.14 (m, 1H), 4.56 (s, 2H), 4.15 (dt, $J = 5.7, 1.5$ Hz, 1H), 4.00 (dt, $J = 5.6, 1.5$ Hz, 2H), 3.65 – 3.37 (m, 6H), 1.62 – 1.52 (m, 2H), 1.34 – 1.25 (m, 26H), 0.88 (t, $J = 7.0$ Hz, 3H).



rac-(2S)-3-benzyloxy-2-hexadecoxy-propan-1-ol (60):

To a 100 mL flame dried round bottom flask with a stir bar was added [(2S)-3-allyloxy-2-hexadecoxy-propoxy]methylbenzene (893.42 mg, 2. mmol) and dissolved in anhydrous Methanol (20 mL) under argon. Tetrakis triphenylphosphine Palladium (231.11 mg, 0.2 mmol) was added and the reaction stirred for 5 minutes. potassium carbonate (1658.40 mg, 12. mmol) was then added and the reaction was refluxed at 75 °C overnight (16 h). The reaction mixture was then concentrated in vacuo, diluted with 2 N HCl, and extracted with DCM (3x). The combined organic layers were washed with brine, dried over anhydrous sodium sulfate, and concentrated in vacuo. Flash chromatography (12 g silica, 0-30% ethyl acetate in hexanes) afforded the product rac-(2S)-3-benzyloxy-2-hexadecoxy-propan-1-ol (425.3 mg, 1.0459 mmol, 52.294 % yield) as a yellow oil.

$^1\text{H NMR}$ (600 MHz, CDCl_3) δ 7.37 – 7.27 (m, 5H), 4.54 (d, $J = 3.2$ Hz, 2H), 3.74 (dddd, $J = 11.3, 7.0, 2.9, 1.2$ Hz, 1H), 3.67 – 3.46 (m, 6H), 2.07 (ddd, $J = 7.0, 5.6, 3.1$ Hz, 1H), 1.60 – 1.54 (m, 4H), 1.35 – 1.21 (m, 26H), 0.88 (t, $J = 7.0$ Hz, 3H). $^1\text{H NMR}$ spectrum is consistent with reported values.²⁸



ammonium;[(1R)-2-(6-aminopurin-9-yl)-1-methyl-ethoxy]methyl-[(2R)-3-benzyloxy-2-hexadecoxy-propoxy]phosphinate (61):

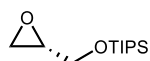
28 Orisada, S.; Ono, Y.; Kodaira, T.; Kishino, H.; Ninomiya, R.; Mori, N.; Watanabe, H.; Ohta, A.; Horiuchi, H.; Fukuda, R. The membrane-bound O-acyltransferase Ale1 transfers an acyl moiety to newly synthesized 2-alkyl-sn-glycero-3-phosphocholine in yeast. *FEBS Lett.* **2018**, *592*, 1829-1836.

To a 10 mL schlenk tube with a stir bar was added [(1R)-2-(6-aminopurin-9-yl)-1-methyl-ethoxy]methylphosphonic acid (172.33 mg, 0.6 mmol), dicyclohexylcarbodiimide (165.06 mg, 0.8 mmol), and (2S)-3-benzyloxy-2-hexadecoxy-propan-1-ol (203.32 mg, 0.5 mmol) dissolved in NMP (3 mL) under argon. DMAP (6.11 mg, 0.05 mmol) was added and the reaction was heated to 100 °C and stirred overnight (21 h). The reaction was then cooled to rt and a few drops of water were added to cause precipitation. The precipitate was filtered off and the filtrate was concentrated in vacuo. Flash chromatography of the filtrate (12 g silica, 100% DCM - 100% DCM:MeOH:NH₄OH 80:20:3) afforded the product ammonium;[(1R)-2-(6-aminopurin-9-yl)-1-methyl-ethoxy]methyl-[(2R)-3-benzyloxy-2-hexadecoxy-propoxy]phosphinate (83.1 mg, 0.1199 mmol, 23.987 % yield) as a white solid.

¹H NMR (600 MHz, CD₃OD) δ 8.35 (s, 1H), 8.22 (s, 1H), 7.29 (q, *J* = 7.7, 5.1 Hz, 4H), 7.23 (s, 1H), 4.50 (s, 2H), 4.37 (dd, *J* = 14.5, 3.2 Hz, 1H), 4.23 (dd, *J* = 14.4, 6.3 Hz, 1H), 3.93 (dh, *J* = 22.0, 5.4 Hz, 3H), 3.75 (dd, *J* = 12.9, 9.3 Hz, 1H), 3.65 – 3.47 (m, 4H), 3.33 (s, 1H), 1.53 (p, *J* = 6.7 Hz, 2H), 1.28 (d, *J* = 14.1 Hz, 28H), 1.14 (d, *J* = 6.2 Hz, 3H), 0.91 (t, *J* = 6.9 Hz, 3H).

¹³C NMR (151 MHz, CD₃OD) δ 149.5, 149.3, 143.6, 138.4, 127.9, 127.3, 127.1, 118.0, 78.2, 78.2, 75.4, 75.4, 72.9, 70.1, 69.7, 64.5, 64.1, 64.0, 63.4, 48.0, 47.9, 47.8, 47.6, 47.5, 47.3, 47.2, 31.7, 29.8, 29.4, 29.4, 29.3, 29.2, 29.1, 25.8, 22.3, 15.5, 13.1. ³¹P NMR (243 MHz, CD₃OD) δ 16.5.

HRMS (ESI+) [M+H] calc. for C₃₅H₅₇O₆N₅P, 674.40519, observed, 674.4052.

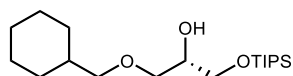


triisopropyl-[[[(2S)-oxiran-2-yl]methoxy]silane (63):

To a flame dried 100 mL round bottom flask with a stir bar was added [(2R)-oxiran-2-yl]methanol (200.02 mg, 2.7 mmol), DMAP (16.49 mg, 0.14 mmol), Imidazole (257.33 mg, 3.78 mmol), and DCM (10 mL) under argon. The reaction was cooled to 0 °C and triisopropylchlorosilane (0.81 mL, 3.78 mmol) was added dropwise. The mixture was then warmed to room temperature and stirred for 3 hours. The reaction was then diluted with water and extracted with DCM (X3). The combined organic phases were washed with brine, dried over sodium sulfate, and concentrated in vacuo. Flash chromatography (12 g silica, 0-5% ethyl acetate in hexanes) afforded triisopropyl-[[[(2S)-oxiran-2-yl]methoxy]silane (262.9 mg, 1.141 mmol, 42.258 % yield) as a clear oil.

¹H NMR (400 MHz, CDCl₃) δ 3.94 (dd, *J* = 11.7, 3.2 Hz, 1H), 3.78 (dd, *J* = 11.7, 4.7 Hz, 1H), 3.14 (tt, *J* = 4.5, 3.0 Hz, 1H), 2.80 (dd, *J* = 5.2, 4.0 Hz, 1H), 2.70 (dd, *J* = 5.2, 2.7 Hz, 1H), 1.22 – 1.03 (m, 21H). ¹H NMR spectrum is consistent with reported values.²⁹

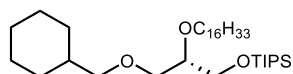
29 Borrel, J.; Pisella, G.; Waser, J. Copper-catalyzed oxyalkynylation of C-S bonds in thiiranes and thiethanes with hypervalent iodine reagents. *Org Lett.* **2020**, *22*, 422-427.



(2S)-1-(cyclohexylmethoxy)-3-triisopropylsilyloxy-propan-2-ol (64):

To a 50 mL flame dried round bottom flask with a stir bar was added triisopropyl-[[[(2S)-oxiran-2-yl]methoxy]silane (230.42 mg, 1. mmol), cyclohexylmethanol (1141.90 mg, 10. mmol), and DCM (4 mL). boron trifluoride etherate (0.03 mL, 0.25 mmol) was added and the reaction stirred for 2 h. The reaction was then concentrated in vacuo. Flash chromatography (12 g silica, 0-5% ethyl acetate in hexanes) afforded (2S)-1-(cyclohexylmethoxy)-3-triisopropylsilyloxy-propan-2-ol (184 mg, 0.5340 mmol, 53.395 % yield) as a clear oil.

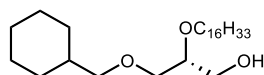
$^1\text{H NMR}$ (500 MHz, CDCl_3) δ 3.83 (h, $J = 5.3$ Hz, 1H), 3.78 – 3.67 (m, 2H), 3.53 – 3.40 (m, 2H), 3.25 (d, $J = 6.5$ Hz, 2H), 2.54 (d, $J = 5.1$ Hz, 1H), 1.77 – 1.53 (m, 6H), 1.28 – 0.86 (m, 25H).



[3-(cyclohexylmethoxy)-2-hexadecoxy-propoxy]-triisopropyl-silane (65):

To a 50 mL flame dried round bottom flask with a stir bar was added Sodium Hydride (65.52 mg, 1.64 mmol) (60% in mineral oil), 1-(cyclohexylmethoxy)-3-triisopropylsilyloxy-propan-2-ol (161.27 mg, 0.47 mmol), and DMF (3 mL). The reaction was stirred for 10 m and then 1-bromohexadecane (285.80 mg, 0.94 mmol) was added and the reaction stirred overnight. The mixture was then diluted with water and extracted with DCM (X3). The combined organic phase was washed with brine, dried over sodium sulfate, filtered, and concentrated in vacuo. Flash chromatography (4 g silica, 0-10% ethyl acetate in hexanes) afforded [3-(cyclohexylmethoxy)-2-hexadecoxy-propoxy]-triisopropyl-silane (219.6 mg, 0.3859 mmol, 82.462 % yield) as a clear oil.

$^1\text{H NMR}$ (500 MHz, cdcl_3) δ 3.73 – 3.70 (m, 1H), 3.59 – 3.36 (m, 6H), 3.24 (dd, $J = 6.6, 1.4$ Hz, 2H), 1.58 (s, 6H), 1.33 – 1.17 (m, 31H), 1.17 – 1.01 (m, 22H), 0.95 – 0.84 (m, 5H).



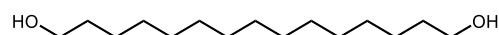
3-(cyclohexylmethoxy)-2-hexadecoxy-propan-1-ol (66):

To a 50 mL flame dried round bottom flask with a stir bar was added [3-(cyclohexylmethoxy)-2-hexadecoxy-propoxy]-triisopropyl-silane (206.56 mg, 0.36 mmol) in THF (2 mL). Tetra-n-butylammonium fluoride (1.45 mL, 1.45 mmol) was added dropwise and the reaction stirred overnight. The reaction was

then quenched with sodium bicarbonate and extracted with ethyl acetate (X3). The combined organic phases were washed with brine, dried over sodium sulfate, filtered, and concentrated in vacuo. Flash chromatography (12 g silica, 0-20% ethyl acetate in hexanes) afforded 3-(cyclohexylmethoxy)-2-hexadecoxy-propan-1-ol (97.7 mg, 0.2367 mmol, 65.217 % yield) as a yellow oil.

$^1\text{H NMR}$ (600 MHz, CDCl_3) δ 3.72 (ddd, $J = 11.1, 6.8, 3.7$ Hz, 1H), 3.65 – 3.57 (m, 2H), 3.56 – 3.41 (m, 4H), 3.27 – 3.21 (m, 2H), 1.75 – 1.53 (m, 7H), 1.35 – 1.10 (m, 30H), 0.96 – 0.85 (m, 5H).

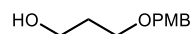
VIII. Preparation of FdUMP Prodrugs



Pentadecane-1,15-diol (S60):

To a 500 mL flame dried 2-neck flask with a stir bar was added lithium aluminum hydride (4.27 mL, 100. mmol) and anhydrous THF (100 mL) at 0 °C. Pentadecanedioic acid (2723.80 mg, 10. mmol) was added in THF and the reaction was warmed to room temperature and then refluxed at 75 °C overnight. The reaction was then cooled to 0 °C and quenched with water under argon. The solution turned from grey to white and was then poured over 300 mL of water and adjusted to pH 1 with HCl and stirred for 1 h to dissolve all inorganic constituents. The mixture was then filtered and washed with water and ice cold ether to afford pentadecane-1,15-diol (1963.8 mg, 8.0349 mmol, 80.349 % yield) as a white solid.

$^1\text{H NMR}$ (600 MHz, CD_3OD) δ 3.54 (s, 4H), 1.52 (p, $J = 6.4$ Hz, 4H), 1.38 – 1.28 (m, 22H). $^1\text{H NMR}$ spectrum is consistent with reported values.³⁰



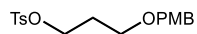
3-[(4-methoxyphenyl)methoxy]propan-1-ol (82):

To a 100 mL flame dried 3-neck flask with a stir bar was added SODIUM HYDRIDE (1599.93 mg, 40. mmol) (60% in mineral oil), THF (20 mL), and 1,3-Dihydroxypropane (3043.60 mg, 40. mmol). The mixture was heated to reflux (70 °C). 1-(chloromethyl)-4-methoxy-benzene (1566.10 mg, 10. mmol) was added dropwise. The reaction stirred overnight (17 h). The reaction was then cooled to room temperature, quenched with 1 M HCl, diluted with water, and extracted with DCM (3X). The combined organic layers were washed with brine, dried over sodium sulfate, and concentrated in vacuo. Column chromatography (24 g silica, 20-80% ethyl acetate in

30 Girlanda-Junges, C.; Keyling-Bilger, F.; Schmitt, G.; Luu, B. Effect of cyclohexenonic long chain fatty alcohols on neurite outgrowth. Study on structure-activity relationship. *Tetrahedron*, **1998**, *54*, 7735-7748.

hexanes) afforded the product 3-[(4-methoxyphenyl)methoxy]propan-1-ol (1811 mg, 9.2285 mmol, 92.285 % yield) as a yellow oil.

$^1\text{H NMR}$ (600 MHz, CDCl_3) δ 4.22 (t, $J = 6.2$ Hz, 2H), 3.69 (t, $J = 6.0$ Hz, 2H), 2.06 (s, 2H), 1.86 (p, $J = 6.1$ Hz, 2H). $^1\text{H NMR}$ spectrum is consistent with reported values.³¹



3-[(4-methoxyphenyl)methoxy]propyl 4-methylbenzenesulfonate (83):

To a flame dried 100 mL round bottom flask with a stir bar was added P-TOLUENESULFONYL CHLORIDE (1582.23 mg, 8.3 mmol), DCM (20 mL), triethylamine (1.16 mL, 8.3 mmol), and DMAP (36.21 mg, 0.3 mmol). 3-[(4-methoxyphenyl)methoxy]propan-1-ol (1163.30 mg, 5.93 mmol) was added slowly and the reaction stirred at room temperature overnight. The reaction was then diluted with water, and extracted with DCM (X3). The combined organic phases were washed with brine, dried over sodium sulfate, filtered, and concentrated. Flash chromatography (24 g silica, 0-20% ethyl acetate in hexanes) afforded 3-[(4-methoxyphenyl)methoxy]propyl 4-methylbenzenesulfonate (1618 mg, 4.6172 mmol, 77.888 % yield) as a white solid.

$^1\text{H NMR}$ (600 MHz, CDCl_3) δ 7.78 (d, $J = 8.3$ Hz, 2H), 7.32 (d, $J = 7.8$ Hz, 2H), 7.17 (d, $J = 8.3$ Hz, 2H), 6.85 (d, $J = 8.7$ Hz, 2H), 4.33 (s, 2H), 4.14 (t, $J = 6.2$ Hz, 2H), 3.80 (s, 3H), 3.46 (t, $J = 6.0$ Hz, 2H), 2.43 (s, 3H), 1.92 (p, $J = 6.1$ Hz, 2H). $^1\text{H NMR}$ spectrum is consistent with reported values.³²



15-[3-[(4-methoxyphenyl)methoxy]propoxy]pentadecan-1-ol (84):

To a 100 mL round bottom flask with a stir bar was added pentadecane-1,15-diol (366.62 mg, 1.5 mmol), THF (1.5 mL), and 50% sodium hydroxide (2.5 mL). TETRABUTYLAMMONIUM BROMIDE (80.59 mg, 0.25 mmol) and 3-[(4-methoxyphenyl)methoxy]propyl 4-methylbenzenesulfonate (175.22 mg, 0.5 mmol) were added. Reaction refluxed at 75 °C overnight. The reaction was then cooled to room temperature, quenched with 1 M HCl, and extracted with ethyl acetate (3X). The combined organic phases were washed with brine, dried over sodium sulfate, and concentrated in vacuo. Flash chromatography (24 g silica, 0-30% ethyl acetate in hexanes) afforded 15-[3-[(4-

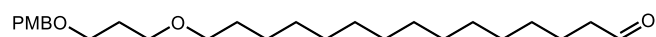
31 Shibahara, S.; Fujino, M.; Tashiro, Y.; Okamoto, N; Esumi, T.; Takahashi, K.; Ishihara, J.; Hatakeyama, S. Total synthesis of (+)-fostriecin and (+)-phoslactomycin B. *Synthesis*, **2009**, *17*, 2935-2953.

32 Urbanek, R. A.; Sabes, S. F.; Forsyth, C. J. Efficient synthesis of okadaic acid. 1. Convergent assembly of the C15- C38 domain. *JACS*, **1998**, *120*, 2523-2533.

methoxyphenyl)methoxy]propoxy]pentadecan-1-ol (100.2 mg, 0.2371 mmol, 47.416 % yield) as a white solid.

$^1\text{H NMR}$ (600 MHz, CDCl_3) δ 7.27 – 7.24 (m, 2H), 6.87 (d, $J = 8.6$ Hz, 2H), 4.43 (s, 2H), 3.80 (s, 3H), 3.63 (t, $J = 6.7$ Hz, 2H), 3.53 (t, $J = 6.3$ Hz, 2H), 3.50 (t, $J = 6.4$ Hz, 2H), 3.39 (t, $J = 6.7$ Hz, 2H), 1.86 (p, $J = 6.4$ Hz, 2H), 1.61 – 1.46 (m, 6H), 1.38 – 1.19 (m, 24H).

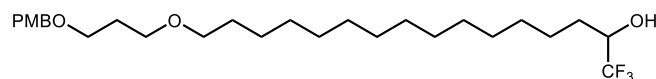
$^{13}\text{C NMR}$ (151 MHz, CDCl_3) δ 159.3, 130.8, 129.4, 113.9, 72.8, 71.2, 67.9, 67.3, 63.2, 55.4, 33.0, 30.3, 29.9, 29.8, 29.7, 29.7, 29.6, 26.3, 25.9.



15-[3-[(4-methoxyphenyl)methoxy]propoxy]pentadecanal (85):

To a 100 mL flame dried round bottom flask with a stir bar was added dimethyl sulfoxide (0.90 mL, 12.62 mmol) and DCM (13 mL) and the mixture was cooled to -78 °C under argon. oxalyl chloride (0.44 mL, 5.05 mmol) was added dropwise and the mixture was stirred for 30 m. 15-[3-[(4-methoxyphenyl)methoxy]propoxy]pentadecan-1-ol (1066.90 mg, 2.52 mmol) dissolved in DCM was added and the reaction stirred for an additional 90 m. triethylamine (2.46 mL, 17.67 mmol) was added and the reaction was warmed to room temperature and stirred for 3 h, during which time, the reaction turned orange. The mixture was then washed with saturated ammonium chloride (X2) and brine and concentrated in vacuo. Flash chromatography (12 g silica, 0-10% ethyl acetate in hexanes) afforded 15-[3-[(4-methoxyphenyl)methoxy]propoxy]pentadecanal (802.7 mg, 1.9083 mmol, 75.596 % yield) as a yellow oil.

$^1\text{H NMR}$ (500 MHz, cdCl_3) δ 9.76 (t, $J = 1.9$ Hz, 1H), 7.29 – 7.23 (m, 2H), 6.90 – 6.84 (m, 2H), 4.43 (s, 2H), 3.80 (s, 3H), 3.53 (t, $J = 6.4$ Hz, 2H), 3.49 (t, $J = 6.4$ Hz, 2H), 3.38 (t, $J = 6.7$ Hz, 2H), 2.41 (td, $J = 7.4, 1.9$ Hz, 2H), 1.86 (p, $J = 6.4$ Hz, 2H), 1.66 – 1.50 (m, 6H), 1.33 – 1.23 (m, 18H).

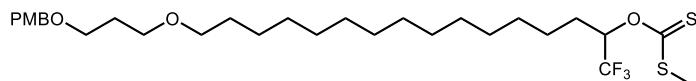


1,1,1-trifluoro-16-[3-[(4-methoxyphenyl)methoxy]propoxy]hexadecan-2-ol (86):

To a 50 mL flame dried round bottom flask with a stir bar was added 15-[3-[(4-methoxyphenyl)methoxy]propoxy]pentadecanal (88.33 mg, 0.21 mmol) in THF (1 mL) under argon and cooled to 0 °C. (TRIFLUOROMETHYL)TRIMETHYLSILANE (74.65 mg, 0.53 mmol) was added, then Tetra-*n*-butylammonium fluoride (0.42 mL, 0.42 mmol) was added dropwise. The reaction turned brown and stirred at 0 °C for 45 m and then was warmed to room temperature and stirred for an addition 3 h. The reaction showed mostly starting material by TLC. An additional 1.0 equivalents of trifluoromethyl trimethylsilane and tetra-*n*-butylammonium fluoride were added and the reaction stirred overnight. The reaction was then quenched with saturated sodium bicarbonate and extracted with ethyl acetate (X3).

The combined organic phase was washed with brine, dried over sodium sulfate, filtered, and concentrated in vacuo. Flash chromatography (4 g silica, 0-20% ethyl acetate in hexanes) afforded 1,1,1-trifluoro-16-[3-[(4-methoxyphenyl)methoxy]propoxy]hexadecan-2-ol (61.9 mg, 0.1262 mmol, 60.077 % yield) as a yellow oil.

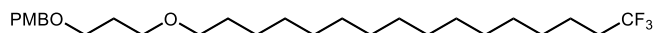
$^1\text{H NMR}$ (500 MHz, CDCl_3) δ 7.32 – 7.23 (m, 2H), 6.93 – 6.85 (m, 2H), 4.44 (s, 2H), 3.90 (ddt, $J = 9.7, 6.6, 3.2$ Hz, 1H), 3.81 (s, 3H), 3.54 (t, $J = 6.3$ Hz, 2H), 3.50 (t, $J = 6.4$ Hz, 2H), 3.39 (t, $J = 6.7$ Hz, 2H), 1.87 (p, $J = 6.4$ Hz, 2H), 1.63 – 1.50 (m, 6H), 1.26 (s, 18H).



O-[15-[3-[(4-methoxyphenyl)methoxy]propoxy]-1-(trifluoromethyl)pentadecyl] methylsulfanylmethanethioate (87):

To a 50 mL flame dried round bottom flask with a stir bar was added Sodium Hydride (75.63 mg, 1.89 mmol) (60% in mineral oil) and 1,1,1-trifluoro-16-[3-[(4-methoxyphenyl)methoxy]propoxy]hexadecan-2-ol (371.10 mg, 0.76 mmol) dissolved in anhydrous THF (4 mL) at 0 °C and stirred for 30 m. carbon disulfide (0.23 mL, 3.78 mmol) was added and the reaction was warmed to room temperature and stirred for 45 m, during which time, the reaction became an orange slurry. methyl iodide (0.24 mL, 3.78 mmol) was added and the reaction stirred overnight at room temperature. The mixture was then poured onto water at 0 °C and extracted with ethyl acetate (X3). The combined organic layer was washed with brine, dried over sodium sulfate, filtered, and concentrated in vacuo. Flash chromatography (12 g silica, 0-10% ethyl acetate in hexanes) afforded O-[15-[3-[(4-methoxyphenyl)methoxy]propoxy]-1-(trifluoromethyl)pentadecyl] methylsulfanylmethanethioate (374 mg, 0.6439 mmol, 85.135 % yield) as a yellow oil.

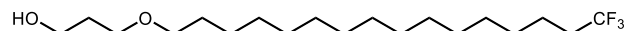
$^1\text{H NMR}$ (600 MHz, CDCl_3) δ 7.28 – 7.23 (dd, $J = 8.5, 2.6$ Hz, 2H), 6.87 (dd, $J = 8.5, 2.6$ Hz, 2H), 6.26 – 6.17 (m, 1H), 4.43 (s, 2H), 3.80 (s, 3H), 3.53 (t, $J = 6.3$ Hz, 2H), 3.49 (t, $J = 6.3$ Hz, 2H), 3.38 (t, $J = 6.7$ Hz, 2H), 2.61 (s, 3H), 1.91 – 1.82 (m, 2H), 1.54 (p, $J = 6.6$ Hz, 2H), 1.43-1.36 (m, 6H), 1.32 – 1.24 (m, 18H).



1-methoxy-4-[3-(16,16-trifluorohexadecoxy)propoxymethyl]benzene (88):

To a 50 mL round bottom flask with a stir bar was added O-[15-[3-[(4-methoxyphenyl)methoxy]propoxy]-1-(trifluoromethyl)pentadecyl] methylsulfanylmethanethioate (54.40 mg, 0.09 mmol) dissolved in dioxane (2 mL). triethylamine (0.07 mL, 0.53 mmol) and hypophosphorous acid (0.150 mL) were added and the reaction refluxed at 110 °C for 30 m. Azobisisobutyronitrile (3.08 mg, 0.02 mmol) was added slowly and the reaction refluxed at 110 °C overnight. The reaction was then cooled to room temperature, diluted with water, and extracted with ethyl acetate (X3). The combined

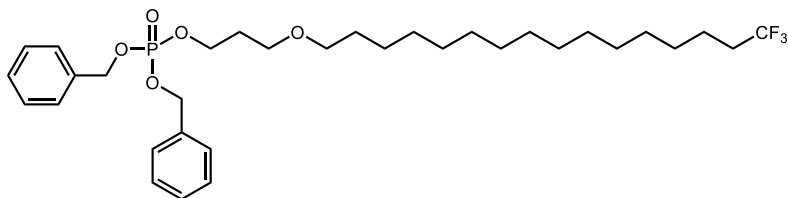
organic phase was washed with brine, dried over sodium sulfate, filtered, and concentrated in vacuo. Flash chromatography (4 g silica, 0-10% ethyl acetate in hexanes) afforded 1-methoxy-4-[3-(16,16,16-trifluorohexadecoxy)propoxymethyl]benzene (37.2 mg, 0.0784 mmol, 83.678 % yield) as a clear oil. ^1H NMR (500 MHz, CDCl_3) δ 7.31 – 7.23 (m, 2H), 6.92 – 6.84 (m, 2H), 4.43 (s, 2H), 3.80 (s, 3H), 3.53 (t, J = 6.4 Hz, 2H), 3.50 (t, J = 6.4 Hz, 2H), 3.39 (t, J = 6.7 Hz, 2H), 2.12 – 1.99 (m, 2H), 1.87 (p, J = 6.4 Hz, 2H), 1.59 – 1.49 (m, 4H), 1.39 – 1.24 (m, 22H).



3-(16,16,16-trifluorohexadecoxy)propan-1-ol (80):

To a 100 mL round bottom flask with a stir bar was added 1-methoxy-4-[3-(16,16,16-trifluorohexadecoxy)propoxymethyl]benzene (221.70 mg, 0.47 mmol) and Pd(OH)/C. A hydrogen balloon was added and the reaction stirred at room temperature overnight. The reaction was then poured over celite, rinsed with ethyl acetate, and concentrated in vacuo. Flash chromatography (12 g, 0-50% ethyl acetate in hexanes) afforded 3-(16,16,16-trifluorohexadecoxy)propan-1-ol (124.2 mg, 0.3504 mmol, 75.009 % yield).

^1H NMR (600 MHz, CDCl_3) δ 3.80 – 3.75 (m, 2H), 3.61 (t, J = 6.7 Hz, 2H), 3.42 (t, J = 6.7 Hz, 2H), 2.09 – 2.01 (m, 2H), 1.83 (p, J = 5.6 Hz, 2H), 1.60 – 1.50 (m, 4H), 1.38 – 1.23 (m, 22H).



[benzyl-[3-(16,16,16-trifluorohexadecoxy)propoxy]phosphoryl]methylbenzene (89):

To a 25 mL round bottom flask with a stir bar was added 3-(16,16,16-trifluorohexadecoxy)propan-1-ol (124.20 mg, 0.35 mmol), 5-methyl-1H-tetrazole (88.38 mg, 1.05 mmol), and DCM (3.5 mL). The solution was purged with argon and cooled to 0 °C. DIBENZYL DIISOPROPYLPHOSPHORAMIDITE (0.14 mL, 0.42 mmol) was added. The reaction stirred for 5 minutes at 0 °C and then 2 hours at room temperature. The mixture was then cooled back to 0 °C and treated with 30% Hydrogen peroxide (0.215 mL) and stirred for 1 hour. The mixture was then quenched with saturated sodium bicarbonate and extracted with DCM (3X). The combined organic phases were washed with brine, dried over sodium sulfate, and concentrated in vacuo. Flash chromatography (12 g silica, 0-30% ethyl acetate in hexanes) afforded [benzyl-[3-(16,16,16-trifluorohexadecoxy)propoxy]phosphoryl]methylbenzene (140.1 mg, 0.2404 mmol, 68.622 % yield).

¹H NMR (500 MHz, CDCl₃) δ 7.40 – 7.28 (m, 10H), 5.11 – 4.96 (m, 4H), 4.14 – 4.06 (m, 2H), 3.43 (t, *J* = 6.2 Hz, 2H), 3.34 (t, *J* = 6.7 Hz, 2H), 2.10 – 1.98 (m, 2H), 1.86 (p, *J* = 6.3 Hz, 2H), 1.57 – 1.48 (m, 4H), 1.36 – 1.22 (m, 22 H).